

POLITECNICO DI TORINO

Master's Degree Course in Electrical Engineering

Master's Degree Thesis

Sizing, simulation and comparison of a Building Integrated and a Building Attached Photovoltaic system



Supervisor:
prof. Filippo Spertino

Candidate:
Juan Ignacio Erenchun G.
Student Id: 239666

Academic Year 2017-2018

Abstract

This thesis project presents the design, simulation and comparison of two different configurations of a photovoltaic system installed on an office building in Santiago, Chile. One is a BAPV type consisting of mono-crystalline modules used as Sun shields on the north facade windows and also mounted on the roof facing the same direction, an installed power of 488.4 kWp is calculated. The second is a BIPV system with mono-crystalline semi-transparent modules on the windows and opaque panels on the walls and the same roof installation as the other case, results in 885.87 kWp installed. The same model of three-phase inverter is used, but 9 are required in the first case and 15 in the latter.

The estimation of the demand profile is performed using the software EnergyPlus and OpenStudio, based on the Reference building model for a large office building developed by the DOE of the United States. After modifications to adjust the internal loads, an annual consumption of 4,200.8 MWh is obtained. This value does not present considerable variations when the solar modules are added. The simulation of the generated power is performed on an hourly basis for a 25-year period using MATLAB R2017a, based on the radiation data provided in “*Explorador Solar*” by the Ministry of Energy of Chile. An annual production of 1,036.1 MWh is computed for Sun shield and 1,788.0 MWh for Curtain wall.

For the Sun shield there is injection to the grid on the weekends, since during the week the consumption is higher, for Curtain wall there is also generation surplus during weekdays in summer. In both cases the energy self-consumed reduces the requirements to the system resulting in a peak-shaving effect due to the coincidence of the demand profile and the sunlight hours. The Sun shield configuration has a higher annual yield and reference yield, of 2,121.4 kWh/kWp and 2,583.2 $kWh \cdot m^{-2}/kW \cdot m^{-2}$, while in Curtain wall are 2,018.4 kWh/kWp and 2,312.0 $kWh \cdot m^{-2}/kW \cdot m^{-2}$. The performance ratio is lower, 82.1% compared to 87.3% of the latter.

An economic analysis is performed, considering the initial investment, the yearly gains and associated costs and the savings that a BIPV system implies when it is constructed. It is concluded that the Sun shield configuration is profitable with an NPV of 575,000 USD and a payback time of 5 years, while Curtain wall is not economically viable with NPV of -1,711,700 USD . The initial investment is 545,362.09 USD and 4,297,745.67 USD respectively but in the second case it is reduced about 30%, to 2,990,252.70 USD , due to savings related to the conventional components being replaced. It is noted that the periodic costs for cleaning the modules take special importance for Curtain wall because they are charged by square meter and the installed area is much bigger in this case, 5,274.67 m^2 compared to 2,664.71 m^2 .

*To my family,
my mother, father,
sisters and grandparents.*

Acknowledgements

First of all, I would like to thank Professor Filippo Spertino for giving me the opportunity to develop this thesis, for the support and guidance provided in this process. I also thank Mr. Renato Macconi from EnergyGlass for the information and insights provided without which this thesis would not have been possible to complete.

Secondly, my deepest gratitude to my family for the support and help they have given me from Chile. To my parents, sisters, grandparents and uncles, for having always been concerned about me since I started my studies and for encouraging me during the development and writing of this thesis.

To the teachers who have taught me during my years of study, who helped me to get to this point. From the physics professors in high school, those at the Pontifical University of Chile where I had the opportunity to do this double degree program and also here in Italy where I finish this process.

Finally, to my friends in Chile and in Italy with whom I have shared over the years. Those I have known for years and we have learned together, perhaps we are not in contact as often, but they are always present. The ones I met recently in Turin, with whom I shared almost every day during this process. To all of you, thank you very much.

Contents

1	Introduction	1
2	State of the art	4
2.1	Solar irradiance	4
2.1.1	The Sun and extra atmospheric irradiance	4
2.2	Solar cells	8
2.3	First generation: Crystalline Silicon technology	12
2.3.1	Manufacturing	12
2.3.2	Structure for crystalline silicon modules	14
2.4	Second and third generation photovoltaics	15
2.5	Main components of a PV system	16
2.6	Losses	20
2.7	Evolution of the prices	21
2.8	Performance indicators	22
3	Geographic context of the installation site	24
3.1	Chile and Santiago	24
3.2	Climate and temperatures	25
3.3	Radiation levels	26
3.4	Air pollution	27
3.5	Electric infrastructure	28
3.6	Installation site	29
4	Demand Profile	30
4.1	Office Buildings	30
4.2	Software used	31
4.3	Reference buildings	32
4.3.1	Large Office reference building	34
5	Design and sizing	39
5.1	Selection of Photovoltaic modules	39
5.1.1	Modules for Sun shield configuration	39
5.1.2	Modules for Curtain wall configuration	43
5.1.3	Modules for Roof installation	47
5.1.4	Inverters	50
5.2	Configuration of the PV plant in the building	53
5.2.1	Sun shield and roof connections	53
5.2.2	Curtain wall connection	55
6	Simulation	59
6.1	The solar irradiance data	59
6.2	From solar irradiance to electric power	60
6.3	Loading the demand profile	66
6.4	Estimation of the power for the next 25 years	67
6.5	Performance indicators	67
6.6	Simulation of the demand in EnergyPlus - OpenStudio	69
6.6.1	Modifications to the original model	69

6.6.2	Adding the PV panels to the model	72
7	Economic analysis	81
7.1	Tariffs	81
7.1.1	BT2 tariff	82
7.1.2	Net billing and PMGD	83
7.2	Net Present Value	84
7.2.1	Initial costs	85
7.2.2	Fixed costs	87
7.2.3	Initial savings	88
7.2.4	Gains	89
7.2.5	NPV, Payback Time and IRR	91
7.2.6	Levelized Cost Of Energy, LCOE	94
7.3	Sensitivity analysis	96
8	Results and discussion	100
9	Bibliography	102
10	Annexes	107
A1	Datasheet for the TSM-DD05A.08 (II) PV module	107
A2	Datasheet for Sunny Tripower 60-US inverter	109
A3	Generic office types from the Energy consumption guide	113
A4	Consumption of each load over a year, for all the cases modelled	113
A5	Annual yield and Performance Ratio for the 25 years	114
A6	Comparison of the power generated and consumed each month, for Sun shield	115
A7	Comparison of the power generated and consumed each month, for Curtain wall configuration	117
A8	Matlab code	119

List of Figures

1	Solar and black-body spectrum at 5,777 K [6]	5
2	Illustration of the Zenith, Azimuth and Solar altitude angles	6
3	Equivalent circuit of a solar cell [8]	10
4	Example of mono and poly crystalline cells in commercial PV modules	13
5	Basic configuration of a three phase inverter	18
6	Diagram of the layout circuit of a solar system with accumulation [16]	19
7	Solar PV total installed power and annual additions [20, 21]	21
8	Evolution of PV technology prices between January 2016 and March 2018 [22]	22
9	Chile in South America	24
10	Temperatures and rainfall levels in Santiago [28]	25
11	Sunny and cloudy days in Santiago [28]	26
12	Average daily GHI for each month in Santiago [30]	27
13	Daily sunlight hours in Santiago [31]	27
14	Installed capacity by technology [33]	28
15	Load profiles for: (a) weekday, (b) Saturday, (c) Sunday, (d) holiday [35]	31

16	Illustration of the Building in consideration [36]	35
17	Thermal zones in the building considered [36]	36
18	Examples of the schedules used in the simulation of the building	38
19	Top 10 PV module suppliers of 2017 according to PV Tech.org [43]	40
20	I-V and P-V curves of the 305 <i>Wp</i> module [10]	41
21	Linear performance warranty provided by Trina solar [10]	41
22	Possible configurations to install the PV modules as Sun shield	42
23	I-V curve of the NS6QL-2080 model [48]	46
24	View of one floor with the PV curtain wall installed on the north facade	47
25	Representation of the relevant angles for the analysis	48
26	Sun chart for the location of the building	49
27	Example of connection of the inverters provided in the datasheet [52]	52
28	Series and parallel connections for the Sun shield configuration	55
29	Series an parallel connections on the windows of Curtain wall configuration	56
30	Series an parallel connections on the walls of Curtain wall configuration	57
31	Series an parallel connections on the roof of Curtain wall configuration	58
32	Calculation logic of the main values in the “Sun shield” configuration	61
33	Definition of the angles for each configuration	62
34	Calculation logic of angle θ , between beam and module plane normal	62
35	Calculation logic of the power produced by the PV system	63
36	Generation in each hour over the year	64
37	Power generated during a day in summer and in winter in Santiago	65
38	Total energy generated each month in the 1 st and 25 th years	67
39	Pie charts of the distribution of the electricity between the loads	71
40	Monthly energy consumption by category, generated in OpenStudio	72
41	Geometric representation of the incident sun beams on the PV configuration	74
42	Representation of the building with the Sun shield and roof installations	75
43	Generation and demand during a month in summer and in winter	76
43	Generation and demand during a month in summer and in winter	77
44	Generation, base and effective demands during a week in summer and in winter	78
44	Generation, base and effective demands during a week in summer and in winter	79
45	Capital Expenditures for a commercial BAPV system [68]	86
46	Percentages for each initial cost for building facades [69]	86
47	Calculation logic of the yearly gains related to power self-consumed or injected	90
48	Calculation logic of the yearly gains related to load reduction and peak shaving	90
49	Positive and negative cash flows in the period evaluated	94
50	Levelized Cost of Energy for various technologies [74]	96
51	Tornado plots for the eight variables sensitized	97
51	Tornado plots for the eight variables sensitized	98
52	Complete datasheet for PV module in Sun shield configuration [10]	107
52	Complete datasheet for PV module in Sun shield configuration [10]	108
53	Complete datasheet for Inverter [52]	109
53	Complete datasheet for Inverter [52]	110
53	Complete datasheet for Inverter [52]	111
53	Complete datasheet for Inverter [52]	112

54	Four categories in which office buildings are classified in the study [58] . . .	113
55	Generation and demand during each month with Sun shield configuration .	116
56	Generation and demand during each month with Curtain wall configuration	118

List of Tables

1	Reference Building energy model input categories [37]	33
2	Inputs for the Form of the building [36]	35
3	Relevant dimensions of the north facade	35
4	Proportion of the surface utilized by each zone	36
5	Values defined for Large Office [38] (rounded to 3 rd decimal)	37
6	Exterior equipment power	37
7	Parameters of selected PV module [10, 44]	41
8	Main values for modules with long side to the wall	42
9	Main specifications sent to EnergyGlass	44
10	Main specifications provided by EnergyGlass [47]	44
11	UGI structure provided by EnergyGlass [47]	45
12	Parameters of bifacial solar cell [48]	45
13	Main values for the Curtain wall installation	46
14	Estimation of the distribution of the cells for one floor	47
15	Relevant values for the Roof installation	50
16	Top 10 inverter suppliers (2016 - 2017) according to Energy Hub [51] . . .	51
17	Main technical specifications of Sunny Tripower 60-US [52, 53]	52
18	Main parameters for the inverters	53
19	MPP voltages in extreme temperatures and number of modules per string .	54
20	Series and parallel connection of the modules for the Sun shield configuration	54
21	MPP voltages in extreme temperatures and number of 8-cell columns per string	56
22	MPP voltages in extreme temperatures and number of 7-cell columns per string	57
23	Series and parallel connections of the modules for the Curtain wall config- uration	58
24	Main technical parameters	60
25	Differences in the years and first and final hours	66
26	Performance indicators for the Sun shield and the Curtain wall, 1 st year . .	68
27	Performance indicators if the roof installation is not considered	69
28	Changes in the exterior equipment power	69
29	Change in the loads associated to the basement	70
30	Reduction in the energy consumed by the building	70
31	Comparison of consumption in base case and both configurations, in (kWh)	73
32	Results for the simulation of the shading at noon, December 21 st	74
33	Comparison between original, base and final cases	75
34	Tariffs applied for the monthly electric bill of the building	83
35	Prices estimation in Net billing and PMGD models	84
36	Discount rate, inflation and conversion from euro to dollar	85
37	Initial costs, in USD	87
38	Yearly additional cleaning costs for each category	88
39	Initial savings for each configuration, in USD	88

40	Gains for the first year of operation, in <i>USD</i>	91
41	Main economical parameter for the projects	92
42	Cash flows, NPV and sum of the non-discounted cash flows, in <i>USD</i>	93
43	LCOE values for each configuration	95
44	Total consumption by load in <i>kWh</i>	113
45	Energy generated, Annual yield and Performance Ration for the 25 years simulated	114

1 Introduction

The electric generation industry has been in constant growth for decades. New advancements in technology develop devices that need this resource to work and are currently present in almost every sector of society. Health, construction, education, transportation, public and private spaces, all need a supply of electricity to carry out their functions, this has led to a worldwide increase in the demand for this type of energy. According to the International Energy Agency (IEA) [1], between 1971 and 2015 the world electricity generation rose from 6,131 *TWh* to 24,255 *TWh*, almost four times greater in less than 45 years.

To supply this demand, for many years the most used source to produce electricity has been fossil fuels, in 1971 they covered 75.1% of the total generation and in 2015 has only been reduced to 66,3% [1]. The most common are coal, oil and natural gas, and are utilized as fuel in thermal plants for their lower costs. The problem is that when they are burnt there are negative externalities for the environment, particulate matter expelled and gases like Sulphur dioxide (SO_2) or Nitrogen oxides (NO_x) pollute the air and greenhouse gases like Carbon dioxide (CO_2) contribute to global warming [2].

An alternative to help solve these problems is the use of renewable energy sources, they use the power provided by natural means to produce electricity. Some examples are photovoltaic, that uses the light of the Sun, solar thermal generation takes advantage of the heat emitted by the Sun, wind turbines harness the kinetic energy of air flows, hydraulic generation captures the potential energy in the water and geothermal uses the heat available underground.

They have the advantage of almost not emitting pollutants and not requiring the constant purchase of external supplies, but there are also disadvantages. Since they use natural resources, they are dependent on their availability and are not always able to provide a non-interrupted electric supply and usually need storage systems. Solar generation has a daily cycle, producing during the day but not at night and it is also affected by the weather, wind is highly variable at all moments. In the case of hydraulic power, it is possible to supply non-interrupted service, but if a longer time-period is considered problems can appear because consecutive years of dry weather can make this resource unavailable for the production of electricity.

Solar photovoltaic and wind technologies are categorized as Non Conventional Renewable Energies (NCRE) and since they are less mature than established methods like thermal generation using fossil fuels, they present higher prices and lower efficiencies. This along with the previously mentioned disadvantages has slowed their adoption but

the advancements done in the last decades have allowed that in recent years they have become competitive and their use has increased considerably.

Another factor that is useful is the change that has been taking place in electric markets, where consumers are no longer passive agents that receive the power that has been generated and transmitted through the network [3], they are active using small generation units to help manage the load they represent to the system and even inject energy to the grid. The use of small generation units along the distribution system, near the consumption, is called Distributed Generation.

It provides many advantages, some of them are the encouragement of the use of renewable sources, for example, with the possibility of using PV modules on the rooftops on the houses to use the available power from the Sun in each household, this also reduces the use of fossil fuels. Additionally, it decreases the losses due to the transmission of the electricity through the network, from the big generation plants to the distribution systems that deliver it to the users and can be helpful in cases of congestion of certain nodes in the network. There is a possibility of higher efficiency by using co-generation [3].

On the other hand, there are throwbacks and challenges to the implementation of the distributed generation. Since the electric systems are designed for passive consumers with the power flowing from generation centers to the users, the distribution lines may need to be reinforced so they can support the inclusion of these generation units. It is possible to cause the inversion of the energy flows [3] with the distribution, providing power to the transmission instead of the other way around, this affects the stability of the system. The use of sources like wind or the Sun makes the power produced very variable which affects the system's reliability, this can be solved with the use of energy storage.

In the context of using photovoltaic technology in distributed generation, the concept of Building Integrated Photovoltaics (BIPV) appears. It involves the use of PV modules to replace conventional building components in its envelope, like windows, walls or rooftops [4] and consider them in the designing of the building, for example PV Skylights or PV Curtain wall [5]. There is a variation that involves the heat recovery for a better thermal efficiency of the building and is called BIPV/T. When the photovoltaic components are not replacing any part of the building but only added as a new structure [5], it is called Building Attached Photovoltaics (BAPV).

The requirements of BIPV have led to the use of diverse PV technologies. There are roofing tiles developed with crystalline silicon, the need for flexible or semi-transparent modules has increased the use of thin film technology, with developments mainly in amorphous silicon [4]. Even with these advances there are still various restrictions for their use on buildings. There is (1) an aesthetical factor that make the people developing the

building reluctant to consider this type of implementation, (2) technical limitations can make unfeasible the adoption, for example big shading structures in the vicinity, (3) the economical factor due to the still high costs associated and (4) a social aspect related to the lack of awareness by the population that can derive in them considering it a developing technology that still needs major improvements.

Considering this information, the objective of this thesis project is to design and simulate two possible configurations of a photovoltaic system for an office building in Santiago, Chile in order to compare the results to determine which is the best option with the current technologies and prices. The first is a BAPV configuration consisting of Sun shields installed on the windows of the north facade. The second is a BIPV system in the form of a Curtain wall that replaces the windows of the same facade with semi-transparent PV modules and on the parts that correspond to walls use opaque versions. To harness as much as possible of the solar resource it will be considered in both cases a PV installation using the roof area.

The scope of the project is to:

- Estimate the load profile that characterizes a typical office building.
- Size the photovoltaic power and determine the inclination and connection of the modules that can be installed in the north facade and the roof in each configuration.
- Size the inverters to perform the power conversion from DC to AC.
- Simulate the energy effects on the building of the addition of the modules.
- Perform a 25-year simulation of the produced energy by each system using the radiation data from the corresponding location.
- Perform an economic analysis of each installation to evaluate the feasibility.

This document is divided into eight sections, this being the first, in section 2 a revision of the state of art of photovoltaic technology is presented, in section 3 a general context of the place of installation is provided, in section 4 the model chosen to represent the office building is described, in section 5 the design of the systems is explained considering the PV modules and inverters in each case, section 6 describes how the simulation was performed and in section 7 the economic analysis is explained.

2 State of the art

In order to understand the current context related to the systems that will be sized and simulated, it is necessary to understand the resource used for energy generation and the available technology that can be employed. In this chapter it will be discussed the solar irradiance, then how solar cells work, the status of the different technologies available and those that demonstrate new possibilities for the future. The components required for the implementation of the system will be explained, the different forms of connection, the associated losses, the evolution of the module prices and finally the most common performance indicators.

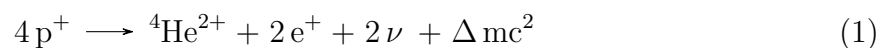
2.1 Solar irradiance

The first approach to begin discussing photovoltaic power generation is to describe the resource used. In this case it is the radiation emitted from the Sun that then reaches the plane of the modules that turn it into electric power. There are many factors that interfere in the way to the surface of the PV panels, the effect of the atmosphere, the location and orientation of the installation, the tilt of the modules change the amount of power that is received in comparison to the one that arrives to the Earth.

2.1.1 The Sun and extra atmospheric irradiance

The source of the solar irradiance, as the name indicates, is the Sun. It is the star at the center of the Solar system, with a diameter of $1.39 \cdot 10^9 m$ at a distance of approximately $1.5 \cdot 10^{11} m$ from the Earth [6]. Its mass is about $2 \cdot 10^{30} kg$ of which 75% is hydrogen, 23% helium and 2% other elements. It is formed by different layers, at the center is the core and on the external side the photosphere represents the visible surface, with a temperature of about $5,800 K$ and it is followed by chromosphere and the corona.

The energy is produced in the core by nuclear fusion reactions, the main process occurs when the hydrogen is turned into helium and energy in the denominated proton-proton chain. Other reactions involving more complex elements also occur but given the composition of the Sun the proton-proton chain is the predominant. A reaction equation [6] that summarizes the processes in the main nuclear reaction is:



Four protons from the hydrogen nuclei are fused and the result is helium, two positrons, two neutrinos and energy produced by a difference in mass. It is estimated [6] that every second the mass of the Sun decreases $4.3 \cdot 10^9 kg$, according to equation $E = m \cdot c^2$ this is

equivalent to an emission of $3.85 \cdot 10^{26} \text{ W}$. This power is transmitted through the layers where it is absorbed, re-emitted and then passed into space.

As it was indicated, the surface of the Sun in the photosphere is at a temperature of about $5,800 \text{ K}$ but since the radiation that emits is the result of modifications that occur in the passing through the different layers, the resulting spectrum can be approximated as the thermal radiation of a black-body at $5,777 \text{ K}$ [6], the biggest part is the range of visible light as shown in the image developed by Enermena [6].

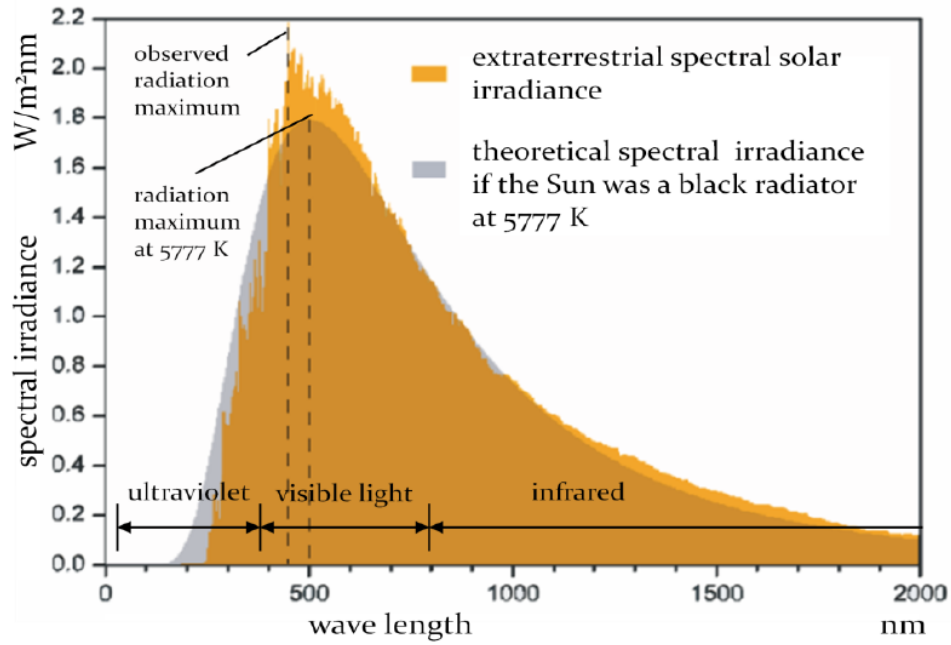


Figure 1: Solar and black-body spectrum at $5,777 \text{ K}$ [6]

Since the radiation is emitted uniformly in every direction with the Sun at the center, when it arrives to the Earth there is less power per unit area, in this case called irradiance. Its value is calculated considering the power divided by the area of a sphere with the radius equal to the Sun-Earth distance and results in the so-called solar constant: $G_{sc} \approx 1,367 \text{ W/m}^2$ that represents the radiant power per square meter incident normally on the planet's atmosphere.

Another concept used in relation to radiation is the irradiation. While irradiance refers to the power per unit of area (W/m^2) the irradiation is used for the energy that arrives on a surface over a period of time (J/m^2). Given that the calculations will be performed with hourly data the irradiance will be expressed in (W/m^2) and the irradiation in (Wh/m^2) and consequently will have the same values.

When working with the Sun beams that arrive on a specific location on the planet, it is important to define the relevant angles that are used. The main ones are the Latitude, the zenith, azimuth, solar altitude and the angle of incidence on a tilted plane.

- Latitude (Φ): Is the angle formed between the line from the location to the center of the Earth and the equator plane, positive towards north.
- Zenith angle (θ_z): The angle between the Earth-Sun line and a vertical line at the location, which intersects the sky vault at a point called zenith.
- Azimuth angle (γ_s): The angle formed by the south direction and the projection on the Sun beam on the horizontal plane, considered positive towards west.
- Solar altitude (α_s): The angle between horizon and the Sun-Earth line.
- Angle of incidence on tilted plane (θ): Angle between the Sun ray and the line normal to the surface of the plane.

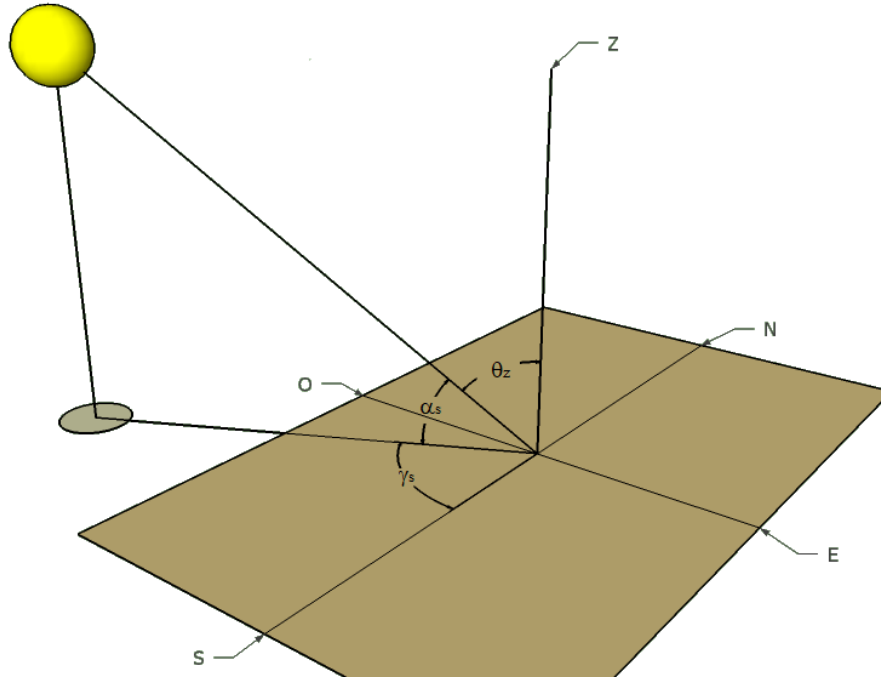


Figure 2: Illustration of the Zenith, Azimuth and Solar altitude angles

Once the solar radiation enters the atmosphere of the planet it begins to undergo attenuating effects like absorption, scattering and reflection. If the solar radiation goes through a longer optical path in the atmosphere the attenuation will be stronger. The shortest path occurs when the sun is at the zenith, product of this the concept of Air mass (AM) is defined as the ratio between the actual length of the beam's path through atmosphere and the path if the Sun were at zenith, it is approximated as:

$$AM \approx \frac{1}{\cos(\theta_z)} \quad (2)$$

The two predominant attenuation phenomena are the absorption and the scattering. The first means that the particles present in the air take the energy from the photons and the latter refers to the change in the direction of the path of some photons due to the interaction with some molecules in the atmosphere.

Atmospheric absorption is a discrete effect, that affects specific sections of the spectrum. It is produced mainly by three-atoms molecules like ozone that take UV bands and carbon dioxide (CO_2) and water (H_2O) that absorb IR bands, as a result there is almost complete extinction of the UV-C, UV-B and IR radiation above $2.5 \mu\text{m}$.

The atmospheric scattering is continuous and occurs mainly due to the N_2 and O_2 molecules present in the air, since it depends on λ^{-4} [6]. This effect produces diffuse radiation and, since shorter wavelengths are more scattered, it has higher frequency. This is also the reason of the blue color of the sky.

Due to these effects approximately 52% of the radiation that enters the atmosphere reaches the surface [6]. Not all is direct radiation there is also a component due to diffuse radiation generated by the scattering effect and another caused by the reflection on the ground. The concept of Global irradiance is defined as the sum of these three components, direct, diffuse and reflected irradiance.

Direct radiation refers to the beams that come in a straight line from the Sun, diffuse radiation does not have a unique direction since it comes from the scattering produced by the particles in the air but arrives from the upper side of the horizontal plane. The reflected radiation depends on the reflectivity of the ground, the albedo (ρ), and comes from under the horizontal plane.

Most common measurements of solar radiation refer to the global irradiance in a horizontal surface (GHI), in this case the only components are the Direct normal irradiance (DNI) on a horizontal surface and the Diffuse horizontal irradiance ($DIFF_h$) because the reflected beams do not reach the surface of the modules. It is calculated as:

$$GHI = DNI \cdot \cos(\theta_z) + DIFF_{hor} \quad (3)$$

Solar modules are usually mounted with a tilt angle (β) to harness the solar resource more efficiently, in this case the global irradiance normal to the plane of the panels (G_t) has to be considered. The direct normal irradiance has to be projected using the incidence angle (θ) instead of the azimuth angle (θ_z) as in the horizontal case, and the diffuse and reflected components must be also added, but are pondered by view factors as shown in equation (4).

$$G_t = DNI \cdot \cos(\theta) + DIF_h \cdot \frac{1}{2} \cdot (1 + \cos(\beta)) + GHI \cdot \rho \cdot \frac{1}{2} \cdot (1 - \cos(\beta)) \quad (4)$$

To make measurements at ground level of the solar resource available in a specific location there are two basic types of instruments that are commonly used, the pyrheliometer and the pyranometer [7]. The first is usually utilized to measure direct radiation, while the second can measure also the diffuse component and can be also used for the reflected component.

The pyrheliometer is also called actinometer, it measures the solar radiation at normal incidence that comes from the Sun and from a small portion of the sky around it. It has an aperture of only 5.7° and uses a tracking mechanism to follow the movement of the Sun during the day.

Pyranometers are also called solarimeters and can measure the global horizontal radiation, which means the direct plus the diffuse, if they are placed on a horizontal surface. Two modifications can be made to estimate specific components, if a shadow band is used to block the beams coming from the Sun, this instrument can be used to compute only the diffuse radiation, two pyranometers can be put together upside-down in order to also measure the ground reflected radiation, in this case it is called an Albedometer.

2.2 Solar cells

The solar irradiance that arrives has to be converted into electric power in order to be used for different applications. This action is performed by the photovoltaic cells present in the modules that are mounted in a solar installation, in the case considered they are placed on a building facade and roof. The cells are made using semiconductors which have the property of allowing the energy of the incident photons to be transferred to the valence electrons of the material.

One of the main characteristics of semiconductors is the energy gap between the valence band and the conduction band. The valence band is where the most external electrons of the atoms are, these are the electrons that perform the chemical bonding. The conduction band involves a higher energy level and allows their motion in crystalline structures. The gap is the energy required to pass from the valence to conduction band, if it is too big the material is considered an insulator, if it is too small, a conductor.

When an electron jumps from the valence band to the conduction band, a positive electric charge appears on the first due to the lack of the electron, this is called a “hole”

and it can be filled when an electron comes back from the conduction band. To take advantage of this effect, the creation of electron-hole pairs, the materials are treated with trivalent atoms to increase the number of acceptors, forming a P-type crystal, and others are treated with pentavalent atoms increase the number of electrons or donors, forming a N-type crystal.

The P-type crystal is created adjacent to the N-type to make a PN junction, there a depletion zone is formed in which the electron-hole pairs recombine leaving the end of the N-type side positively charged and the end of the P-type side negatively charged. This creates an electric field in the depletion zone. In open circuit conditions two currents are created, one due to the electrons that diffuse from the N side to the P side and it is called Diffusion current (I_{diff}) and the other is produced by the electric field in the junction (I_{drift}), under dark conditions they are equal, and the resulting current is null.

If a forward bias is applied to the PN junction, the depletion zone becomes smaller and more electrons pass from the N side to the P side, therefore I_{diff} increases, when a reverse bias is applied the depletion zone gets bigger and there is only a small current due to the thermal generation of electron-hole pairs in the direction of I_{drift} . It behaves as a rectifier.

The exposure of the junction to the light makes it necessary to take the photoelectric effect into account. This phenomenon occurs when the photons from the incident radiation pass part of their energy to electrons in the valence band and that allows them to jump into the conduction band. The energy of the photon must be above a critical value to be able to create the electron-hole pair, it is dependent on its wavelength (λ) according to equation (5), “h” is the Plank constant and “c” the speed of light.

$$E_{ph} = h \cdot \frac{c}{\lambda} \quad (5)$$

In solar cells the N-type crystal is thinner and exposed to the Sun, so the radiation can reach the junction. The photovoltaic effect makes the depletion zone smaller because electrons absorb the energy from the photons and jump back to the N side, this also implies that holes pass to the P side and thus a current is generated (I_{ph}). It makes the electric field decrease and I_{diff} increases. In open circuit conditions they are counterbalanced, and results is zero current and an equilibrium voltage, V_{oc} .

When a load is connected, the output current and voltage are non-linear and follow an I-V characteristic curve normally in the first quadrant. It is usually defined by four parameters, the first two are the values of current and voltage at which the solar cell works at full performance, for the last two occur when the power is 0.

- V_{mpp} : The voltage at the maximum power point.
- I_{mpp} : The current at the maximum power point.
- V_{oc} : The voltage in open circuit, due to the balance between I_{diff} and I_{ph} .
- I_{sc} : The current in short circuit, I_{ph} goes through the short circuit and not through the PN junction.

The maximum power point is obtained making the derivative of the power, as $P = I \cdot V$, equal to zero [9]. The resulting value can be understood as the load required to have the cell working in its most efficient state:

$$-\frac{dI}{dV} = \frac{I}{V} = \frac{1}{R_{load}} \quad (6)$$

These parameters are also used to define the fill factor, which allows to compare the performance of different cells.

$$FF = \frac{V_{Pmax}}{V_{oc}} \frac{I_{Pmax}}{I_{sc}} \quad (7)$$

To represent the behavior of a solar cell an equivalent circuit is used. A current source represents the production of I_{ph} proportional to the irradiance, a diode in anti-parallel symbolizes the PN junction where I_{diff} passes, a resistance in parallel (R_{sh}) represents leakage paths that occur in edge insulation and finally a resistor in series (R_s) considers the resistance of the semiconductor, the electrodes and the contacts [8].

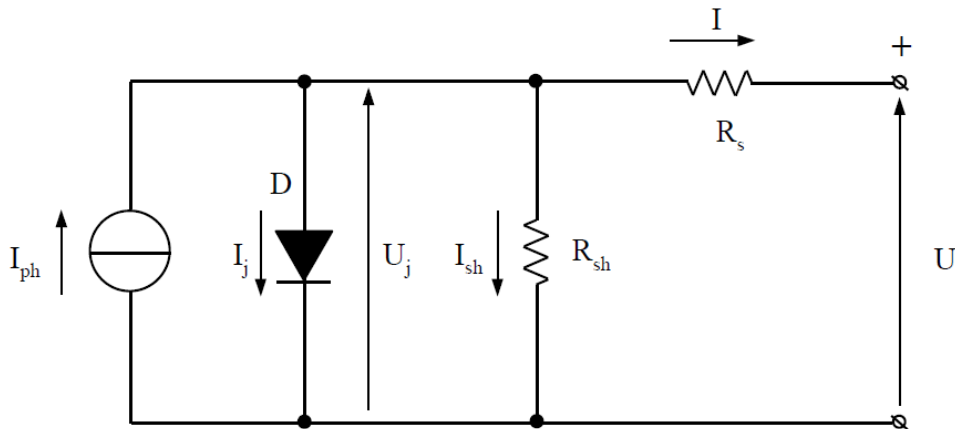


Figure 3: Equivalent circuit of a solar cell [8]

The equations that define the variables present in the circuit are described. The photo-generated current (8) depends on a constant from the material, G is the irradiance and

A is the receiving area.

$$I_{ph} = k_{mat} \cdot G \cdot A \quad (8)$$

The junction current is the difference between I_{diff} and I_{drift} , “q” is the charge of an electron, “m” is the quality factor of the junction, “k” is the Boltzmann’s constant and “T” is the temperature expressed in Kelvin.

$$I_j = I_0 \cdot \left(e^{\frac{qU_j}{mkT}} - 1 \right) \quad (9)$$

The output current I and voltage U (following the nomenclature of figure 3) result from a balance of the other variables, including the effects of the shunt and series resistances:

$$I = I_{ph} - I_j - \frac{U_j}{R_{sh}} \quad (10)$$

$$U = U_j - R_s \cdot I \quad (11)$$

The normal operation of a silicon based solar cell is in the first quadrant of the I-V plane, with both variables positive. If the current or the voltage becomes negative it passes to the fourth and the second quadrant, respectively, in both cases there is a thermal limit due to the increase of the cell temperature that should be avoided so no damage is done to the cell. In the second quadrant there is also the limit of the breakdown voltage that causes a sudden increase in the current and can cause the failure of the cell.

The irradiance and temperature on the cell can change its I-V characteristic. Irradiance has an effect mainly on the current, with changes in I_{sc} and I_{mpp} approximately proportional to the level of irradiation, the voltage instead has minor variations. On the other hand, an increase in temperature has a bigger effect on V_{oc} and V_{mpp} , decreasing due to the rise in the drift current, while I_{sc} gets bigger and I_{mpp} smaller.

The total maximum power has a behavior with temperature similar to the V_{mpp} because the change of current due to thermal effects is negligible at MPP [8]. For practical applications these changes are modelled using thermal coefficients α for current, β for voltage and γ for power. It is approximated that I_{sc} depends only on the irradiance and V_{oc} only on the temperature.

There are losses in the conversion from irradiance to electric power. As previously indicated the photons need a sufficient level of energy to make an electron pass the energy gap, lower frequency radiation will not have an effect on the cells. Also, higher energy

frequencies even from the visible and ultraviolet spectrum have an excess over the gap of the material and is lost as well.

Part of the photons from the radiation are reflected by the surface of the modules that contain the cells and others are blocked by the frontal electrodes. There are losses due to the recombination of electron-hole pairs in the PN junction, and as shown in the equivalent circuit, from the resistance of the electrodes and the leakage paths on the edge insulation.

Different technologies are utilized to create solar cells. The most traditional and widely used in the present are known as First generation photovoltaics, they use crystalline silicon, present a higher efficiency than others and have proven durability with modules from the decade of 1970 still working [4], a disadvantage is the high price associated.

A second generation has been developed with the aim of using less material in the manufacturing, a thinner layer, but trying to maintain the efficiency. A third generation is starting to develop with the intention of using the thin film fabrication methods but reaching a lower price per Wp while using nontoxic materials that present less limitations to acquire [4].

2.3 First generation: Crystalline Silicon technology

The first generation in photovoltaics is mainly composed of mono-crystalline and polycrystalline silicon technology. These are single junction solar cells formed from silicon wafers and are connected in series, usually of 60 or 72 cells, to form a module. The construction requires a highly purified silicon to ensure a better performance, but this kind of process also results in higher prices.

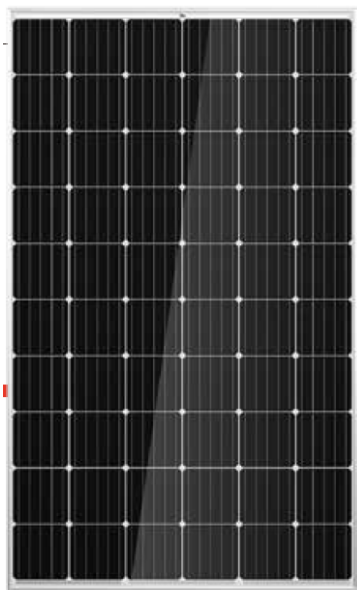
2.3.1 Manufacturing

The manufacturing process first requires to get metallurgical grade silicon, with a purity between 98% and 99%, the process is performed at around 2,000 °C to pass from SiO₂ to Si and CO that later becomes CO₂ with a low emission rate. This material is used in the steel and aluminum industry. To be used in the electronics and photovoltaic industry an impurity concentration between 10⁻⁷ and 10⁻⁸ is required so a second step is performed.

In this second step three sub-stages can be differentiated, in the first the material is reduced to powder and a hydrochloric gas is used in a “fluidized bed” reactor to get trichlorosilane (SiHCl₃) and hydrogen, the second step uses fractional distillation to separate the SiHCl₃ from the hydrogen. The last sub-step involves melting the high purity silicon at around 1,300°C to create the ingots that later are cut to get the solar cells.

Ingots are created differently for mono-crystalline and poly-crystalline, in the first case a rod-shaped “seed” is inserted in the melted silicon and then is slowly pulled while rotating to create a homogeneous, cylindrical-shaped crystal, it is performed in an inert ambient to avoid adding impurities. In the second case a rectangular shaped mold is used to contain the melted material, a controlled cooling is performed, and crystals are formed vertically aligned to the surface. The special conditions required to create the ingots of mono-crystalline silicon imply a high cost, on the other hand with poly-crystalline it is cheaper, but the resulting performance is lower.

Once the ingots are formed, they are cut into slices with square form. With mono-crystalline the cylinder ingot creates circular wafers and more material has to be removed to have a shape closer to a square, this leads to the characteristic shape with the corners cut. For poly-crystalline the ingot is directly cut into square wafers, which means less waste of material. The difference is illustrated in figure 4, 4a shows a m-Si module and the spaces left by the missing corners are noticeable while in 4b a p-Si is shown and all the cells are fully square shaped.



(a) Mono-crystalline module [10]



(b) Poly-crystalline module [11]

Figure 4: Example of mono and poly crystalline cells in commercial PV modules

The ingots had previously been doped with acceptors (boron) to make P-type wafers. After they have been cut they are chemically cleaned in a process called etching, then the upper side is doped with donors (phosphorus) to create a small N-type layer. After that an anti-reflection layer is applied to reduce losses. The last step is the production of the electrodes in each side, on the front an Al-Ag alloy is used to create the fingers and bus bars, on the back an Al plate is connected.

2.3.2 Structure for crystalline silicon modules

The cells are arranged into modules where they can be connected in series or in parallel to produce a specific output when the panel is exposed to the Sun. The structure of the module provides physical support to the cells and also protection from the environmental conditions. They usually present similar structures with the following components, from front to back:

- Front glass: with a thickness between 3 and 4 *mm* it must present high transparency to allow the radiation beams to reach the cells with minimal losses. Provides protection from agents like snow, hail and dust.
- Solar cells encapsulated in Ethylene Vinyl Acetate (EVA), a hot melted adhesive that provides waterproofing, protects from humidity.
- Back-sheet made of glass or plastic like tedlar to provide support for physical stresses caused, for example, by wind.
- Frame, usually aluminum to keep the components in place.
- A junction box that contains by-pass diodes and plug-in connectors to be able to associate different modules in series or parallel and also connect to the inverters.

Before the cells are encapsulated in the EVA material, ribbons are connected to each bus bar. This is done to be able to connect the cells between each other, the ribbons are put in contact with the back of the other cells to make the required connections.

There are some variations to the standard design of these cells, developed to overcome the physical limitations on the efficiency to achieve higher values, which would lead to more economically attractive PV systems. One of the modifications results in the Passive Emitter and Rear Cell (PERC) technology, introduced in 1989 and commercialized since 2012 reaches an efficiency above 22% [12]. It is obtained by reducing the recombination losses in the emitter and in the rear side, this is done applying a passivation layer using SiO_2/SiNx or AlOx/SiNx and then the connection is made only by line, segmented or even point contacts.

Another type is the bifacial solar cells, they work producing power using the irradiance received on both sides, not only the front. The back side is no longer opaque and allows to harness the diffuse and reflected radiation, the absence of the rear Al plate also has the benefit of a lower heat absorption rate which means that the cells can operate at a lower temperature and results in a higher power output per square meter. There is no global agreement on how to model the combination of both factors in the increase of the cell efficiency. In the manufacturing process the P type wafer receives a p^+ printed layer

on the front and an n^+ layer to serve as a back-surface field, then the anti-reflection layer is applied followed by screen printed metallic contacts [13].

2.4 Second and third generation photovoltaics

Currently, first generation PV cells dominate the market providing high efficiency and proven durability, but there are other technologies being developed. Second generation photovoltaics refers mainly to technologies that use amorphous silicon (a-Si), Cadmium telluride/cadmium sulphide (CdTe/CdS) or Copper indium gallium diselenide (CIGS). They are present in the market at similar or lower prices than traditional cells [14] but currently can achieve lower efficiencies, some reaching 14.7% [4].

Also known as thin film technologies, they are manufactured in a simpler process that does not require to form the wafers, which implies lower costs and less waste of material. In this case they are deposited on low cost substrates like glass, polymers or metal foils in thin films of about $1 - 10 \mu m$, it is possible because they can perform a more efficient absorption of the solar spectrum [4]. The effects of economies of scale are not yet at the level present in crystalline silicon, so it is expected that in the future there will be improvements in performance and reductions in the costs [14].

This technology also provides the advantage of being able to build flexible modules when a substrate with these characteristics is used. On the other hand, there are some throwbacks apart from the lower performance in comparison to crystalline silicon, there is also a higher rate of degradation by the exposure to the Sun, especially in a-Si, and the materials required for the production of CdTe/CdS and CIGS are scarce [4], which is a factor that increases the costs.

The third generation deals with this last problem by using abundant and non-toxic materials to make the thin film cells, while trying to maintain a high efficiency [4]. In this case the development is mainly in investigation phases, some of the technologies in this category include Copper zinc tin sulphide (CZTS), Dye-sensitized solar cells (DSSC), Organic (OPV), Perovskite, Polymer and Quantum dot cells.

CZTS has reached an efficiency of 12.0% in laboratory and it is considered similar to CIGS but using abundant and non-toxic elements [4] a problem to be solved is that can present defects called cation disorder that reduce the V_{oc} [15], DSSCs are made with economic materials, are semi-flexible and semi-transparent and are expected to have commercial applications by 2020 [4], they have achieved cell efficiencies of 11.9% but there is still work to do with long-term stability under light and thermal response [15].

Organic and polymer cells use small molecules or large with repeated structural units (polymers) to absorb light. Perovskite cells usually are made with a hybrid organic-

inorganic lead [15] and have showed a big increase in performance in a short time with 3.8% in 2009 and 21.0% in 2015 [4]. Quantum dot cells use nanocrystals called quantum dots to harvest light and the band gaps can be tuned in a wide range changing the size of the dots which allows to also use IR radiation [4].

These technologies show great potential for higher performance at lower costs using available resources and simpler manufacturing processes. Although they are mostly in research levels of development, there is potential for big scale production with properties like transparency or flexibility and reduced costs.

2.5 Main components of a PV system

A complete photovoltaic system requires other components besides the solar modules to be able to use the power that is generated. These additional components are usually called Balance of System and can include a DC/DC converter to perform the Maximum Power Point Tracking (MPPT), a DC/AC converter because it is necessary to convert the DC power that comes as an output of the configuration of PV panels to AC so it can be utilized, an storage system to collect the energy and use it at the moments when it is needed, and other safety and monitoring devices to control the correct operation.

Depending on the objective of the system they can operate in two different configurations. If the power will be consumed completely in the place where it is generated, then there is no connection to an external electric network and the system is classified as “Stand Alone”, it usually requires the use of storage of energy to utilize equipment that needs electricity in moments when the solar resource is not available or too low, like at night or cloudy days. The other category is “Grid Connected”, as the name says the photovoltaic system is connected to the electric network and can consume when there is low production and can act as generator and inject power at moments of low consumption.

The following is a description of the main components of a photovoltaic system.

- Photovoltaic array: The solar modules that receive the solar irradiance and use it to produce electric power. Depending on the technology used, each module can provide a peak power between 10 Wp and 350 Wp approximately. To achieve higher voltages and currents they are connected in series making “strings” of modules and also in parallel.

The specifications for each module are provided considering specific conditions in which the results can be replicated. The electrical data like the peak power, MPP current and voltage, the V_{oc} and I_{sc} are specified under Standard Test Conditions

(STC), this means an irradiance of 1000 W/m^2 , a cell temperature of 25°C and an air mass of 1.5.

Another relevant parameter is the Normal Operating Cell Temperature (NOCT), that is the equilibrium temperature reached by the cells in the modules when the irradiance is 800 W/m^2 , the ambient temperature is 20°C and the wind speed is 1 m/s . Typical values for NOCT are in the range of 40°C to 50°C .

- Maximum power point tracker (MPPT): The solar radiation that reaches the modules changes constantly during the day, either by the movement of the Sun in the sky or by the interference of other factors like clouds or shading obstacles. The changes in the temperature of the cell also cause variations on the output power. This leads to the need to constantly track the point in which the panels are producing the maximum power.

A DC/DC converter is used, and it is controlled by an algorithm that performs the MPP tracking. The most commonly used is the Perturb and Observe (P&O), it performs and increase or decrease of the voltage and checks the behavior of the power, if it increases the same action is performed, if it decreases then the opposite. Other algorithms used are Constant Voltage, that is less accurate, and Incremental Conductance, more accurate since there is no problem with local maximums but requires too much computational processing.

On stand-alone systems it is usually done in the charge regulator for the battery and on Grid connected a chopper is usually used with has typical configurations like Buck for a converter that reduces the voltage, Boost to increase the voltage or Buck-Boost to be able to perform both actions.

- DC/AC converter: An inverter is used to pass from DC power to AC that can be utilized by the different devices of the facility or to inject to the electrical network. Depending on the amount of power that the system can generate it is possible to use a single-phase inverter or a three-phase one. Some converters also provide the possibility to change the power factor to be provided to the grid.

A typical configuration for the DC/AC converters is the H-bridge, with two legs for single-phase applications and three leg variation for three-phase uses. The main components are the transistors that have to be controlled to be able to generate a sinusoidal waveform. This is usually done with the Pulse Width Modulation (PWM) technique that compares a high frequency triangular waveform, named the carrier, with the sinusoidal waveform, the modulating, that has the desired frequency of the

output. The modulation index is the parameter controlled and is calculated as the division on the amplitudes of the modulating and the carrier.

The resulting PWM signal is used to control the ON/OFF state of the transistors in the H bridge, in the same leg the negated signal is used for the other transistor, so they are not active at the same time, which would cause a short circuit. For the three-phase case three signals are used usually with a phase shift of 120° between them. Usually a filter is applied after the H-bridge to provide a sinusoidal waveform with a low THD. Figure 5 shows a basic schematic of a three phase inverter.

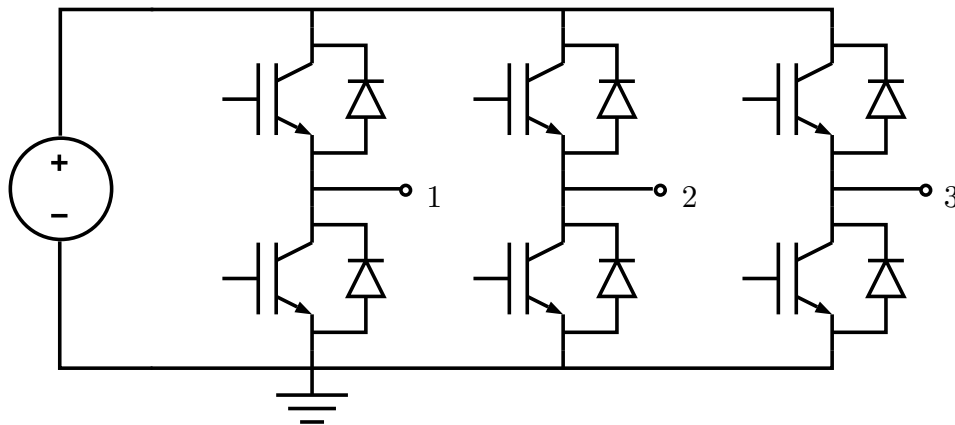


Figure 5: Basic configuration of a three phase inverter

- Storage unit: The power generated by a photovoltaic system is very variable during the day since it is dependent on factors like the weather, the hour or the season. By itself it cannot provide an uninterruptible service and a natural solution is the use of a storage device to accumulate the energy that is not used in the moment of production, so it is available later when needed. Batteries are normally used for this application [8], especially on stand-alone installations.

Batteries are electrochemical accumulators and can be based on different technologies, although the prices have been decreasing over the last years the cost they represent is still high. Lead acid is the most mature but presents problems with environmental impacts, another type that is gaining importance is the lithium-ion (Li-ion) for its good properties of energy density and efficiency [16] other battery technologies used are Sodium-sulphur (NaS), Nickel-cadmium (NiCd) and Nickel metal hydride (NiMH).

Some of the main specifications for electrochemical storage are:

- Energy density: The amount of energy that can be stored per unit of volume (Wh/l) or mass (Wh/kg).

- Nominal voltage: The voltage provided by the battery when a load is connected.
- Maximum input voltage and current: Highest values to charge the battery.
- Capacity: The charge (Ah) that can be provided in a period usually of 10 hours.
- Depth of Discharge (DOD): The percentage of charge that can be extracted from the full charged battery without causing any damage.
- Battery life: The number of charge-discharge cycles respecting the DOD limit.
- Self-discharge rate: The charge lost in stand-by mode over the full capacity.

For grid connected applications it is possible to avoid the cost associated to the acquisition of the storage system because at moments of lower generation the demand can be supplied by the electric network. Nevertheless, using an accumulation unit provides some benefits to both the consumer and the electric system. With an appropriate control system, it allows to perform demand side management like load shifting [16] or peak shaving by supporting local critical loads [18]. Benefits to the network include ramp and frequency response and reactive support [17] with big enough storage capacity.

The following image illustrates the main components of a grid connected photovoltaic system that includes a storage system.

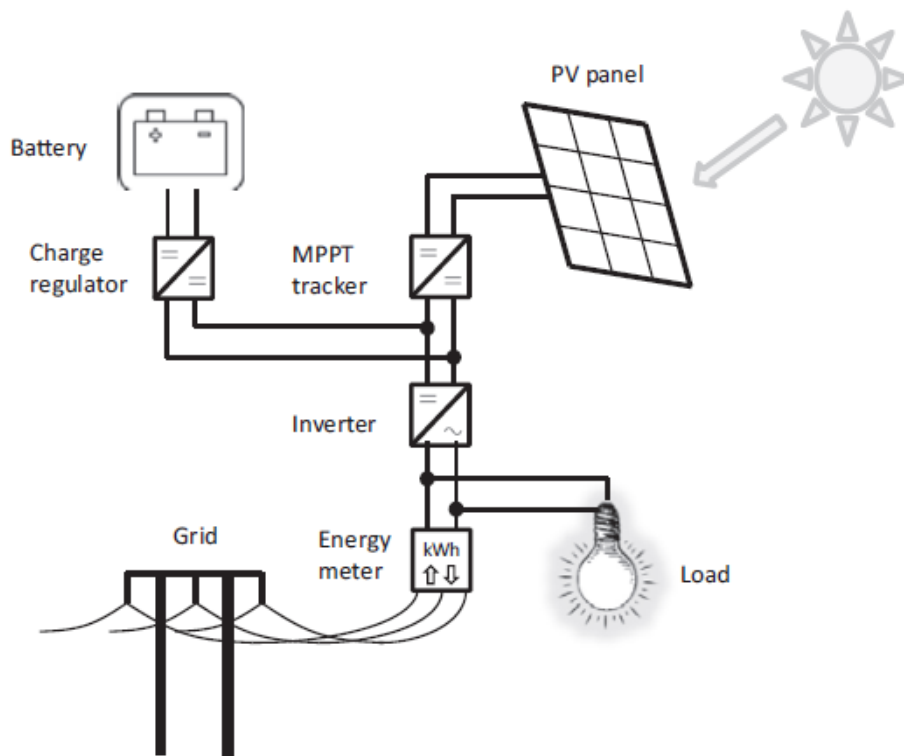


Figure 6: Diagram of the layout circuit of a solar system with accumulation [16]

2.6 Losses

Besides the losses inherent to the operation of photovoltaic cells, there are others that occur when the complete PV system is working. The modules do not produce the power indicated by the specifications every moment because those are obtained under laboratory conditions, the irradiance is not always 1000 W/m^2 as in STC, also the air mass differs from 1.5. There is reflection that occurs on the cover glass of the module and there is dust deposition that blocks part of the incident radiation.

There are also losses due to the real temperature of the cells, ambient temperature and the incident radiation from the Sun change the value from the reference of 25°C and that affects the output values. The wiring to connect the modules between themselves and to the other components, plus the use of diodes, fuses and other safety measures also reduces the final performance.

The use of the MPPT and the conversion from DC to AC performed by the inverter are not ideal, although the efficiencies of both processes are high, with typical values over 97% and 90% respectively, they add losses that reduce the final output.

Another source of losses is generated when cells are connected with each other. In order to achieve higher voltage and current levels to supply the demand of the loads, the solar cells are connected in series and in parallel. When cells are connected in series, in the ideal case all produce the same amount of current but in real applications there are some factors that induce changes between the outputs of similar cells and cause mismatches in their I-V curves.

Manufacturing defects or shadows cast by external objects are the main causes and results in a decrease of the total generated power to values much lower than what the output would be if the defected cell is not connected ($P_{mismatch}^{max} \ll P_{Ns-1}^{max}$) [8]. Also, when a higher current than the one that the defected cell can provide is required, that cell acts as a load with a reverse voltage. If a short circuit occurs between the terminals of the string, then the weak cell is under the biggest stress because the sum of all the other voltages is applied to it.

The solution to this problem is the use of bypass diodes connected in parallel to the cells to provide a path for the current and thus avoid the limitation imposed by the weaker cell. This is usually applied to groups of cells in the modules and in some applications when the shading patron is well known, bypass diodes can be also connected in parallel to modules to avoid that they act as a load when not under direct irradiance.

In the case of parallel connections, the currents are added and the voltages should be the same, if there are cells in one string that are damaged or shaded they will produce

a lower current than the others and the resulting voltage will be lower because there are fewer good cells. The lower voltage causes that part of the current of the system is absorbed by the damaged cell, which increases its temperature and can cause failure, the worst case is in open circuit because all the other currents pass through the shaded string in reverse direction.

To avoid this effect blocking diodes are connected in series in each string to stop the currents that would go through the cells in the opposite direction. The losses due to the mismatch of the I-V curves of the cells in PV systems is between 2% and 4% [8], instead the losses produced by shading will depend of the specific situation of the photovoltaic installation.

2.7 Evolution of the prices

One of the main factors that has limited the adoption of the photovoltaic technology in the past has been the high costs that are associated. New advances in the technology and the development of economies of scale has led to a reduction of the PV modules' prices in the last decade, which has driven the development of new photovoltaic projects around the world. According to Solar Power Europe [19] between 2000 and 2015 there was a 29% year-on-year increase of the installed PV power, from about 5 GW to 229 GW.

By 2017 the installed PV power in the world has reached 402 GW, with 98 GW being added between 2016 and 2017 [20]. In the last five years China has been increasing its installed power and last year was responsible for about 53 GW, more than half the increase of the period. The ten year evolution is shown in figure 7.

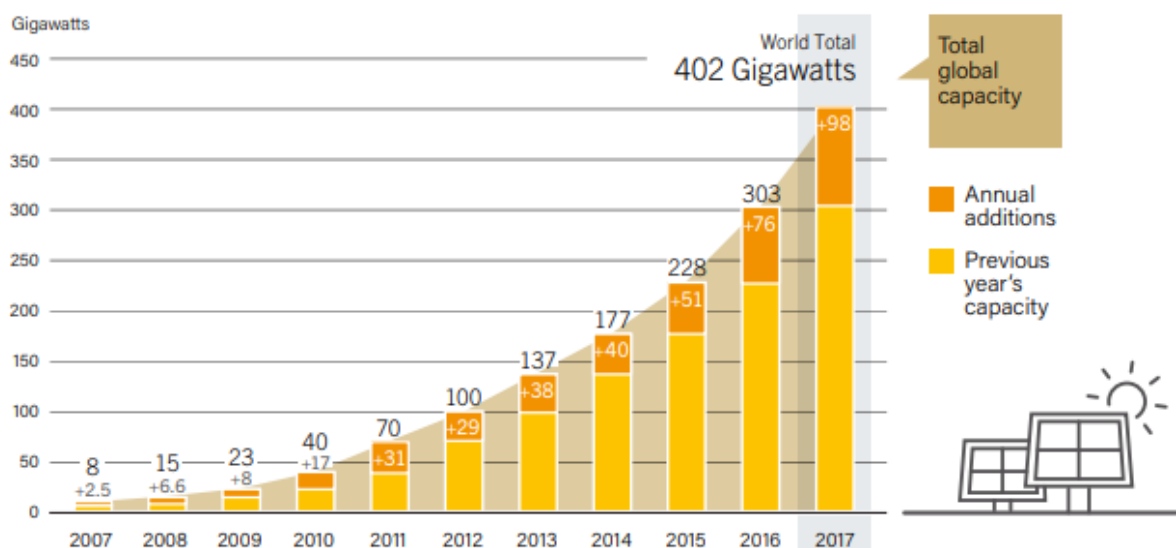


Figure 7: Solar PV total installed power and annual additions [20, 21]

This trend means a growing demand that has driven price reductions in the industry [20], and manufacturers are in constant need to develop advancements to increase the performance and efficiency. This has resulted in a decrease of the cost per peak Watt of the technology, figure 8 shows the changes in approximately two years. The prices of modules for large buyers decreased about 0.2 USD/Wp in the period considered, but the rate is lower during the last year, it reaches a value of 0.3 USD/Wp in March 2018. For small buyers they are a little more expensive and are closer to 0.4 USD/Wp in the same date.

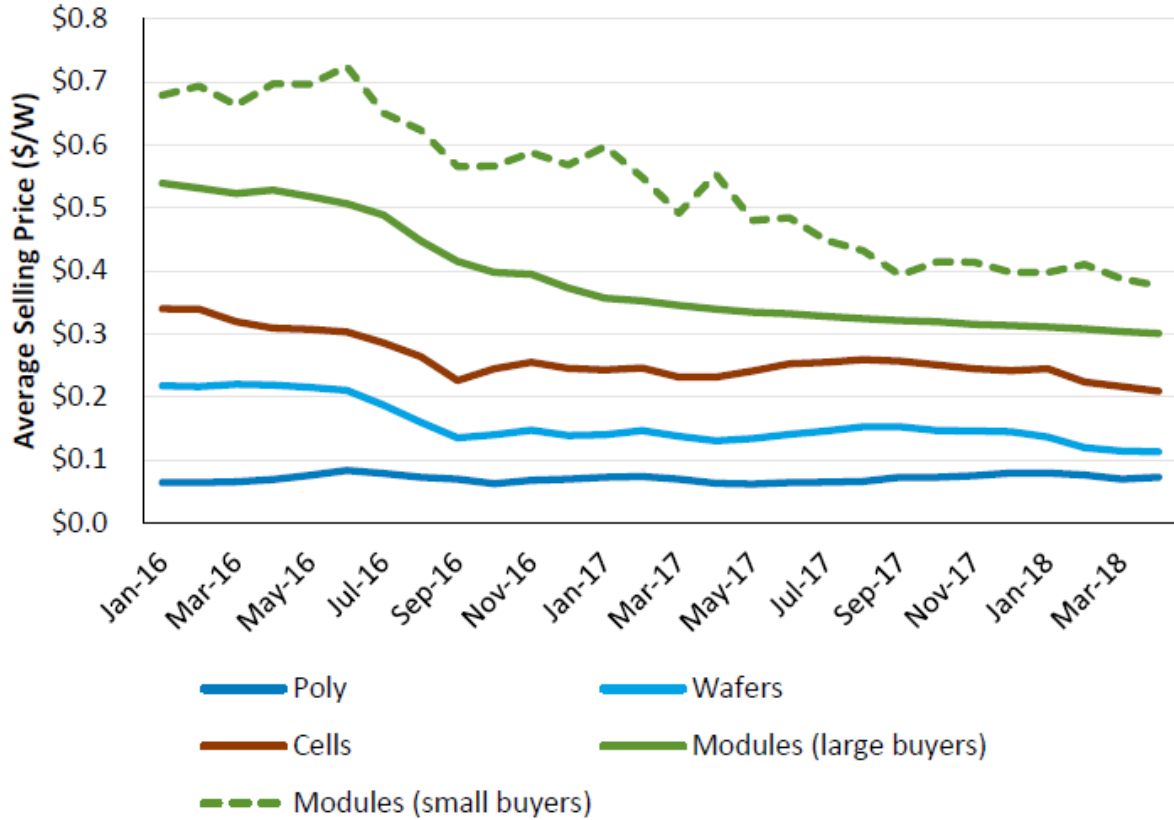


Figure 8: Evolution of PV technology prices between January 2016 and March 2018 [22]

2.8 Performance indicators

To assess the performance of a PV installation some indicators are usually utilized in order to compare systems with different rated power.

The Specific Yield (Y_f) represents the amount of energy that the system is able to generate for one kWp installed or, from a different point of view, the equivalent hours that the PV array has to work at the peak power to produce the same amount of energy [23]. It is calculated as the total generation (E_{tot}) over a year divided by the installed power of the system, as it is shown in equation 12. The resulting value depends on factors like the location of the installation, the orientation and tilt of the modules and parameters

like the thermal coefficient.

$$Y_f = \frac{E_{tot}}{P_{nom}} \quad \left[\frac{kWh}{kWp} \right] \quad (12)$$

The Reference Yield (Y_r) is used to assess the solar resource at the place of installation, it represents the equivalent hours during which the reference irradiance at STC (G_{STC}) is received by the modules and depends mainly on the factors related to weather, location and orientation [23]. It is calculated as the global radiation incident on the module plane in the period ($H_g \text{ kWh/m}^2$), divided by the reference irradiance, as the following equation:

$$Y_r = \frac{H_g}{G_{STC}} \quad \left[\frac{kWh \cdot m^{-2}}{kW \cdot m^{-2}} \right] \quad (13)$$

The Performance Ratio (PR) is the proportion of the real AC generation in relation to the expected production [24]. This is usually calculated as the specific yield over the reference yield and is useful to quantify the losses of the system in the conversion from DC power to the AC power that will be used later. It is represented in equation 14:

$$PR = \frac{Y_f}{Y_r} = \frac{E_{tot} \cdot G_{STC}}{H_g \cdot P_{nom}} \quad (14)$$

3 Geographic context of the installation site

3.1 Chile and Santiago

Chile is a country located in the southern hemisphere, in South America. It limits by the north with Peru, by the northeast with Bolivia and by the east with Argentina. The total area of the country corresponds to 756,102 square km [25] this value considers the continental territory and the land in Oceania but excludes the Antarctic territory. According to the National Institute of Statistics [26] the total estimated population to the year 2017 is 18.4 million inhabitants.

The map shown in figure 9 illustrates the location of Chile in South America and the limiting countries:



Figure 9: Chile in South America

Geographically, Chile is characterized by its longitudinal extension, it starts in the north at latitude $17^{\circ}30'S$ and reaches $56^{\circ}30'S$ in the south, covering about 4270 km long. This characteristic leads to the presence of a great variety of climates [26].

In general terms, the northern part of the country is characterized by dry, desert

climate, while the southern zone by a rainier climate with lower temperatures. The central zone presents Mediterranean climates and concentrates most of the country’s population. It is in this part where the capital, Santiago, is located.

Santiago de Chile is the capital of the country and the most populated city. It is located at coordinates 33°27’S 70°40’W and is at a height of 570 m above sea level. The total area is 641 square kilometers with an approximate population of 6.68 million people, which corresponds to about a third of the country’s total [25].

3.2 Climate and temperatures

The climate of Santiago corresponds to the Mediterranean type, with dry and warm summers, while in winter there is more rain and low temperatures. The Köppen Climate Classification indicates that it is of the ”dry-summer subtropical” type, of subtype “Csb”. According to Weatherbase [27], the average annual temperature in the city is 14.4 °C. The highest temperatures are in January (summer) with averages of 21.1 °C and the lowest in July (winter) with 8.3 °C.

The following graph, shown in figure 10, summarizes the main behaviors of the temperatures and also rainfall over a year. In this case, it presents the mean values of the daily maximum and minimum temperatures for each month. It is based on 30 years of hourly weather model simulations [28].

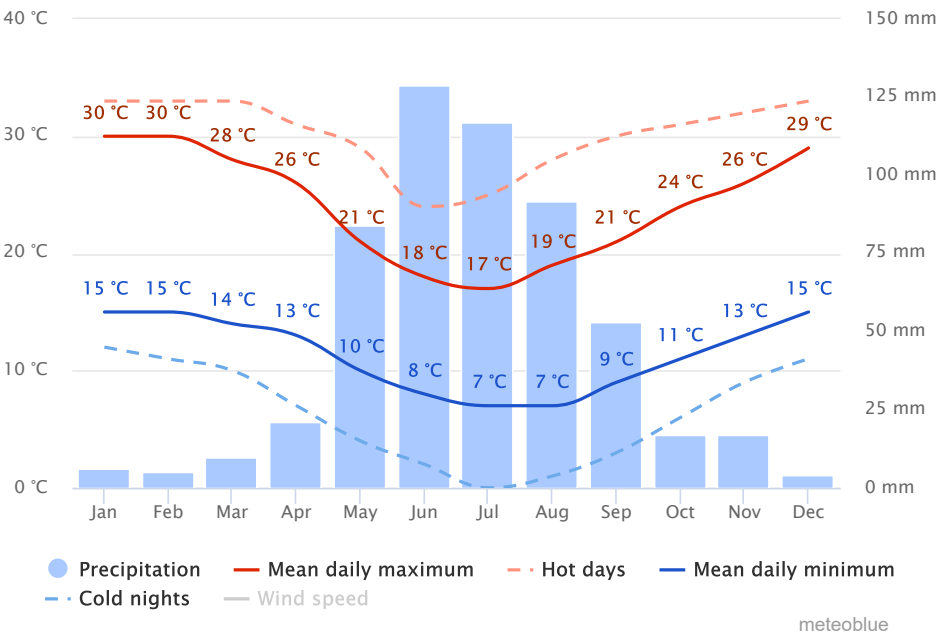


Figure 10: Temperatures and rainfall levels in Santiago [28]

Regarding the rains in the city, an average of 340.4 mm of water falls in a year. Of

the 76 days that it rains on average annually, most of this amount occurs in the winter months. In June, an average of 78.7 mm falls and it rains around 7 days of the month, while in January there are usually no rainfalls [27].

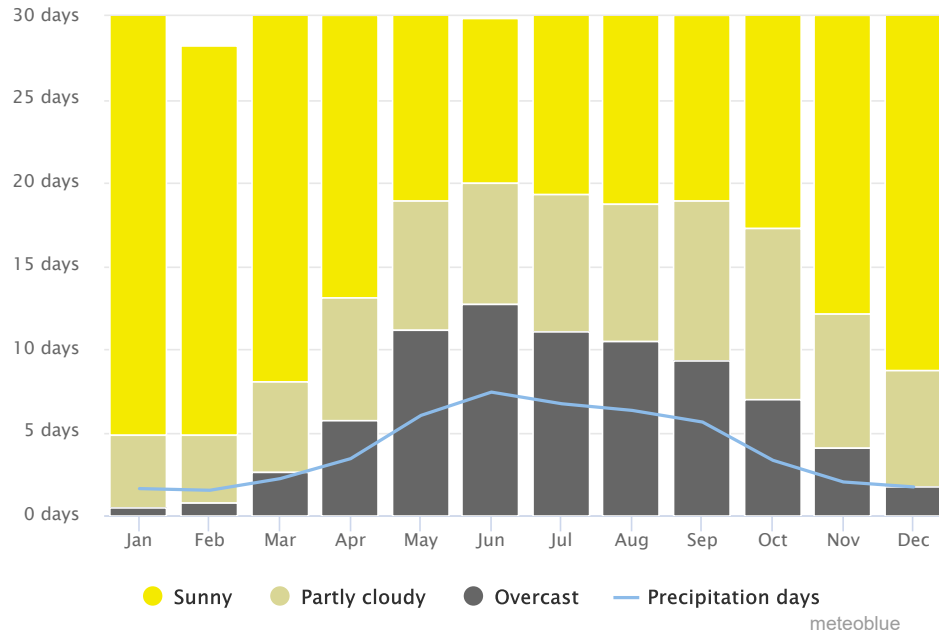


Figure 11: Sunny and cloudy days in Santiago [28]

The graph shown in figure 11 indicates the amount of sunny days, partly cloudy and cloudy in each month of the year. It is possible to observe how in the summer months it is possible to have around 25 sunny days in a month, while in winter this number is reduced to only 10. Sunny days are defined as days that have clouds less than 20% of the time, partly cloudy when the value is between 20% and 80% and overcast days when it is greater than 80% [28].

3.3 Radiation levels

Chile is known for the high levels of radiation in the north, it is possible to reach values greater than $8 \text{ kWh/m}^2/\text{day}$. These show a decrease when advancing in latitude to the south, however, in the Santiago area it is still possible to obtain significant levels of GHI [29], this fact makes the option of photovoltaic generation to produce electric power very attractive.

Figure 12 shows the behavior of the average daily radiation levels in the city throughout the year. In the summer months, daily values of more than 7 kWh/m^2 are reached, while in winter no more than 3 kWh/m^2 are exceeded daily. The total yearly value of GHI is

1,882.92 kWh/m^2 . The data are obtained from the Solar Explorer service delivered by the Ministry of Energy of Chile [30].

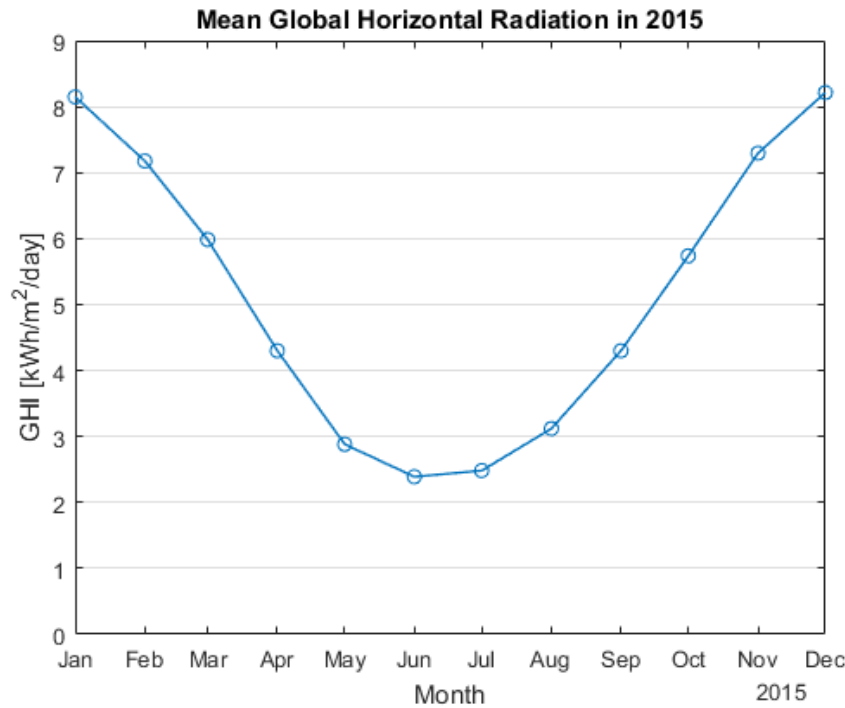


Figure 12: Average daily GHI for each month in Santiago [30]

It is important to consider the hours of sunlight that are received on the surface of the city throughout the year. Given the latitude in which it is located, it has as a result that during the summer months there are more than 13 hours of light, reaching almost 14 and a half hours in December, while in winter they are limited to around 10 hours, with the minimum in June [31]. Figure 13 illustrates the behavior for one year.

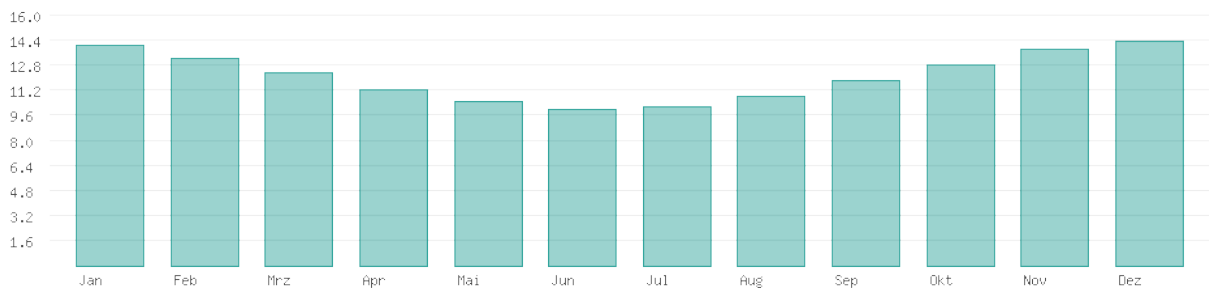


Figure 13: Daily sunlight hours in Santiago [31]

3.4 Air pollution

Another factor that should be considered about the city in which the installation of the photovoltaic system will be carried out is the level of contamination. Santiago is

considered one of the most polluted cities in South America, with concentrations of PM_{10} particles that reach $123.9 \mu g/m^3$ in winter periods and $80.3 \mu g/m^3$ in summer periods and $PM_{2.5}$ concentrations of 71.3 and 34.3 in the same periods [32].

It is noted that the sector of Santiago with the lowest levels of pollution corresponds to Las Condes with maximums of $45.46 \mu g/m^3$ of monthly average concentrations of $PM_{2.5}$ and $80.05 \mu g/m^3$ of PM_{10} in months of winter. As a comparison, these values reach levels of $80.92 \mu g/m^3$ and $140.6 \mu g/m^3$ in other areas of the city [34]. These data indicate that this area is a good choice as the site in which to place the installation to be simulated.

3.5 Electric infrastructure

Some general information about the electric system in Chile will be described. On March 2018 [33], the total installed capacity in the country is 22,517 MW which is divided in three systems, the main one is the National Electric System (SEN) which represents a capacity of 22,350 MW, a 99.3% of the total. It operates at a frequency of 50 Hz and a voltage of 220 V for the distribution system.

Considering a categorization by technology, in SEN the main source is thermal generation with approximately 57% of the capacity, conventional hydroelectricity represents 15% and Non Conventional Renewable Energy (NCRE) accounts for 28% [33]. Figure 14 illustrates this distribution, it can be noted that solar photovoltaic technologies cover an 8% of the total installed power.



Figure 14: Installed capacity by technology [33]

Regarding electric generation projects under construction, considering the ones that will begin operations between April 2018 and March 2014, about 36% of them are from NCRE with solar PV representing a 7% of the total. This goes according to the policy “Energía 2050” that defines as an objective that 70% of the total generation of the country is supplied by renewable energy sources by the year 2050.

3.6 Installation site

According to what it was just explained in 3.4, choosing the district of Las Condes as the place to locate the building in which the project will be carried out would take advantage of a lower level of pollution, considering the average values for the city in which it is located. This is an urbanized area in which there are buildings mainly for residential use, but also commercial. For example, the main offices of LATAM airlines, Motorola and other brands are situated in this area.

Given that the necessary infrastructure is available, the direct connection to the electric grid can be considered, which allows to plan the installation as a "Grid connected" type. In the same way it is possible to choose a place close to wide avenues and mostly surrounded by houses or buildings of small height, this decision is made to avoid losses due to the shading effect on the solar panels that will be installed on the facade.

Regarding the orientation of the building, the wider facades will be facing north and south to have access to a bigger area to install the modules. Since the city is located in the southern hemisphere it is important to notice that the system should be facing north, in this way it is ensured that the panels will receive the optimal amount of irradiation and subsequently will achieve a higher level of energy production.

4 Demand Profile

To carry out the complete simulation of the photovoltaic systems in consideration, it is necessary to take into account two fundamental aspects. On the one hand, we have the photovoltaic generation produced by the panels, which depends on the levels of radiation that reach them during the year. On the other hand, the demand profile of the building in which the installation will take place.

In this chapter the methodology followed to simulate the consumption of an office building in the city will be explained and the effect of the installation of the photovoltaic modules in each case, mainly over to the use of air conditioning in summer and heating in winter.

4.1 Office Buildings

Buildings can be classified into different categories according to their purpose, some of the most common examples are residential, commercial and industrial use. Each one presents a different type of typical electrical consumption. Office buildings are classified as commercial.

While residential consumption tends to present a greater energy demand in early morning hours and in late evenings, since during the day the inhabitants go to work or study, the industrial types are usually constant, using machinery that remains in operation.

In the case of commercial consumption, the demand profile is characterized by a greater use of electricity during the day and a reduction during the night. This behavior can be observed in image 15, it shows the normalized load profiles for office buildings [35]:

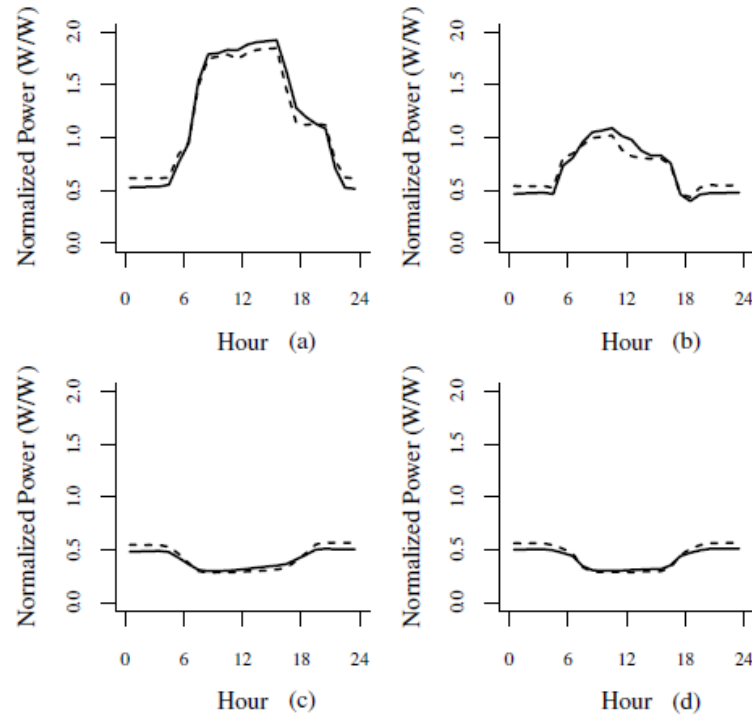


Figure 15: Load profiles for: (a) weekday, (b) Saturday, (c) Sunday, (d) holiday [35]

In addition to the feature described above, it is shown that there is a reduction in consumption on weekends and holidays. The effect is due to the lower flow of people on Saturdays and in the case of Sundays and public holidays, as the use of the facility is practically non-existent, there is a slight reduction in demand during the day as natural lighting allows the interior lights to be switched off.

This characteristic of commercial consumption profiles makes this type of building a good option for installing the photovoltaic system, since the hours of greatest demand coincide with the hours of sunlight. This effect allows the energy generated to be used directly on site, which implies positive effects such as greater efficiency due to lower transport losses and possible reduction of peak demand. This is why it was decided to simulate the photovoltaic system in an office building.

4.2 Software used

To simulate the behavior of the building in which the installation will be performed, three computer programs were used. The main one is the EnergyPlus software, in which the energy simulation of the construction is carried out. In addition, it was necessary to install the OpenStudio plug-in and SketchUp software which provide a graphical interface that makes easier the use and modification of the model on which one works.

Next, a brief explanation of each of the programs used is given:

- **EnergyPlus:** It is an open-source, console-based program developed by the U.S. Department of Energy's (DOE) Building Technologies Office (BTO) [39]. It is aimed to perform a whole building energy simulation, it considers a Surface Heat Balance manager, an Air Heat Balance Manager and a Building Systems Balance manager. These three parts are solved simultaneously to provide feedback from one to the other in order to obtain a physically realistic solution [40]. The program was used in its 8.9.0 version.
- **OpenStudio:** It is an open-source collection of software tools created to support the use of the programs EnergyPlus and Radiance. It includes the OpenStudio application, which consists of a graphical interface that allows to manually change variables related to the building envelope, loads, HVAC and schedules. A SketchUp plug-in is also included and provides an extension to the program to be able to create geometry that can be used in an EnergyPlus analysis [41]. Also, a Results Viewer and a Parametric Analysis Tool are provided.

The OpenStudio 2.5.1 Release was used in order to properly generate the Large Office reference building developed by DOE.

- **SketchUp:** A 3D modelling program, originally developed by Google and later acquired by Trimble. With the OpenStudio plug-in new options become available to create structures that can be later uploaded as an OpenStudio file and then simulated using EnergyPlus. The SketchUp Make 2017 version was used because it is the latest compatible with OpenStudio.

4.3 Reference buildings

Once the software required for the simulation is installed, the characteristics of the building must be modeled in order to represent a realistic consumption. It is necessary to have a clear idea about the relevant parameters should be considered, for example, the power that is used for lighting or air conditioning and the input variables to the model as climate information. A correct calibration of these factors is essential to obtain a model output with values that are appropriate for the case to be represented.

The Reference Building models developed by the U.S. Department of Energy (DOE) are used, which are created to be run in EnergyPlus. There are 16 types of buildings, each available in 17 locations in the United States [36], representing the different climatic zones of the country. They are specifically designed to perform energy simulations of buildings under typical operations for research purposes [37].

The model was developed taking into consideration previous projects like Advanced Energy Design Guides (ADEGs) and the Commercial Buildings Energy Consumption Sur-

vey (CBECS), the ASHRAE standards, and also the experience with real buildings. The necessary inputs were classified into four categories: program, form, fabric and equipment [37]. The building characteristics that each category represents are summarized in table 1:

Program	Form	Fabric	Equipment
Location	Number of floors	Exterior walls	Lighting
Total floor area	Aspect ratio	Roof	HVAC system types
Plug and process loads	Window fraction	Floors	Water heating equipment
Ventilation requirements	Window locations	Windows	Refrigeration
Occupancy	Shading	Interior partitions	Component efficiency
Space environmental conditions	Floor height	Internal mass	Control settings
Service hot water demand	Orientation	Infiltration	
Operating schedules			

Table 1: Reference Building energy model input categories [37]

Original geometry for the buildings was developed by the Lawrence Berkeley National Laboratory (LBNL) and describes the shape, the area and number of floors, and the distribution of thermal zones. The occupancy data were taken from ADEGs and ASHRAE Standard 62.1-2004, ventilation is based on the Standard 62-1999 and the schedules on ASHRAE 1989. The hot water services are provided by natural gas water heaters.

For the Plug and Process loads several assumptions were made to determine the intensity values and are assigned to the thermal zones according to the activity performed [37]. The elevators are included as a different zone and the number is established considering one every 4,181 m^2 of total area.

The Form category values are estimated based on opinion of experts and, as shown in table 2, describes mainly parameters related to the dimensions and shape of the building. The Fabric category focuses on the construction types and the thermal properties of the walls, roofs, floors, and windows [37]. The envelope of the construction mainly describes the insulation requirements for the roof and walls, the U-values for the different components are specified, which represent an overall coefficient of heat transfer and can have different values to adapt to the weather requirements of each climate zone considered. In this category the infiltration of air from the outside is also considered, it is adapted according to a function of wind speed and temperature difference across the envelope.

The last category is the building equipment, considers the: interior and exterior lighting, the heating, venting and air conditioning (HVAC), the service hot water (SWH) equipment, and commercial refrigeration systems. The lighting is defined using a Light Power Density (LPD) factor, the exterior lights consider parking lots, facade and exterior doors lights and are modeled to work on an astronomical clock, which means that the turn-on/turn-off times are synchronized with the sunrise and sunset hours [37].

The HVAC system is estimated according to the specifications of ASHRAE (2004) and the resulting values are focused on the modelling the performance and not on construction practices [37]. The equipment is then sized for each building type. The equipment also considers fans and cooling equipment efficiencies.

4.3.1 Large Office reference building

Now that there is a basic knowledge of the way in which the DEO of the USA developed the models of the Reference buildings, the specific description of the selected model will be made. This corresponds to the so-called Large Office and the 3B climate zone is chosen.

OpenStudio is used to download the measures that allow to enter the parameters of the chosen building into the simulation that will be performed. These measures come from the Building Component Library [42] and are intended to create the DOE Prototype Building for EnergyPlus specifying the options of (1) Building Type, (2) Template and (3) Climate zone.

As previously indicated, the type of building to be modeled is Large Office, the template refers to the ASHRAE standard to be assigned to the building and affects the loads, type of construction and mechanical systems, the 90.1-2013 is selected because it has more updated values, for example, for the schedules of the lights. For the climate zone, which represents the environment in which the building will be immersed during the simulation, the ASHRAE 169-2006-3B version is chosen.

Zone 3B is selected because it is the type of climate that resembles the one in Santiago. As indicated in section 3.2, the capital of Chile is classified as “Csb” by Köpper and one of the US cities in zone 3B is Los Angeles [37] and Köpper also classifies it as “Csb”. Once loaded in the OpenStudio interface, the weather files and design days corresponding to Santiago are downloaded from the EnergyPlus website [39].

Figure 16 represents the building being modelled in EnergyPlus, from the measure downloaded from BLC. In table 2 the main inputs from the Form category are summarized. It should be noticed that the model does not consider shading over the building during the day, but the shadows cast by elements of the geography of the location are already considered in the irradiation file, as it will be explained in section 6.1.

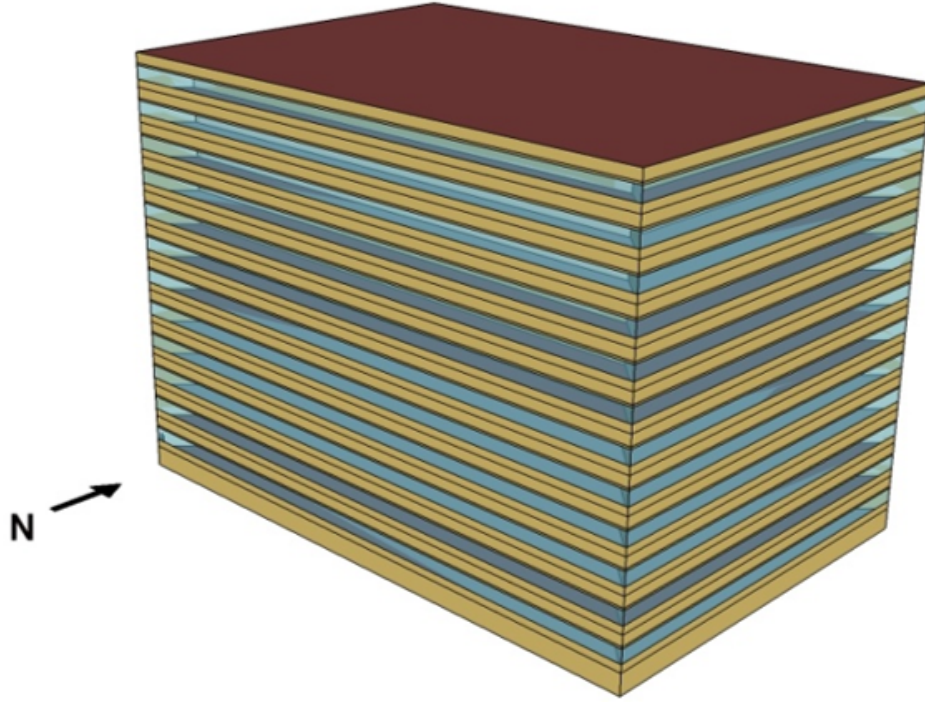


Figure 16: Illustration of the Building in consideration [36]

Input	Value
Floor dimensions	$73.15 \times 48.77 \text{ m}$
Number of floors	12 + 1 (basement)
Total area	$46,320.38 \text{ m}^2$
Aspect ratio	1.5
Window fraction	0.40 (above-grade walls)
Shading	0
Floor to floor height	3.96 m
Floor to ceiling height	2.74 m

Table 2: Inputs for the Form of the building [36]

With this information it is possible to calculate the total area of the north facade of the building. This will be used for the design of the system in Curtain wall configuration. In addition to the total value, it is useful to consider the surface that corresponds to the windows and the surface that corresponds to the walls, it is calculated using the window fraction, table 3 presents the results.

Window surface	$1,390.4 \text{ m}^2$
Wall surface	$2,085.7 \text{ m}^2$
Total surface	$3,476.1 \text{ m}^2$

Table 3: Relevant dimensions of the north facade

Each floor is divided into thermal zones, the same distribution is applied for the 12

floors, the basement presents its own configuration with a main area and a data center. The zones of the other floors are a central core, a perimeter section the goes approximately 4.72 m from the windows to the center and a small IT closet.

At first the model did not include the data center in the basement and de IT closets in the other floors, but these were added as part of an update performed by the Pacific Northwest National Laboratory (PNNL) to enhance all the previous models [38]. Figure 17 represents the distribution of the thermal zones in each floor and the basement in the prototype building.

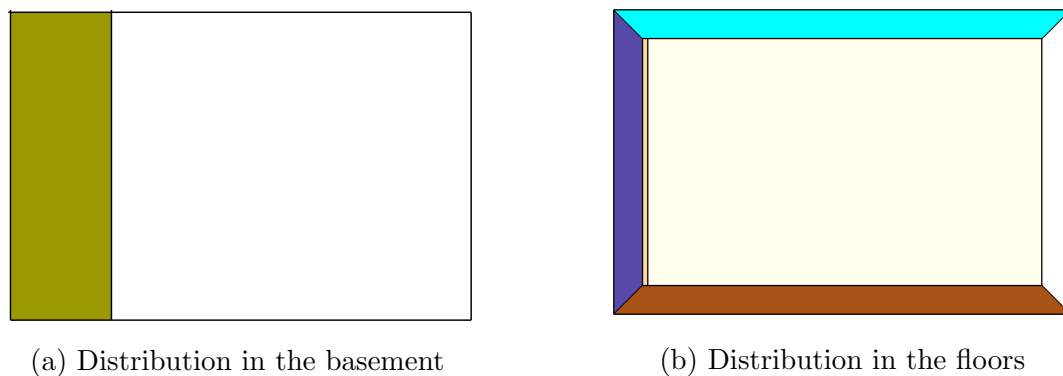


Figure 17: Thermal zones in the building considered [36]

To classify the type of use that is assigned to each room, four Space Types are defined: Data Center for the IT closet, Main Data Center for the one in the Basement, Whole-Building for the rest of the Basement and the Core and Perimeter zones in the other floors. The forth one is called Plenum and it is associated with the infiltration of air to the building and it is linked to the spaces between the different floors. Table 4 shows the percentages of the floor area that each thermal zone uses and the space type associated.

	Core	Perimeter	IT closet	Datacenter
Basement	72%	0%	0%	28%
Floors	70%	29%	1%	0%
Space type	WholeBuilding	WholeBuilding	Data Center	Main Data Center

Table 4: Proportion of the surface utilized by each zone

The electrical consumption of the building depends to a large extent on the equipment, plug and process loads. In the model this is simulated as a load expressed in (W/m^2) for each category and a different value is assigned depending on the Space type. The amount of people in each zone is also described, in this case in ($people/m^2$). Once the Large Office prototype building is uploaded to the OpenStudio interface the following values are defined:

Variable	Unit	WholeBuilding	Main Data Center	Data Center
People	p/m^2	0.054	-	-
Lights	W/m^2	8.826	8.826	8.826
Electric equipment	W/m^2	8.070	484.376	215.278

Table 5: Values defined for Large Office [38] (rounded to 3rd decimal)

The HVAC system uses natural gas for the heating and electricity for the cooling. Each thermal zone has an air loop associated with cooling and heating thermostat schedules. For the data centers the cooling activates for temperatures over 27°C and the heating under 18°C, while for the rest of the spaces the range goes between 21°C and 24°C.

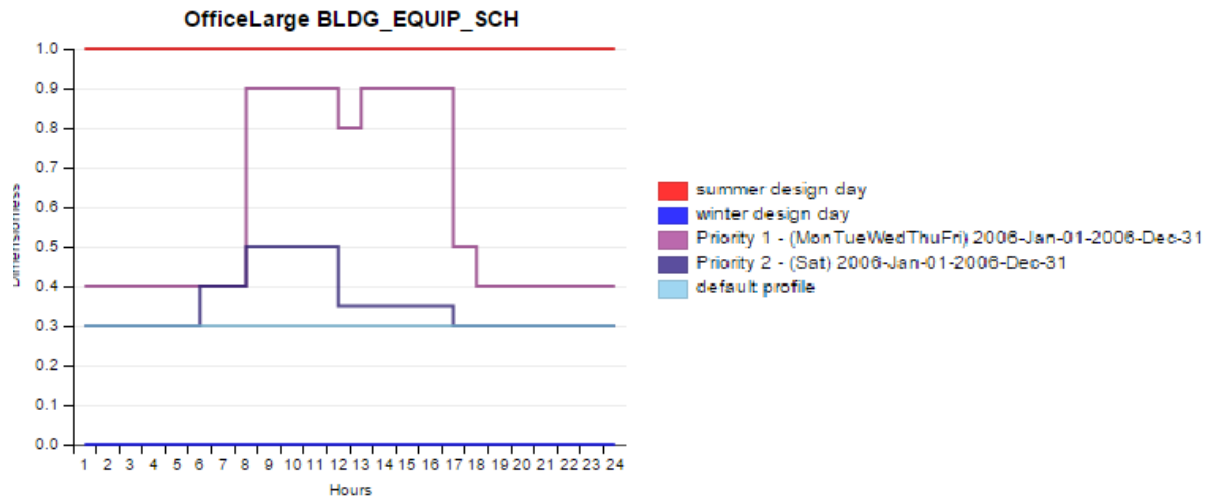
The external equipment is defined separately, it considers the elevators, the fans and the lights associated to each one, and the exterior lightning. In this case the factors are described using the peak power in Watts (W). Given the total area of the building, the model includes 12 elevators, each one of 20,370.33 W and 62.67 W from the lights and fans. The total values that the model uses are:

Load	Power [W]
Elevators	244,443.956
Lights and Fans	752
Non dimming lights	12,979.2
Sensing exterior lights	43,305.089

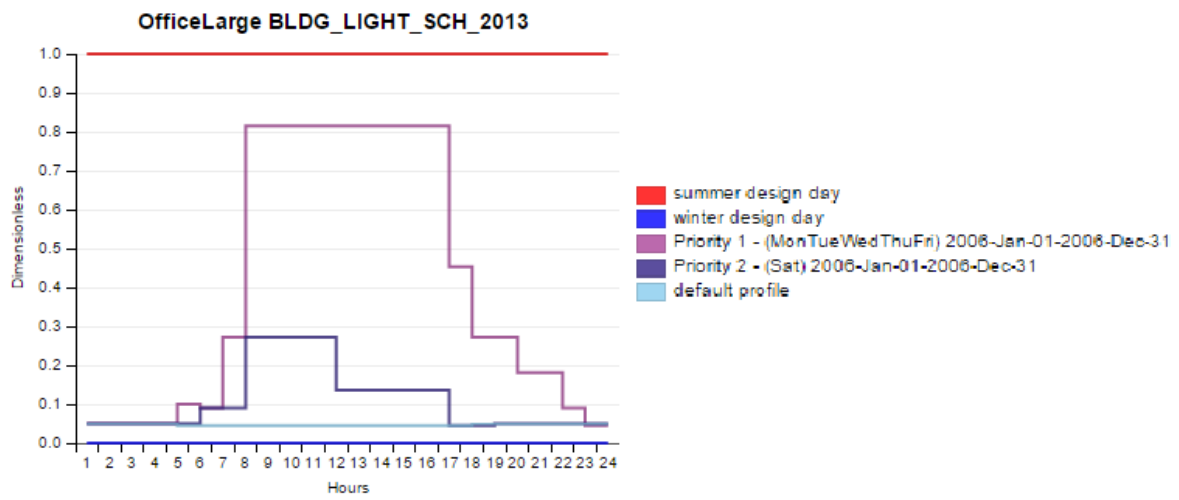
Table 6: Exterior equipment power

The final relevant part to consider from this model of a large office building, generated in OpenStudio using the measure from BCL [42], are the schedules. These are used to simulate the hourly operation of the equipment previously described, the temperatures used for the air conditioning and the heating, and also the behavior of the people during each hour. It takes in consideration differences between work days and weekends, summer and winter periods, but it is important to note that this representation does not contemplate vacation periods or national holidays.

As an example, the schedules for the elevators and for the lights are shown in figure 18. In both cases the usage is higher during the day and it is reduced considerably during the night, with different curves for weekdays, Saturdays and Sundays (called default), this way a normal operation is represented.



(a) Elevators schedule



(b) Lights schedule

Figure 18: Examples of the schedules used in the simulation of the building

5 Design and sizing

First of all, it is important to define the way in which the system being planned will run. It can be a “Stand alone” or “Grid connected” type, it is possible that there is the need to use a storage system or to operate without one. As explained in section 3.6 for the specific case of this installation, being located in a city and having easy access to the electric network, the “Grid connected” configuration is chosen.

Regarding the use of energy storage equipment, it implies an additional expense for the total cost of the project, so it is preferable not to have this element. Given the high consumption associated with the office building with which the simulation is being carried out, most of the time the generated energy will be consumed directly, so it would not be practical to have a system of accumulation.

5.1 Selection of Photovoltaic modules

Two different configurations will be considered for the photovoltaic installation on the building. The first is a Sun shield type, considered in the category of Building Attached Photovoltaics (BAPV), in it the modules are mounted on the windows of the north facade to block the sun that hits the interior of the offices and at the same time it collects the irradiation that hits the plane of the modules to generate electricity.

The second configuration is a Curtain wall type, considered in the category of Building Integrated Photovoltaics (BIPV), transparent modules replace the windows of that facade of the building and opaque ones are also installed covering the rest of the walls. In both cases the modules to be used must be selected to know their technical specifications, that will be used to estimate the energy production.

5.1.1 Modules for Sun shield configuration



To estimate the energy that will be produced by the photovoltaic installation with Sun shield configuration, it is necessary to select a solar panel model to know its specific characteristics. With its dimensions, it is possible to calculate the necessary number of modules that need to be purchased according to the space available on the facade of the building. The operating voltage, current and thermal coefficients are used to define a form of connection with the inverters.

The parameters of maximum power, thermal coefficient, NOCT and performance reduction over the years are used to estimate the production of electrical energy obtained from the radiation incident on the modules. It is also very important to know the price at which they are purchased, as this value influences in the profitability of the project.

Various suppliers of solar modules were investigated. Given that only the north facade of the office building is considered, there is a limited area and the objective is to supply a high consumption, as it is a 12-story building. Therefore, high efficiency is prioritized when choosing between the different options available in the market.

To ensure the quality of the selected products, the top 10 best solar module suppliers of the year 2017 are taken into consideration, according to PV Tech.org these are [43]:

Top-10 Module Suppliers in 2017

Ranking	Producer	
1	JinkoSolar	
2	Trina Solar	
3	Canadian Solar	
4	JA Solar	
5	Hanwha Q-CELLS	
6	GCL-SI	
7	LONGi Solar	
8	Risen Energy	
9	Shunfeng (incl. Suntech)	
10	Yingli Green	

© PV-Tech &
Solar Media Ltd, Jan. 2018



Figure 19: Top 10 PV module suppliers of 2017 according to PV Tech.org [43]

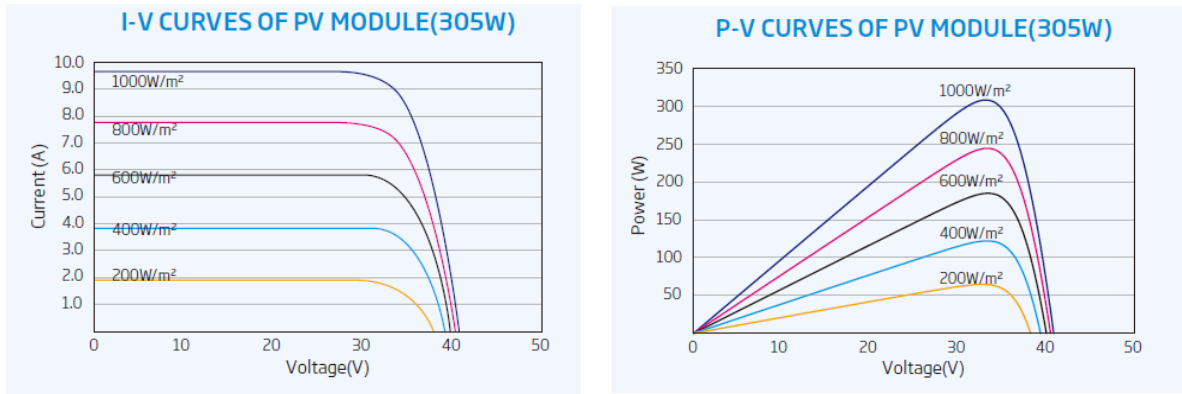
Priority is given to the modules that present the highest price-peak power (USD/W_p) ratio, which also have high efficiency. The company Trina Solar is chosen, with the model TSM-DD05A.08 (II). It is a 60-cell mono-crystalline silicon module, considered to have an excellent performance in low light conditions. For the price a 10% discount over the original value is considered, as it is offered by some providers for purchases over 100 panels. Its main technical features are the following [10], the currents and voltages at Standard Test Conditions (STC) are presented and then table 7 summarizes the others:

- $V_{MPP} = 32.6 \text{ V}$
- $V_{OC} = 39.8 \text{ V}$
- $I_{MPP} = 9.19 \text{ A}$
- $I_{SC} = 9.77 \text{ A}$

Parameter	Value	Unit
Peak Power Watts (P_{max})	300	Wp
NOCT	44	$^{\circ}C$
Thermal coeff. of P_{max} (γ_P)	-0.39	$\%/^{\circ}C$
Thermal coeff. of V_{OC} (β_V)	-0.29	$\%/^{\circ}C$
Thermal coeff. of I_{SC} (α_I)	0.05	$\%/^{\circ}C$
Efficiency (η)	18.3	$\%$
Dimensions	$1650 \times 992 \times 35$	mm
Price	168.01	USD
Price over power	0.56	USD/kWp

Table 7: Parameters of selected PV module [10, 44]

The I-V and P-V curves are provided in the datasheet [10] for the module of 305 Wp , since the values are similar, the images are shown in figure 20:



(a) I-V curves of module

(b) P-V curves of module

Figure 20: I-V and P-V curves of the 305 Wp module [10]

The linear performance warranty is specified for 25 years for this module, it is shown in figure 21:

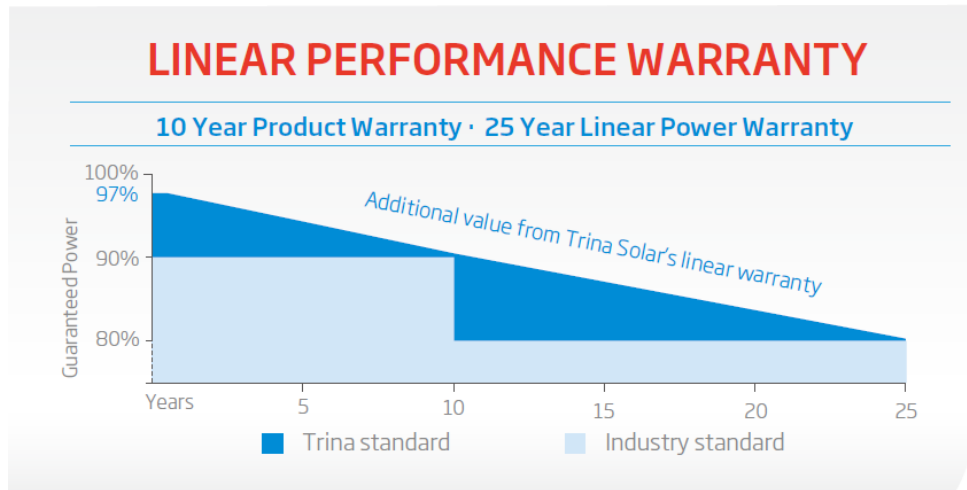


Figure 21: Linear performance warranty provided by Trina solar [10]

For the calculations made in the simulation, an annual performance decrease was estimated considering that the difference between the guaranteed powers in the first year and the 25th is 17%. The annual value is estimated in equation 15.

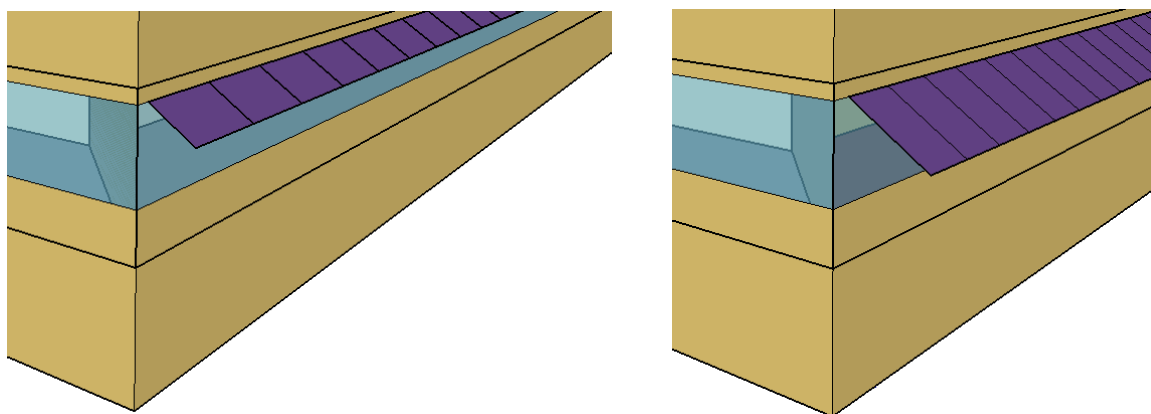
$$\text{Yearly performance decrease:} \quad 1 - (1 - 0.17)^{1/25} = 0.74\% \quad (15)$$

Given the dimensions of the PV panels and the building, it is possible to calculate the number of modules that can be installed on each floor. It is obtained that there are 44 modules per floor if they are oriented with the longer side towards the wall, that is, the 1.65 m side is aligned with the facade of the building. Since there are 12 floors, a total of 528 modules are needed.

On the other hand, if the modules are oriented with the shorter side to the wall, that is, with the 0.992 m side parallel to the facade, the number of panels per floor rises to 73. A total of 876 modules is obtained. The resulting values in each case are summarized below:

Parameter	Unit	Long side	Short side
Number of PV modules		528	876
Installed power	<i>kWp</i>	158.4	262.8
Total area	<i>m</i> ²	864.23	1,433.84
Total price	<i>USD</i>	88,709.28	147,178.51

Table 8: Main values for modules with long side to the wall



(a) Modules with the shorter side to the wall (b) Modules with the longer side to the wall

Figure 22: Possible configurations to install the PV modules as Sun shield

Figure 22 presents a Sketchup representation that illustrates how the modules are oriented in the Sun shield in the cases previously described. To decide which configuration

is preferable, the results of the building's energy simulation with Sketchup, OpenStudio and EnergyPlus will be used. The distribution that leads to better operation of air conditioning systems and internal lights will be used for the analysis. It will also be considered the shading between panels of consecutive floors.

In both cases the modules are mounted an azimuth angle of 180 since it is assumed that the wall is facing north, and with a fixed tilt angle of 33° with respect to the horizontal plane. This is done because a mechanic system to constantly adjust the angle to the optimum value during the day increases too much the costs and it is usually not considered for these type of applications [45].

The tilt angle is selected using the value of the location's latitude, which is indicated in section 3.1, to have a better performance considering the whole year. That is because during summer the sun is higher in the sky and the modules would be better closer to a horizontal tilt, while in winter the opposite is true, the sun is lower and a better performance is achieved closer to a vertical inclination. With this configuration the modules perform better in spring and autumn and a compromise is made for the other two seasons.

5.1.2 Modules for Curtain wall configuration

The other configuration that is considered is the Curtain wall, in this case semi-transparent modules are used to replace the glass used in the windows and opaque modules are used to cover the rest of the walls in the north facade. This disposition implies that the panels will be mounted in a vertical inclination, which means that they will not receive the irradiation with the optimal angle. To get accurate information about the prices and technical specifications of an installation of these characteristics the company EnergyGlass was contacted.

EnergyGlass is a company that provides support to designers and builders in projects related to the inclusion of energy generation in the architectonic elements of the construction using BIPV solutions, in order to do that they also produce stratified photovoltaic security glasses and ceramics [46]. Among the projects that the company has developed is the Porta Susa railway station in Turin, where structural photovoltaic glass was used, with an installed power of 600 *kWp*.

As part of the information delivered to the company, it was indicated that the building facade has a total area of 3.474,2 *m*² of which 60% corresponds to walls and 40% to windows, insulating glass required. The specifications were the following:

	Area m^2	Length m	Height m
Walls	2,084.5	73.11	1.58
Windows	1.389,7	73.11	2.38

Table 9: Main specifications sent to EnergyGlass

The solution proposed by the company has the aim of obtaining the best ratio between performance, design and price, the main parameters they consider for a BIPV solution. Performance refers to the peak power of the BIPV elements and the energy production, design to the aesthetic aspects like color and disposition, and the price is given in a €/m² basis and it is indicated that includes the architectural construction elements [47].

To obtain a good performance given the vertical disposition of the modules, the components suggested [47] are high efficiency solar cells of mono-crystalline PERC technology, these have the characteristic of making better use of diffuse radiation present in the atmosphere. It is also indicated that they should be bifacial solar cells to increase the performance by harnessing the irradiance from both sides, reaching 5 to 6% more energy production in the transparent modules and 7 to 8% in the opaque ones.

Insulating Glass Units (UGIs) are used to contain the solar cells in both cases. For opaque it is suggested [47] the use of white or light grey back glass for aesthetic purposes, since it hides the building's structure, and to increase the performance by reflecting the light to the back of the cells. For transparent, the solar cells in the UGI present a bigger separation between themselves for higher transparency, the back glass is transparent to receive the diffuse light also coming from inside the building, it has more layers to increase insulation.

The technical data provided are presented in table 10, the prices were indicated in Euro, but here are converted to dollar, the rate is specified in section 7.2, to express all values in the same currency:

Parameter	[Unit]	Transparent	Opaque
Power	Wp/m^2	130	180
Price	USD/m^2	353.16	282.53
Transparency		40%	10%
U_g	$W/(m^2K)$	1.1	-
Perfor. decrease	%/year	0.95%	0.95%

Table 10: Main specifications provided by EnergyGlass [47]

The costs are indicated as EXWORKS, which means that the buyer has to pay for the transportation expenses. The configuration proposed also includes the BIPV cabling system, which includes edge connectors hidden in the frame system, or back Slim Junction

box. The structure of the UGI for the transparent and opaque cases is also provided, it is shown in table 11, HTS stands for Heat Soak Test, PVB for Polyvinyl butyral a resine with high optical clarity.

Transparent	Opaque
6 mm extra clear glass Tempered + HST	6 mm extra clear glass Tempered + HST
1.52 PVB Solar with solar cells inside	1.52 PVB Solar with solar cells inside
6 mm float glass toughened	6 mm float glass toughened and white or grey screen print
16 mm with Argon	
6 mm float glass LE tempered	

Table 11: UGI structure provided by EnergyGlass [47]

The model of the solar cells suggested is the NS6QL from Neo Solar Power corporation (NSP), as previously indicated it is a high efficiency cell, can reach values over 21.3 % and the bifacial technology allows a power gain from the rear side between 5% and 20%. The main relevant parameters are summarized in the following table:

Parameter	Value	Unit
Peak power (P_{max})	5.204	Wp
Open circuit voltage (V_{OC})	0.661	V
Short circuit current (I_{SC})	9.764	A
Max. power voltage (V_{MPP})	0.565	V
Max. power current (I_{MPP})	9.201	A
Thermal coeff. of P_{max} (γ_P)	-0.40	$\%/K$
Thermal coeff. of V_{OC} (β_V)	-2.00	mV/K
Thermal coeff. of I_{SC} (α_I)	3.70	mA/K
Efficiency (η)	21.1	$\%$

Table 12: Parameters of bifacial solar cell [48]

The I-V curve is provided in the datasheet [48] for the model NS6QL-2080, since the values are similar, it is shown in figure 23:

(Cell Efficiency 20.8%)

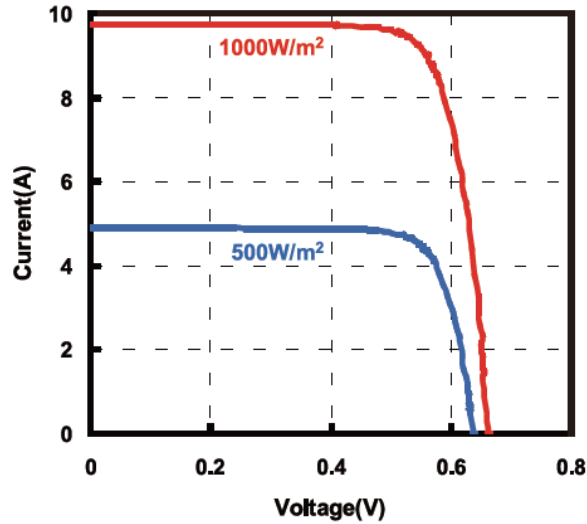


Figure 23: I-V curve of the NS6QL-2080 model [48]

With this information it is possible to estimate the installed power for the Curtain wall configuration. Table 13 shows the values for the semi-transparent modules in the windows, the opaque ones on the walls and the total values as the sum of the two previous:

Parameter	Unit	Transparent	Opaque	Total
Total area	m^2	1389.7	2,084.5	3,474.2
Installed power	kW_p	180.658	375.212	555.870
Price	USD	490,777.58	588,933.10	1,079,710.68

Table 13: Main values for the Curtain wall installation

It is indicated that for this type of applications they use custom modules, specially designed for the situation. It is necessary to estimate the disposition of the PV cells in the windows and in the walls, also how they will be divided into modules. This is done to be able to calculate the number of inverters that are needed in this case and to simulate the effect over the building with EnergyPlus and OpenStudio.

The estimation is performed separately for the windows and for the walls. In the first case a 40 % transparency is used, which means that 60 % of the window will be covered with the solar cells. Dividing the covered surface by the area of a single cell it is obtained that approximately 2820 cells are needed for each window, for a more symmetrical distribution an arrange of 8 by 360 cells per window is considered, which provides around 40% transparency as desired.

For the walls there is a 90% coverage, following the same procedure it is estimated that approximately 6,230 cells are needed per floor, again with the objective of symmetry the cells are distributed in an arrange of 14 by 445. In both cases the cells are separated from

each other by uniform distances, vertically and horizontally. In table 14 this information is summarized and figure 24 illustrates a view of the facade with this distribution.

Parameter	Unit	Transparent	Opaque
Covered area	m^2	69.308	155.602
Cell distribution		8×360	14×445
Horiz. separation	mm	46.2	7.53
Vert. separation	mm	36.2	12.63

Table 14: Estimation of the distribution of the cells for one floor

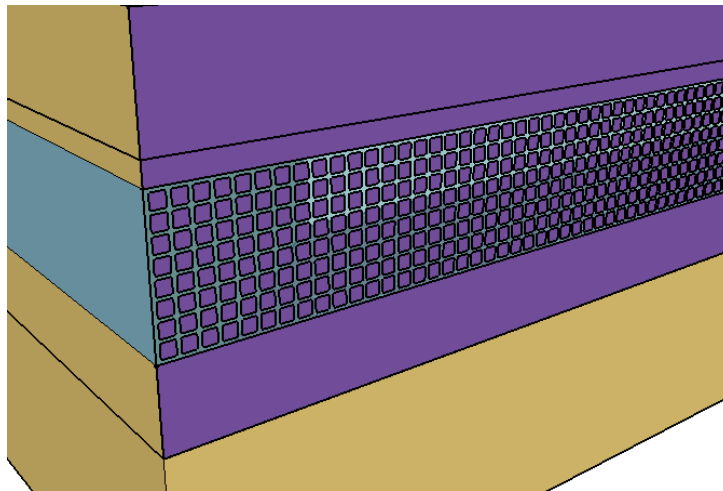


Figure 24: View of one floor with the PV curtain wall installed on the north facade

5.1.3 Modules for Roof installation

The surface in the roof of the building can also be exploited to harness the solar resource. Since in both considered configurations the roof is not used, it can be sized and applied in the same way as in the two previous cases. It will not have an impact when comparing the two settings, but it is important to be able to supply a larger percentage of the building's consumption.

The same model selected for the Sun Shield configuration will be used, since the same criteria applies in this case. They will be installed with the larger side parallel to the ground in order to fit more rows of PV modules along the roof, since the dimensions are the same as in the other floors, the number of panels per row is 44 as estimated in section 5.1.1.

The next step is to decide on the number of rows that will be installed in the roof. The main factor that determines this decision is the shading between the panels that are one in front of the other. To take this into consideration the worst case is considered, which is in the winter solstice because the sun reaches its lower point in the sky and consequently produces the greatest shadows in the year.

To estimate an appropriate distance between the rows a trigonometric analysis is performed. The logic is illustrated in figure 25 and the values of the altitude and azimuth of the sun are needed. The altitude (α_s) of the sun is the angle between the horizon and the Earth-Sun line, the azimuth (γ_s) is the angle formed between the sun ray and the line of the south, with positive values to the west.

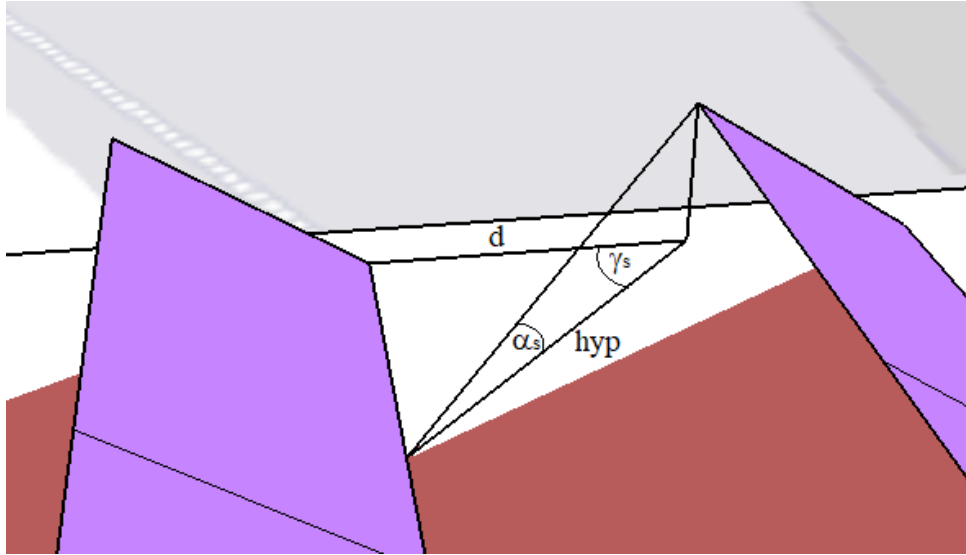


Figure 25: Representation of the relevant angles for the analysis

To obtain the values for the altitude and the azimuth it is necessary to use the sun chart for the location, obtained from SunEarthTools.com [49], it is shown in figure 26. The lowest curve should be considered for the winter solstice, a window of six hours without any shading is assumed to optimize the number of rows to install in the roof.

This is because if the whole day is taken into account, the resulting distance to avoid shading is too long and fewer rows of modules can be installed. Instead, given that the hours near sunrise and sunset are characterized by a lower irradiance, a bit of shading is accepted during this time to favor a greater installed power.

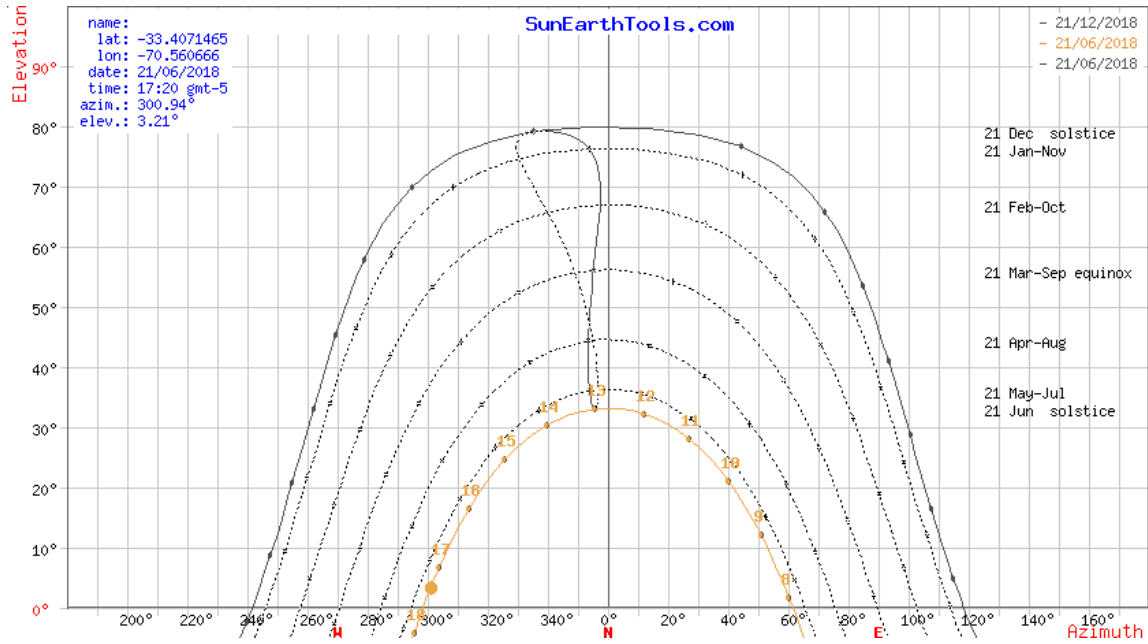


Figure 26: Sun chart for the location of the building

For the given date the sunrise and sunset hours are 7:45 h and 17:42 h respectively, for the window in consideration, the limits for the shading are around 9:45 and 15:45. For these hours the chart indicates that the elevation and the azimuth are 18,8° and 43,2 °. The values can be used in the following trigonometrical equations to calculate the distance required:

$$\text{hyp} = h \cdot \tan(\alpha_s) \quad (16)$$

$$d = \text{hyp} \cdot \cos(\gamma_s) \quad (17)$$

- “h” is the height of the upper end of the solar module that is casting the shadow.
- “hyp” is the projection on the floor of the sun beam.
- “d” is the distance between the rows.

Knowing that the tilt angle of the modules is fixed as 33° and the length is 0.992 m, the height “h” is approximately 0.54 m, using this parameter a distance “d” of 1.16 m is obtained. The depth of the building is 48.74 m which means that 25 rows of 44 modules each can be installed on the roof. A total of 1100 modules are required for this part of the system and adds a peak power of 330 kW. Table 15 summarizes the relevant values used and obtained in this calculation.

Variable	Value	Variable	Value
Time window	6 hours	Modules per row	44
Sun elevation	18.8°	Number of rows	25
Azimuth	43.2°	Total modules	1100
h	0.54 <i>m</i>	Installed power	330
hyp	1.59 <i>m</i>	Total area	1,800.48 <i>m</i> ²
d	1.16 <i>m</i>	Total price	184,811 <i>USD</i>

Table 15: Relevant values for the Roof installation

The same calculation is performed in the case with the modules oriented with the shorter side to the ground and results in a distance of 1.92 *m*. This allows only 15 rows of 73 modules each, the power achieved is 328.5 *kWh*, slightly lower, so it is confirmed that the configuration used in the previous paragraphs is preferable.

Another factor that supports this conclusion is the way in which the bypass diodes are connected in the modules, three Schottky diodes are installed, one every 20 PV cells [50]. The orientation used for the roof panels makes it possible for the shade produced between rows in early mornings and late afternoons to be aligned with the groups of 20 cells inside the module. This allows the other groups that still receive direct irradiation to continue generating energy without major problems.

5.1.4 Inverters

The inverters are an essential part for the operation of the project, since they are in charge of the conversion of DC power generated in the solar modules in AC so that it can be used by the different devices that must work in the offices of the building. The replacement of one of them means large losses due to the high associated prices and the time that the whole system spends without being able to operate while waiting for the replacement to arrive [24].

For this reason, it is necessary to select a quality inverter that ensures normal operation. To do this, the main suppliers were also investigated, according to Natural Energy Hub [51], the best suppliers of inverters in terms of profits between 2016 and 2017 were:

Number	Company	Country
1	SMA Solar Technology AG	Germany
2	Huawei Technologies	China
3	TMEIC	Japan
4	SolarEdge Technologies	Israel
5	ABB	Switzerland
6	Sungrow Power Supply	China
7	Schneider Electric	France
8	Enphase Energy	USA
9	Omron Corp	Japan
10	Fronius International	Austria

Table 16: Top 10 inverter suppliers (2016 - 2017) according to Energy Hub [51]

To select the model that will be used a compromise is made between the performance of the inverter and the total price associated to the number of elements required. The company SMA Solar Technology is selected with the model Sunny Tripower 60-US, this three-phase, string inverter with a rated power of 60 kW , makes it possible to require a smaller number of these converters to transfer the energy generated by the photovoltaic system from DC to AC. Even though the price is higher, the also higher power results in a lower cost per Watt for this type of components, so this solution allows to obtain a better total cost. A different number of converters is used for the configuration as Sun shield and Curtain wall.

According to the manufacturer [52] this inverter is characterized by a high efficiency, low weight and simpler installation. It uses the SMA Inverter Manager and a Local Commissioning and Service (LCS) tool to provide a better performance. An example of the connection and the use of these tools is shown in figure 27. It allows one independent MPP input, but up to 16 strings can be connected using a DC combiner, it also has the option to modify the power factor that is being injected.

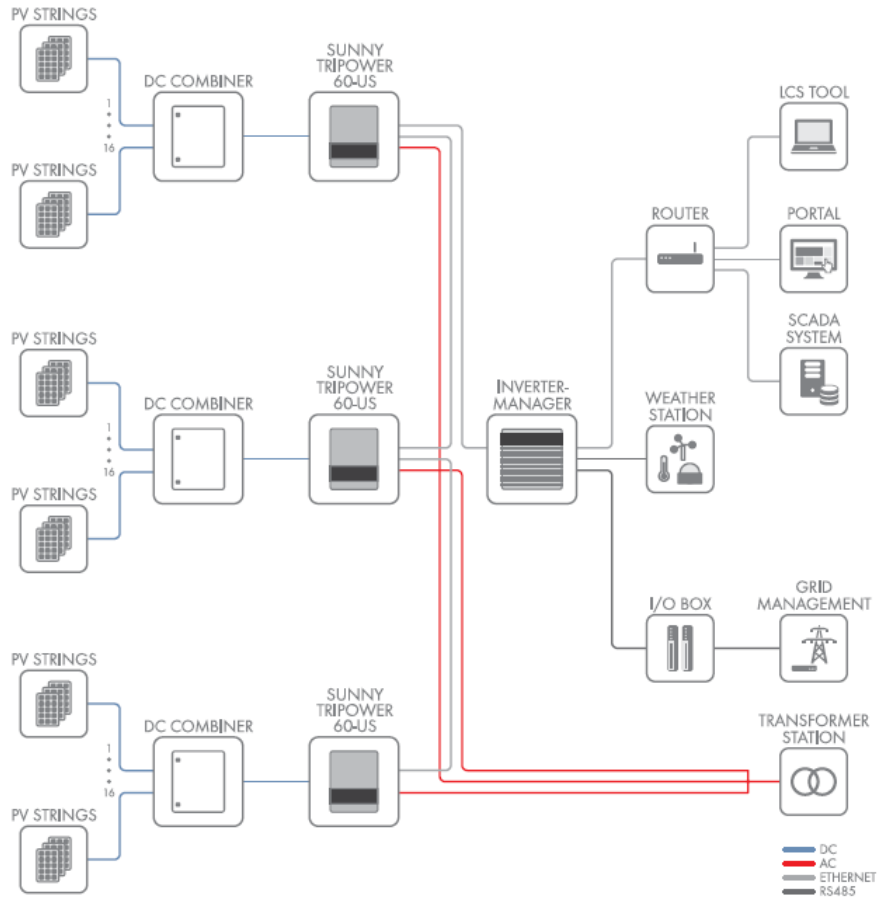


Figure 27: Example of connection of the inverters provided in the datasheet [52]

The main technical specifications are summarized in table 17, since the rated voltage at the output of the inverter can be 400 V or 480 V phase-to-phase, there is no need for an additional transformer since the voltage used in the grid and equipment is 220 V phase-neutral.

Parameter	Value	Unit
Rated Power (P_{ac})	60	kW
MPPT window	570 to 800	V
Max. input Voltage V_{DC}	1,000	V
Max. input Current I_{DC}	110	A
Efficiency (η_{inv})	98.3	% (@630 V_{DC})
MPPT efficiency (η_{MPPT})	99.9	%
Rated power frequency f	50, 60	Hz
Rated grid voltage	400 , 480	V
Power Factor	1 to 0.8	(lagging and leading)
Topology	Transformerless	

Table 17: Main technical specifications of Sunny Tripower 60-US [52, 53]

For this inverter it is specified that the maximum efficiency is 98.8%, but this is not the real value that will have at the operation point, this is why in table 17 the European

efficiency is noted and that value will be used in the simulation. To perform the maximum power point tracking this converter includes the OptiTrac algorithm developed for the SMA inverters [53], it has the property of ensuring the operation at MPP in conditions of partial shading.

To estimate the number of inverters required in each configuration the installed power in each case is considered, the sum of the rated power of the inverters required has to be similar to that value. A slight oversizing is preferred, to have as a warranty in case one of the converters malfunctions during its lifetime, the strings that were connected to it can be redistributed to the others that are still in normal operation.

In table 18 the results for the Sun Shield and Curtain wall configurations are shown, the installed power includes the roof in both cases, the resulting number of inverters and total rated power are listed. It is possible to observe that the rated power of the total number of converters is higher than the installed power, which confirms the oversizing that was intended.

Parameter	Unit	Sun shield	Curtain wall
P_{nom}	kWp	488.4	885.87
$N_{inverters}$	-	9	15
P_{rated}	kW	540	900
Price [54]	USD	53,906.34	89,843.90

Table 18: Main parameters for the inverters

5.2 Configuration of the PV plant in the building

To determine the configuration in which the PV modules will be connected between themselves and to the inverters the extreme conditions must be considered. The MPPT window and also the maximum values for the input voltages and currents must be taken into account. For the modules it is important to check that after the series and parallel connections the resulting current and voltage are within accepted ranges. From table 17 the input voltage is 1000 V the maximum input current is 110 A and the window is between 570 V and 800 V at a grid voltage of 400 V .

5.2.1 Sun shield and roof connections

For the sun shield configuration, the dimensions of the building limit the number of modules per floor to 44, the same happens in the rows on the roof. As a first approach, it can be estimated dividing the installation in strings of 22 modules and connect them in parallel to the inverters. This has to be checked considering the modules' output voltages in extreme temperatures, because this parameter makes the MPP voltage increase in colder situations and decrease when it is hotter.

The information used for these modules is already shown in table 7. The voltage thermal coefficient will be used in $V/^{\circ}C$, taking in consideration that $V_{OC} = 39.8V$, the result is $\beta_V = -0.115V/^{\circ}C$ and it is used in the following equation, T_c is the cell temperature:

$$V_{MPP}(T_c) = 32.6 - 0.115 \cdot (T_c - 25) \quad (18)$$

The extreme values used for the cell temperature are $75^{\circ}C$ and $-7^{\circ}C$, this last one because the lowest ambient temperature recorded in the database is around $-2^{\circ}C$ during daylight hours and due to the irradiance, the cells are warmer. Given that at STC the maximum power point voltage is $V_{MPPT} = 32.6V$ the results are:

Temperature	V_{MPP}	MPPT window	$N_{s(min)}/N_{s(max)}$
$75^{\circ}C$	$26.85 V$	$570 V$	21
$-7^{\circ}C$	$36.28 V$	$800 V$	22

Table 19: MPP voltages in extreme temperatures and number of modules per string

To calculate the maximum and minimum number of modules per string the MPPT window of the inverter is considered. At $75^{\circ}C$ the voltage has its lowest value, by multiplying it by the number of modules in series, the minimum value for the voltage of the string is obtained, this has to be compared with the lower end of the MPPT window to estimate $N_{s(min)}$. At $-7^{\circ}C$ the voltage reaches its highest and the maximum value for the string is calculated, comparing with the upper end of the window $N_{s(max)}$ is estimated. The results indicate that selecting 22 modules per string is within the inverter's operating range.

The next step is calculating the number of strings to connect in parallel to each inverter, since in this connection the currents are added, this is the limiting variable. The total value must be lower than $110 A$. Since the current thermal coefficient is very low, it is neglected. Each string provides $9.19 A$ in open circuit conditions so a maximum of 11 strings can be connected to each inverter.

To have a more even distribution between the 9 inverters, it is decided to connect 8 strings in parallel to 8 of the inverters and 10 strings to the other one. As previously indicated, this measure allows the system to be kept fully operational in the event of a failure of one of the converters. In table 20 the values used for the connections are summarized.

$N_{inverters}$	$N_{s(max)}$	N_s	$N_{p(max)}$	N_p
8	22	22	11	8
1	22	22	11	10

Table 20: Series and parallel connection of the modules for the Sun shield configuration

Figure 28 illustrates the way the modules are connected in this configuration, the strings are distinguished by lighter and darker tones of blue and grey, and the parallel connections are differentiated by the change in color, in the roof the last five rows are grey to represent the ten strings connected in parallel.

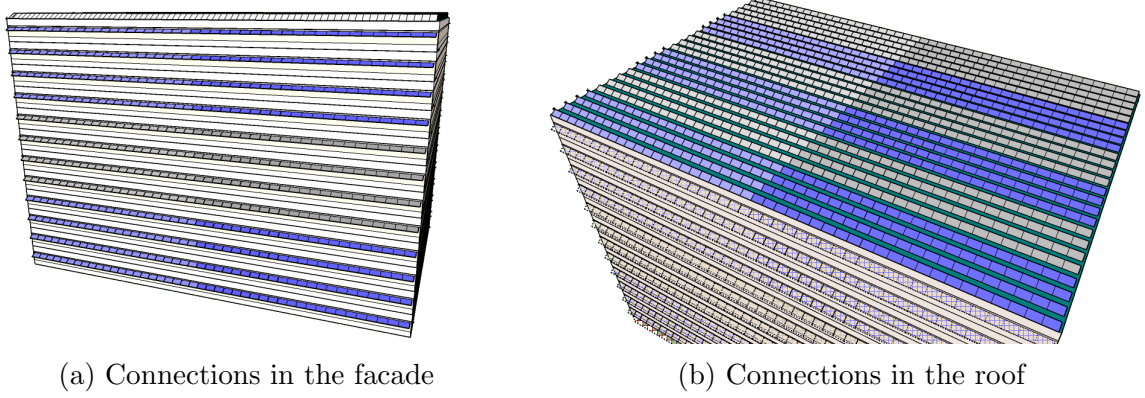


Figure 28: Series and parallel connections for the Sun shield configuration

5.2.2 Curtain wall connection

As previously explained, in this configuration the modules are custom made so it is necessary to estimate their size and the number of cells that each one contains to do a proper calculation of the number of inverters that are required. EnergyGlass can produce glasses of dimensions up to $2 \times 5m$, which means that for the windows one glass can be used and repeated horizontally. For the walls 2 glasses would be required because the height is greater than $2m$.

Like in the Sun shield configuration, the parameters of the cells are used to calculate the extreme conditions that limit the number that can be connected in series. The data from table 23 are used and since the ambient conditions considered are equivalent, the temperature values are the same, the equation in this case is:

$$V_{MPPT}(T_c) = 0.565 - 0.002 \cdot (T_c - 25) \quad (19)$$

The resulting values for the MPP voltage of one cell are $0.465V$ in hot conditions and $0.629V$ in cold. For the window glasses it is approximated that 8 cells are placed vertically, if they are connected in series, it is possible to calculate the amount of these 8-cells columns that can be connected to each inverter. The results are summarized in table 21:

Temperature	$V_{MPP}(8 - cells)$	MPPT window	$N_{s(min),col}/N_{s(max),col}$
75 °C	3.72 V	570 V	153
-7°C	5.08 V	800 V	158

Table 21: MPP voltages in extreme temperatures and number of 8-cell columns per string

Considering those limits, a possible solution is to connect in series 154 of these columns of cells which can be divided in seven glass modules with 22 columns each that respect the dimensions that EnergyGlass can deliver. Each floor would end up with two strings of 154 columns and one string of 52, this latter one can be connected in series with other two from adjacent upper floors, forming a string of 156 columns.

To calculate the number of strings that can be connected in parallel to the inverter the same procedure is performed as in the Sun shield case, the current is $I_{MPP} = 9.201A$ and the thermal coefficient is $\alpha_I = 3.7mA$ so again, it can be neglected. This results in a maximum of 11 strings, for symmetry reasons 7 will be connected, which corresponds to three floors per inverter, in other words, four inverters are used for the modules of the windows. The configuration is illustrated in figure 29, the change in the colors distinguishes a different parallel connections and the smaller and darker parts on the right represent one string connected through the three floors.

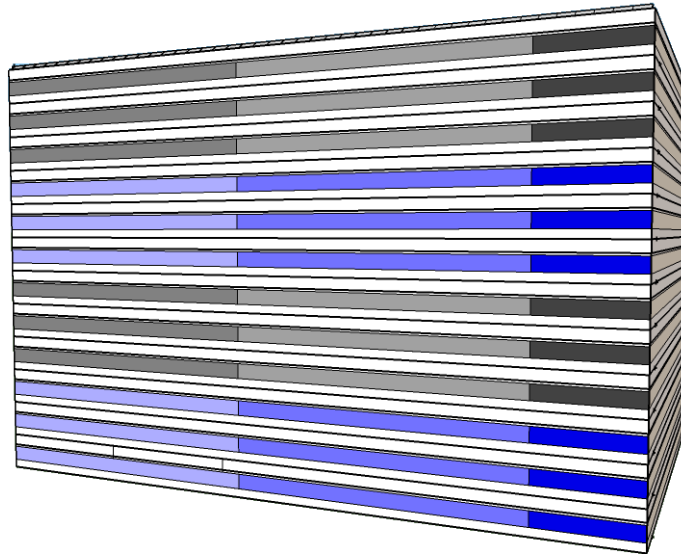


Figure 29: Series an parallel connections on the windows of Curtain wall configuration

In the walls it was considered that the columns would be of 14 cells each. Given the limitation of the maximum dimensions of the glasses, this can be arranged in two glasses with 7-cells columns. The following tables shows the results for the number that can be connected in series:

Temperature	$V_{MPP}(7 - cells)$	MPPT window	$N_{s(min),col}/N_{s(max),col}$
75 °C	3.225 V	570 V	175
-7°C	4.445 V	800 V	179

Table 22: MPP voltages in extreme temperatures and number of 7-cell columns per string

In this case strings of 178 columns are formed, to do it the two rows of glasses that are one on top of the other in each floor can be arranged to connect their columns in series, this results in 5 identical strings per floor, then it is possible to make ten parallel connections, from the strings of two floors, which results in 6 inverters for the modules on the walls.

Figure 30 illustrates the configuration, again the tones of the colors in each floor represents one string and the change between yellow and purple means a different connection in parallel to a new inverter.

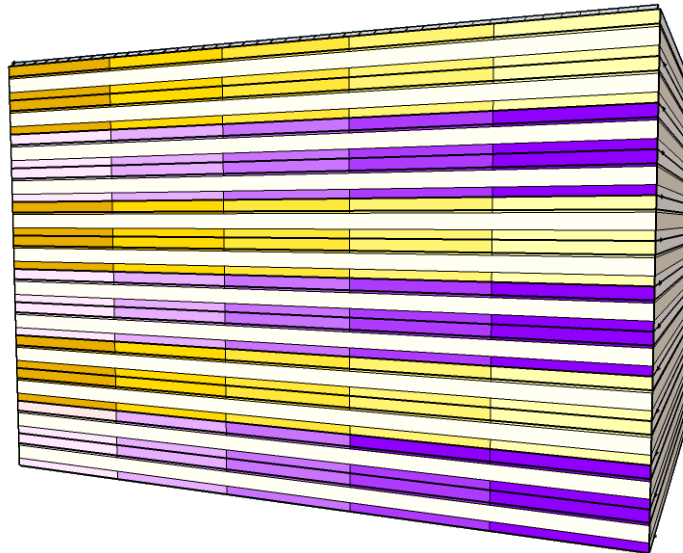


Figure 30: Series an parallel connections on the walls of Curtain wall configuration

Finally, five inverters are needed for the roof installation in this case, it is already calculated that there are 50 strings of 22 panels each, now ten strings are connected to one converter. Figure 28b depicts the distribution using the color to differentiate the connection to each inverter and the tones as contrast between strings in the same row.

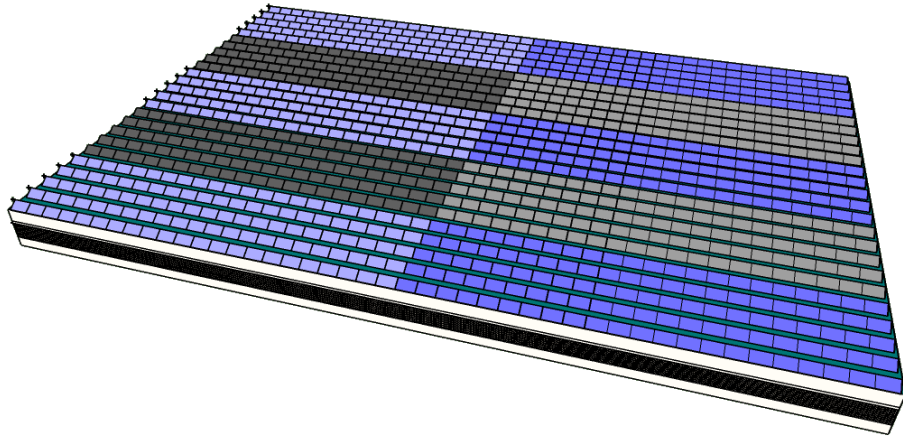


Figure 31: Series an parallel connections on the roof of Curtain wall configuration

To summarize the connections in the Curtain wall configuration table 23 is presented.

Category	$N_{inverters}$	Cells/col	Ns	Np
Windows	4	8	154 col.	7
Walls	6	7	178 col.	10
Roof	5	-	22 mod.	10

Table 23: Series and parallel connections of the modules for the Curtain wall configuration

6 Simulation

The following chapter describes the methodology followed to simulate the generation of electrical energy by the solar panels selected in each case, based on the radiation records in the chosen location. Then the simulation of the office building is explained in the cases of “Sun shield” and “Curtain Wall” implementations, and the variations noted in comparison with the original building.

6.1 The solar irradiance data

The first step to estimate the energy generated by the photovoltaic system is to obtain the data of the solar radiation of the area. To achieve this objective the “Solar Explorer” (*Explorador Solar*) service provided by the Ministry of Energy of Chile was used, which has a public database of solar irradiation throughout the continental territory of the country [30].

The data downloaded were obtained from satellite information and atmospheric models that span from 2004 to 2016, with a spatial resolution of 90 meters. This database was obtained thanks to the collaboration of several entities such as the German Society of International Cooperation (GIZ), the Department of Geophysics of the University of Chile, among others. A total of 67 measuring stations, considered of high quality, were used throughout the country to validate the horizontal global radiation magnitudes obtained [55].

Clear sky radiation was calculated in 10-minute intervals. It is indicated that they took satellite images to include the cloudiness situations using 20 daily images for places in latitudes below 45°. The topography of the place was also considered to determine moments of shade and thus adjust the direct and global radiation. Then, for the years indicated above, the hourly averages were calculated and delivered in the file in comma separated format (csv), which is downloaded and then used in this analysis. In addition to radiation, the following values are included:

- Temperature [°C]
- Wind speed [m/s]
- Shadow [1/0] (considers night and topography)
- Cloud presence [1/0]

6.2 From solar irradiance to electric power

In order to work with the data obtained from the radiation in the area the Matlab software, in its R2017a version, was used. In addition to this input, it was necessary to enter the parameters related to the selected solar panels, the inverters, the building and relevant economic variables for the subsequent final analysis.

The necessary parameters for the beginning of the simulation are summarized in table 24:

PV modules	P_{max} $\gamma_{P_{max}}$, thermal coefficient NOCT Yearly performance reduction Dimensions Price
Inverter	Rated power η_{AC-DC} , conversion efficiency η_{MPPT} , MPPT efficiency Price Maintenance downtime
Building	Dimensions Number of floors
NOCT and STC	$G_{STC} = 1000 \text{ W/m}^2$ $G_{NOCT} = 800 \text{ W/m}^2$ $T_{a_{STC}} = 25^\circ\text{C}$ $T_{a_{NOCT}} = 20^\circ\text{C}$
Losses	η_{LOSS} (Due to wiring, dust, reflection)

Table 24: Main technical parameters

First, the number of panels needed is computed, for the Sun shield configuration it is done using the dimensions of both the building and the panels. With these data, the value of the maximum power of the installation, the total area that receives solar radiation and the total price of the modules are reached. The calculation logic is illustrated in figure 32, the values obtained were also presented in section 5.1.1.

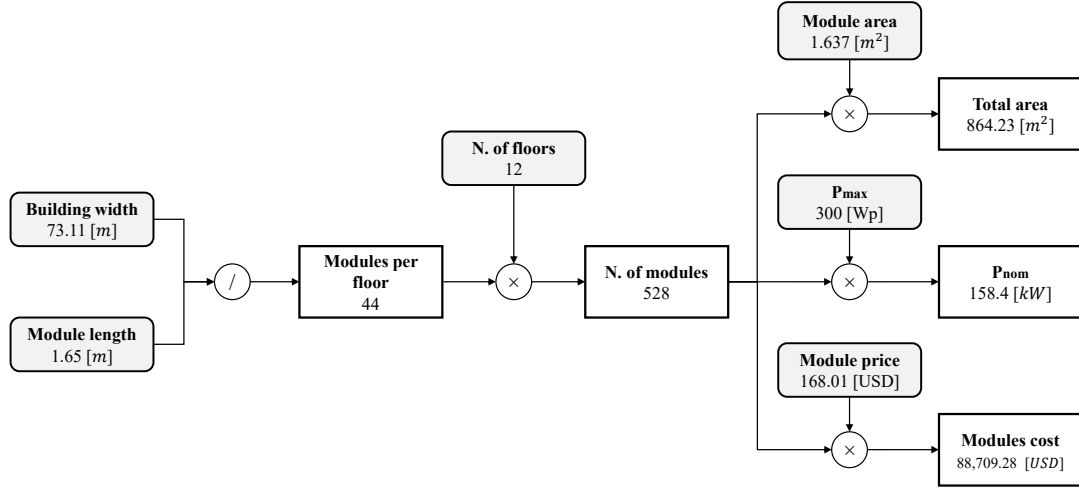


Figure 32: Calculation logic of the main values in the “Sun shield” configuration

In the case of the Curtain wall configuration the power and price are provided per unit of surface, the areas for the windows and the walls are directly calculated according to the dimensions of the building. The final values are obtained by simple multiplication.

The next step is uploading the file with the radiation data for Santiago. It is loaded as a table and then converted into “timetable” since this format allows easier handling of the data associated with a specific time. Then it is useful to check that the time intervals of the file are regular, after that, the missing data are removed. Since it is noted that the values for 2016 are not complete, it is decided to use the mean values for ten years with the data up to 2015.

From the data provided in the file, the values of the temperatures, the global horizontal irradiation, the direct normal irradiance and the diffuse horizontal irradiance are used. It is necessary to calculate the global irradiation incident in the module plane (G_t), since in both cases it is tilted with respect to the horizon, 33° in the case of Sun shield and 90° on Curtain wall. To do this, equation (4) is used, besides the variables obtained from the file, it requires the surface albedo (ρ) and the angle θ between the sun beam and the normal to the module plane.

The values used for the surface albedo is 0.24 as indicated in the modelling of the “Solar Explorer” [56]. It is possible to estimate the value of θ each hour using equation (3), which relates the global horizontal irradiance with the direct normal irradiation and the diffuse horizontal irradiation, if β is the tilt angle of the modules, then the following equation for θ can be deduced:

$$\theta = \arccos\left(\frac{GHI - DIF_h}{DNI}\right) - \beta \quad (20)$$

The logic of the angles involved is illustrated in figure 33 and for the calculations to get the global in-plane irradiance in figure 34.

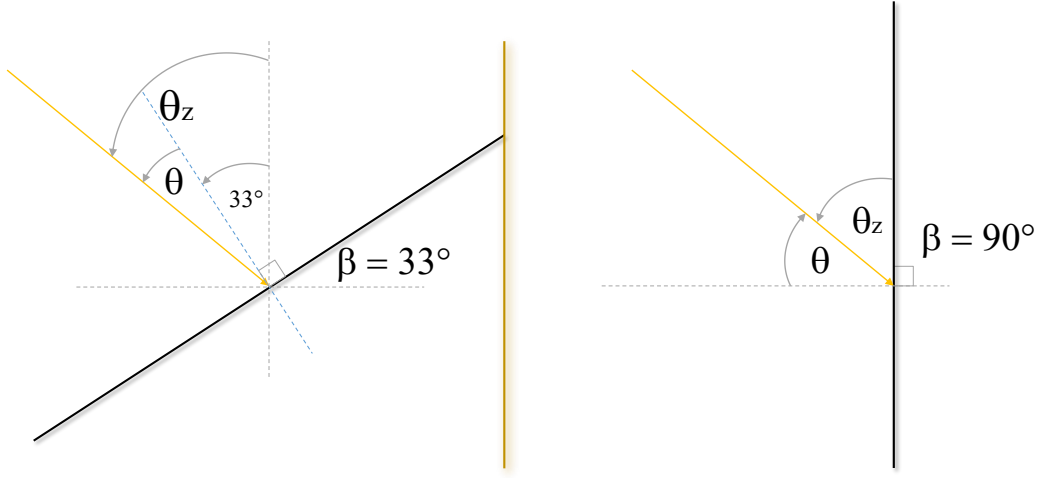


Figure 33: Definition of the angles for each configuration

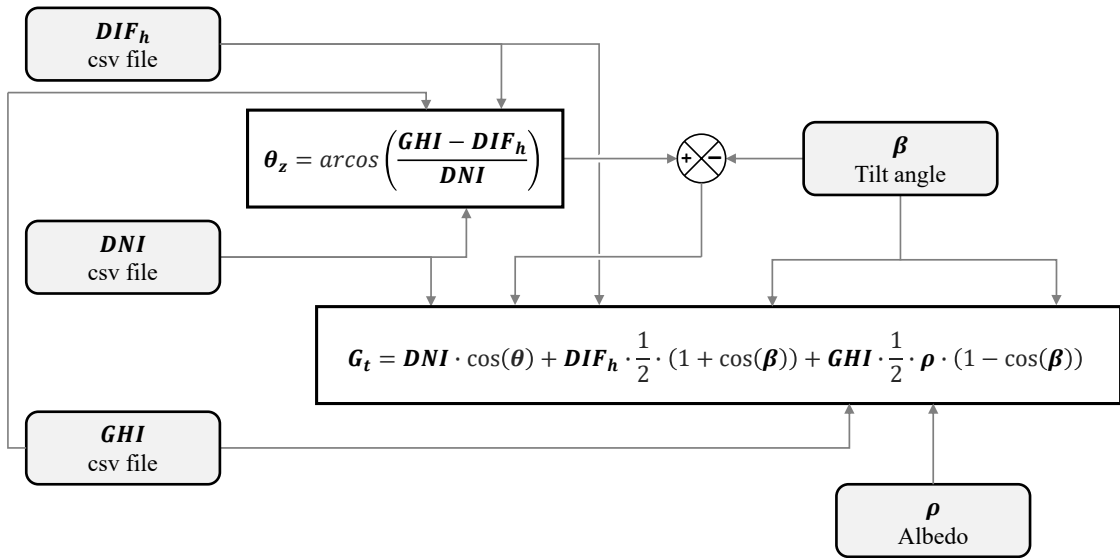


Figure 34: Calculation logic of angle θ , between beam and module plane normal

With these definitions and the available information, it is possible to calculate the global in-plane irradiance for each case. Then the hourly values for both the temperature of the cells under the influence of irradiation and the generated AC power are estimated. The following formulas are used:

$$T_c = T_{air} + (NOCT - T_{aNOCT}) \cdot \frac{G_t}{G_{NOCT}} \quad (21)$$

$$P_{ac} = P_{nom} \cdot \left(\frac{G_t}{G_{STC}} \right) \cdot f_{incl} \cdot \eta_{LOSS} \cdot \eta_{inv} \cdot \eta_{shad} \cdot [1 + \gamma_{Pmax} \cdot (T_c - T_{aSTC})] \quad (22)$$

The factor f_{incl} is inserted into the generated power formula to take into account the effect of the additional irradiance that the bifacial cells allow to harness, in the case of Sun shield it is used as $f_{incl} = 1$. For the Curtain wall instead, it is used as $f_{incl} = 1.06$ and $f_{incl} = 1.08$ for the windows and the walls respectively, to include the gains added by the use of the bifacial cells in each case.

The following graph illustrates how the downloaded data and the parameters are used in the formulas (21) and (22) to get the hourly AC power that comes from the PV generation.

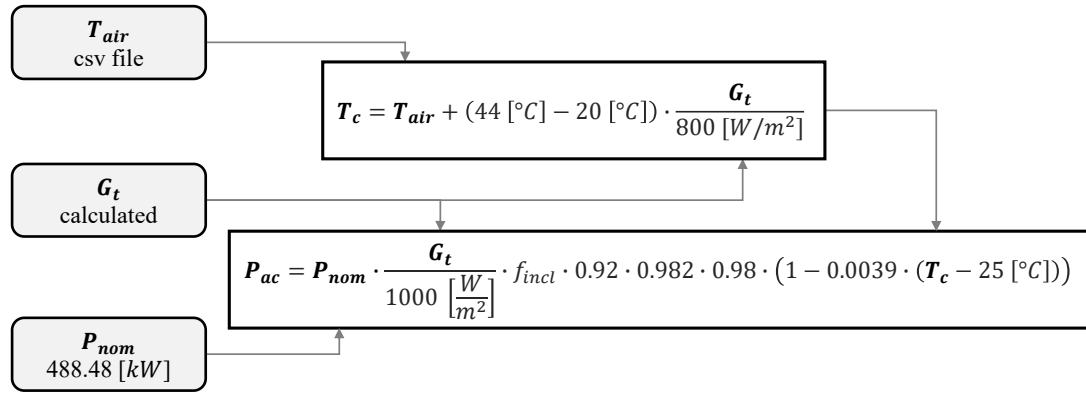
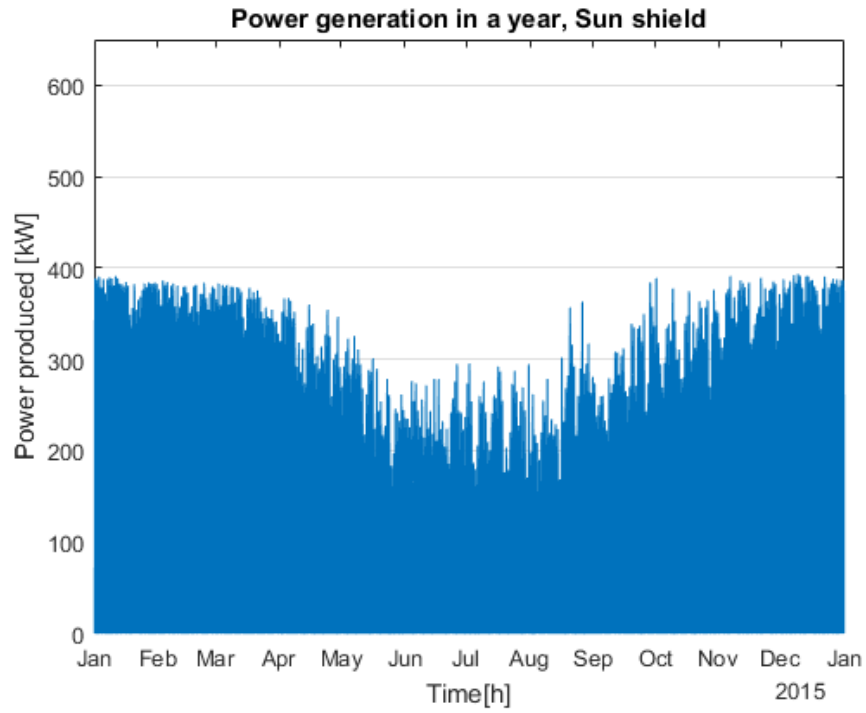


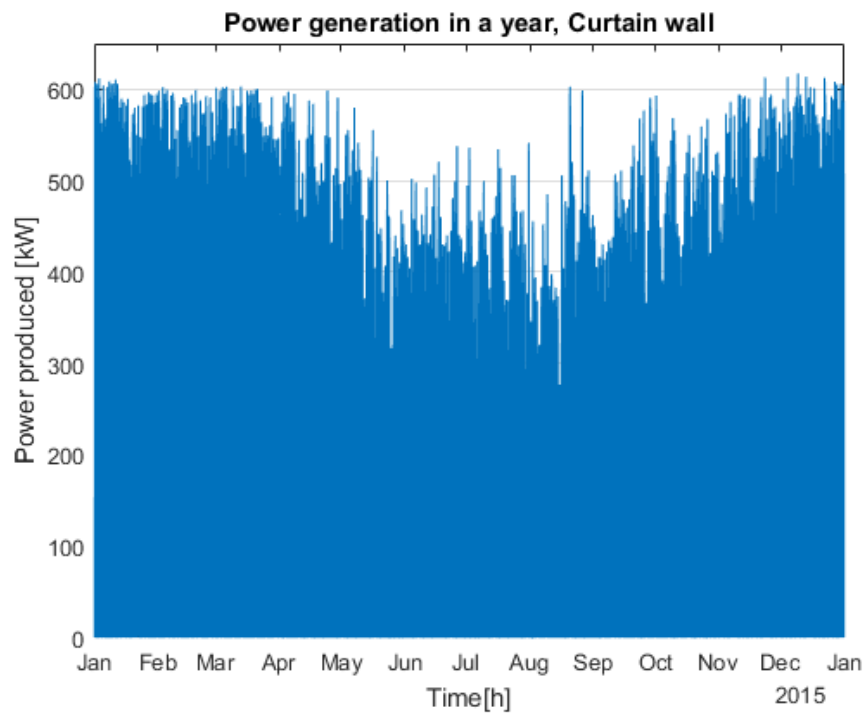
Figure 35: Calculation logic of the power produced by the PV system

Both resulting arrays of the hourly values are added to the main table to have all the data organized in one single element. Figure 36 shows the profiles for the power generated hourly over the year, while figure 37 illustrates the energy generated on a sunny day in summer and in winter, also the evolution of the temperatures of the cells in each case. The dates considered are January 16th and July 16th.

In figure 36a is possible to observe that in summer the energy generated is approximately 60% higher the amount produced in winter, values around 400 *kW* are obtained in the warm season, while the values are around 250 *kW* in the colder months. Figure 36b shows that for the Curtain wall the production difference is reduced and now it is only one third higher than in winter, and reaches 600 *kW* and 400 *kW* respectively.

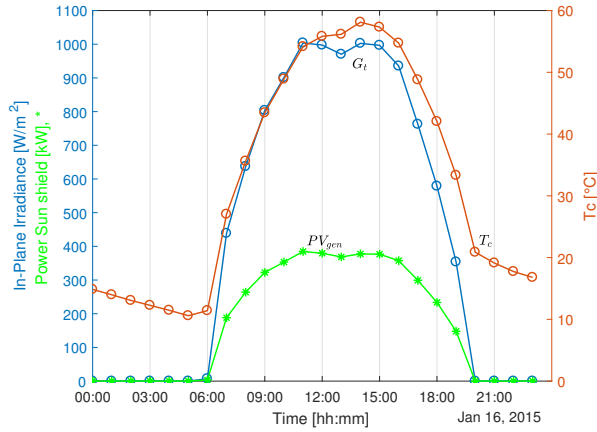


(a) Generation with Sun shield

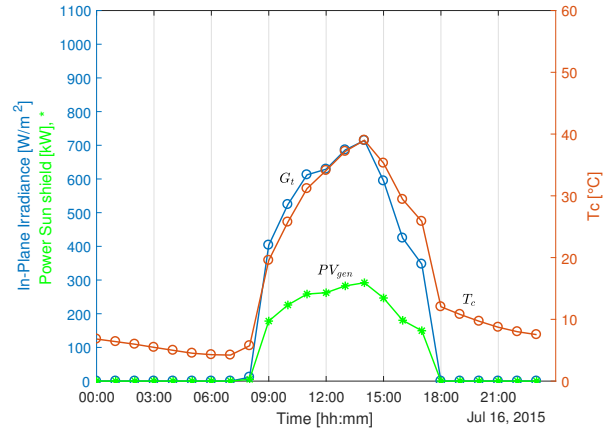


(b) Generation with Curtain wall

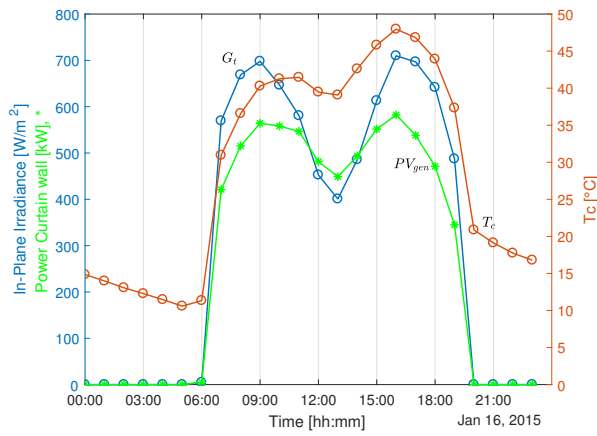
Figure 36: Generation in each hour over the year



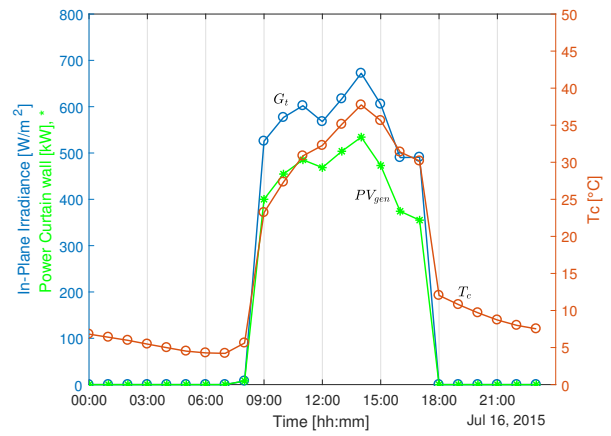
(a) Sunny day in summer, Sun shield



(b) Sunny day in winter, Sun shield



(c) Sunny day in summer, Curtain wall



(d) Sunny day in winter, Curtain wall

Figure 37: Power generated during a day in summer and in winter in Santiago

Comparing the graphs 37a and 37b it is possible to verify the reduction both in maximum irradiance and power generated previously mentioned. Another factor that reduces the total energy produced in the day is the lower number of sunlight hours, which goes from 14 to 10. It should also be noted that the cell temperature reaches values under 40 °C, compared to 60 °C in summer, this results in a higher efficiency of the modules in winter. As a final remark, the temperature range to which the cells are subjected during the year remains restricted to approximately 0 °C and 60 °C.

The diagrams 37c and 37d show a clear difference between the in-plane irradiance in both configurations and also between seasons. During summer there is a reduction of the irradiation received on the module near noon because the incident angle of the DNI is too big in a vertical inclination, the effect of the tilt angle can also be noted in the maximum irradiance reached, which is around 700 W/m^2 compared to the 1000 W/m^2 in the Sun shield.

During winter the irradiance shows a more constant behavior throughout the day, this happens because the sun elevation is lower and the incident angle of the DNI is

more favorable for a vertical inclination. For the same reason both configurations present a similar maximum irradiation received, reaching approximately $700W/m^2$ because the incident angle is worse for the Sun shield configuration. Regarding the cell temperatures for Curtain wall, the range is reduced and goes from around $40^{\circ}C$ to $50^{\circ}C$.

6.3 Loading the demand profile

In the same way, the demand profile data obtained in the simulation with EnergyPlus and OpenStudio are loaded. In this case three files are used, one with the base demand curve of the building, that is, without having installed any of the photovoltaic system configurations. The other two correspond to the consumption that occurs with the Sun shield system and that of Curtain wall.

As with the radiation file, they are loaded as tables and then transformed into timetables. Given the way in which EnergyPlus performs the simulation for a year, in this case the hourly values are provided between 1:00 on January 1st, 2009 and 0:00 on January 1st, 2010. This presents a difference with the dates of the measurements of irradiation, as shown in the following table:

Date.Hour	temp [$^{\circ}C$]	ghi [W/m^2]	Date.Hour	Ele.Facility [J]
2015-01-01 00:00	12.88	0	2009-01-01 01:00	$9.06 \cdot 10^8$
2015-01-01 01:00	12.08	0	2009-01-01 02:00	$9.04 \cdot 10^8$
\vdots	\vdots	\vdots	\vdots	\vdots
2015-01-01 06:00	10.46	20.09	2009-01-01 07:00	$9.50 \cdot 10^8$
\vdots	\vdots	\vdots	\vdots	\vdots
2015-12-31 22:00	16.90	0	2009-12-31 23:00	$1.00 \cdot 10^9$
2015-12-31 23:00	15.85	0	2010-01-01 00:00	$9.58 \cdot 10^8$

Table 25: Differences in the years and first and final hours

Two changes are performed to these the dates, the first is to add six years to all the rows, so they coincide with the ones of the irradiation measurements, which are from 2015. The second is to adjust the hours so only data from 2015 are contained in the table, that is, do not have the value of 0:00 of January 1, 2016. To achieve this, the “retime” command is used, which allows assigning the same hours to both tables and estimating the missing data by means of a linear extrapolation.

Finally, the consumption in (kWh) must be calculated, since the file obtained through OpenStudio delivers the energy values in Joules (J). To achieve this, the formula shown in equation (23) is used and the results are added to the main table.

$$1[kWh] = \frac{1[J]}{3.6 \cdot 10^6} \quad (23)$$

6.4 Estimation of the power for the next 25 years

Since the suppliers of the solar modules guarantee a level of performance for 25 years, this period is considered for the subsequent economic analysis. The evolution of the power generated in each year must be estimated, a weighting associated with the downtime of the system is applied annually due to maintenance, this reduces the total production. A value of 0.75% is used, it is estimated in a study that uses empirical data with inverters of the same brand [24].

Then a cycle is implemented to calculate the power that corresponds to each year applying an annual performance reduction of 0.74% for the Sun shield modules and of 0.95% in the case of Curtain wall. A table with the hourly data of the 25 years for both configurations is created, which is used later in the economic analysis. Figure 38 shows the difference between the respective power in year 1 and in year 25.

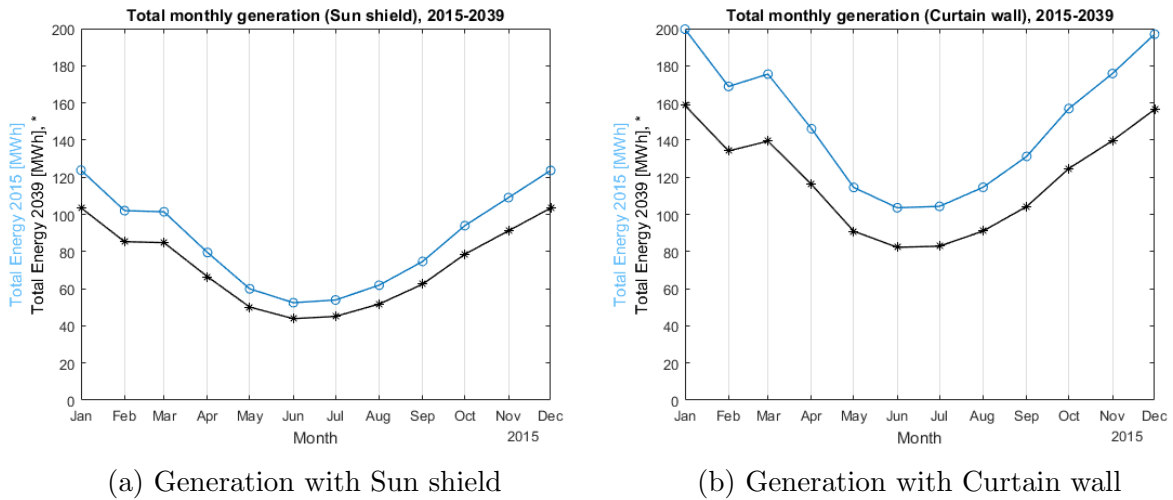


Figure 38: Total energy generated each month in the 1st and 25th years

Although the reduction between the 25 years is a 17%, in terms of the energy that is available there are differences that can be noticed between summer and winter. For the Sun shield configuration, in January and December the decrement is over 20 *MWh* each month, while in the June and July is slightly over 8 *MWh*. In the same periods for Curtain wall the reductions are around 40 *MWh* and 21 *MWh* respectively due to the higher level of power that is installed.

6.5 Performance indicators

Finally, some indicators of the performance of the PV system are calculated, these are the annual Specific Yield, Performance Ratio and the value of the generation over the consumption. These are determined using equations (12) and (14) from section 2.8, the

PR in the Curtain wall installation has to be calculated considering the incident irradiance on the vertical plane for the windows and wall covers, and on the tilt angle for the roof modules. The energy production in each case can be obtained directly from the power, since those data are sampled hourly, the sum of all the values in (kW) results in the total energy in (kWh).

The proportion of generation over consumption is calculated as the division of the total energy produced in the year over the total yearly demand. For this particular case, during weekdays the generation of the Sun shield is always lower than the consumption, so the self-consumed electricity is equal to the annual production. On the other hand, during weekends the load is lower, and part of the energy is delivered to the network. The production of the Curtain wall application is higher and most days there are hours in which it is injecting electricity to the grid, this effect will be explained in more detail in the next section. The main results are summarized in the following table:

Parameter	Unit	Sun shield	Curtain wall
E_{tot}	kWh	1,036,097.17	1,788,027.65
Y_f	kWh/kWp	2,121.41	2,018.39
Y_r	$kWh \cdot m^{-2} / kW \cdot m^{-2}$	2,583.16	2,311.99
PR		82.12 %	87.30 %
E_{tot}/E_{cons}		24.90 %	42.79 %
E_{roof}/E_{tot}		67.57 %	39.15 %

Table 26: Performance indicators for the Sun shield and the Curtain wall, 1st year

The Curtain wall configuration can generate approximately 73% more energy in a year than the Sun shield, mainly because there is a bigger surface to collect the incident irradiation. In both cases the production from the roof installation is included, which represents a 67.57% of the energy in from the Sun shield and a 39.15 % of the Curtain wall. If only the modules in the north facade are considered, the difference of production between both configurations is increased to a 224%.

The annual energy yield is higher for the Sun shield configuration, mainly due to the better angle to receive the irradiance, the same applies to the reference yield meaning that in the first case there is access to a better solar resource. The difference is accentuated when the roof is not considered, for Y_f goes from 5.1% to 8.39% and for Y_r from 11.73% to 18.96%.

The Performance Ratio instead is higher with the Curtain wall configuration, which means that there are fewer losses in the conversion from the energy that arrives to the surface of the modules to the AC power that is later used. It is also higher the value of the generation over the consumption, it covers more than 2/5 of the load of the year and the Sun shield only one quarter. If the roof installation is not considered, the curtain wall

is still able to supply more than one quarter of the consumption while the Sun shield less than 1/10. Table 27 shows the values when there is no roof installation.

Parameter	Unit	Sun shield	Curtain wall
E_{tot}	kWh	336,031.52	1,087,961.99
Y_f	kWh/kWp	2,121.41	1,957.22
Y_r	$kWh \cdot m^{-2} / kW \cdot m^{-2}$	2,583.16	2,171.46
PR		82.12 %	90.13 %
E_{tot} / E_{cons}		8.07 %	26.04%
E_{roof} / E_{tot}		0 %	0 %

Table 27: Performance indicators if the roof installation is not considered

6.6 Simulation of the demand in EnergyPlus - OpenStudio

To generate the file of the demand profile it is necessary to perform the simulation of the building in EnergyPlus. The reference building described in section 4.3 was used to this end, but there were some modifications made to the model in order to adjust the resulting consumption.

6.6.1 Modifications to the original model

The first step was adjusting the external loads, as mentioned in section 4.3.1 this category considers the elevators, the lights and fans associated to them, and external lights related to parking lot and illumination of the facade. To achieve a lower consumption, it is assumed that the building does not have a parking lot and doesn't illuminate artificially the facade.

Regarding the elevators, the model estimated their number according to the total surface of the facility. Given the dimensions of the building the model considered a total of 12 elevators, with the aim of higher efficiency only 4 elevators are considered, the same proportion applies to the equipment associated to them. In the following table it is shown the comparison of the power obtained with the change.

Load	Power [W], 12 elev	Power [W], 4 elev
Elevators	244,443.956	81,481.319
Lights and Fans	752	250.667
Non-dimming lights	12,979.2	0
Sensing exterior lights	43,305.089	0

Table 28: Changes in the exterior equipment power

Secondly, the temperature range of the thermostat is modified. The original values were 21°C and 24 °C, but it can be considered acceptable to relax it between 20°C and

26 °C [57]. In addition, on Sundays the upper limit is increased to 30°C to represent that is turned off since the occupancy is almost 0. With these ambient conditions it is still pleasant for the occupants on the days of the week that the building is used, but the electric requirement from the use of the air conditioning will be reduced.

The next action that is performed to reduce the total load is to use the basement of the building as a storage facility for supplies for the offices installed in the other floors. The amount of people is reduced to half the original and the loads related to the lights and equipment are modified using load definitions provided by OpenStudio for an office building. A definition for lights used in storage is applied and for the equipment there is no definition related to a storage room, so the one for a mechanic/electric room is used.

Finally, the perimeter zone of the south side in the first floor is changed to a lobby for the building, this means slight increase in the people and interior lightning in that space, but a big decrease in the electric equipment consumption. The definitions for the three parameters are used as provided in OpenStudio.

These changes in the basement and the perimeter zone have to be applied in the model, it is done creating two new Space types and applying them of the Main data center and to the core basement, in one case, and to the perimeter on the other case. Their respective properties must be modified to use the new definitions indicated in order to have a different result when running the simulation. Table 29 shows the changes in the loads according to the new definitions.

Variable	Unit	WholeBuilding	Main Data Center	Storage	Lobby
People	p/m^2	0.054	-	0.027	0.108
Lights	W/m^2	8.826	8.826	7.750	12.594
Electric eq.	W/m^2	8.070	484.376	2.906	0.753

Table 29: Change in the loads associated to the basement

With these modifications it has been possible to reduce the total consumption of the building in the year. In table 30 a comparison is shown in terms of the total energy utilization in the year and the consumption per unit of area of the building between the “Original case”, using the model as it was loaded from the measure, and the “Base case”, in which the changes are applied to obtain the model that will be used as a starting point for the Sun shield and the Curtain wall configurations.

Variable	Unit	Original	Base
Energy	kWh	8,963,758.05	4,200,817.27
Specific energy	kWh/m^2	193.522	90.693

Table 30: Reduction in the energy consumed by the building

Two studies are consulted to validate that these changes have produced reasonable results. The Energy consumption guide [58] presents a classification of office buildings into four categories: (1) naturally ventilated cellular, (2) naturally ventilated open-plan, (3) air-conditioned, standard and (4) air-conditioned prestige, the representation of each one is displayed in annex A3, according to the description provided for each one the modified reference building is in the middle between (2) and (3). There is an air-conditioning system, but there is a lower percentage of window presence in the facades.

The typical energy consumption values for these buildings go between 54 and 128 kWh/m^2 for good practices. As indicated in table 30 in the “Base case” this value is 90.693 kWh/m^2 , if the definition of treated floor area (TFA) used in the article is applied as 90% of the gross area, then the resulting value is 95.467 kWh/m^2 , which is within the normal range.

A more recent second study [59] presents values for the yearly specific energy demand for three cities that belong to different climate zones. When the energy required by the heating loads is not considered, the resulting values vary between approximately 50 and 90 kWh/m^2 for colder and warmer conditions respectively. The value obtained in the simulation is similar to the upper limit of that range, and so it can be considered a reasonable estimation.

In figure 39 two pie graphs are shown, both represent the way in which the total electric consumption in the year is distributed between the different loads present in the building. In the two cases the biggest loads are, in first place the interior equipment and in second the interior lighting. With the changes applied the interior equipment presents a reduction of its percentage and gets closer to a half of the total. On the other hand, the interior lightning consumption is not significantly reduced and the portion in the chart increases to approximately a quarter of the total.

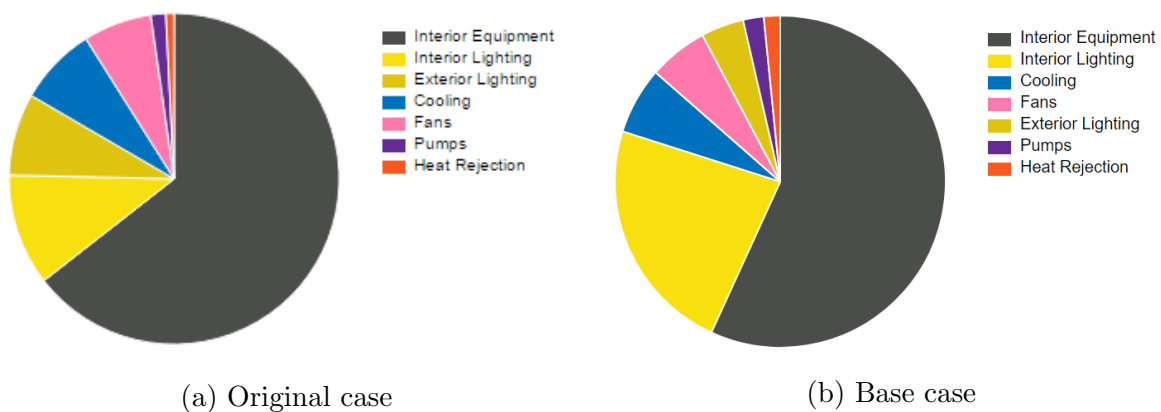


Figure 39: Pie charts of the distribution of the electricity between the loads

The monthly consumption of the building is plotted in figure 40 and displays the behavior of each of the loads. The loads related to the lightning and the equipment

remain relatively constant each month, while the cooling, heat rejection, pumps and fans display a seasonal variation with higher values in summer and lower in winter. During the cold period the heating load is higher, but it is not showed because it uses natural gas instead of electricity.

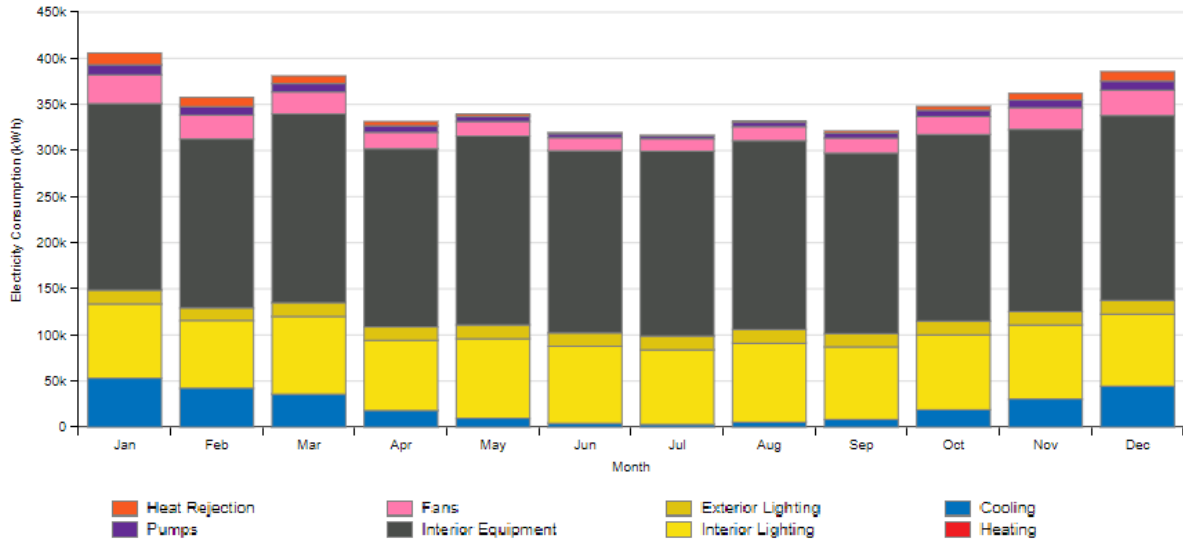


Figure 40: Monthly energy consumption by category, generated in OpenStudio

6.6.2 Adding the PV panels to the model

Once the base case is established, the solar modules can be added for each configuration. This is performed using Sketchup with the OpenStudio plug-in. The OpenStudio model has to be opened in Sketchup and then the modules are added in the windows and the roof, it is done creating a new shading surface group and then drawing a rectangle with the dimensions specified in the datasheet.

For the Sun shield and the roof configurations it is tilted to be at 33° and copied to fill each floor. In the Curtain wall case each cell is added to the windows in vertical inclination and for the walls an opaque surface that covers the whole area is used, both configurations have been illustrated in figures 22 and 24.

In the case of the Sun shield configuration the option with the longer side of the module parallel to the facade and the one with the shorter side are drawn separately. Each one is used to perform the energy simulation and analyze the effect that they have in the final consumption. The change in the length of the shadow can have positive effect for the cooling during summer, but a negative one for the heating in winter and for the lightning in the whole year, making it necessary to turn the lamps on earlier because of the reduction of natural light.

Load	Base	Long side	Short side
Cooling	274,050.75	261,614.73	261,384.26
Interior Lighting	968,652.50	973,729.72	986,479.44
Exterior Lighting	176,009.78	176,009.78	176,009.78
Interior Equipment	2,387,972.22	2,387,972.22	2,387,972.22
Fans	242,561.69	230,263.47	228,513.67
Pumps	84,583.11	82,233.53	82,210.49
Heat Rejection	66,987.22	65,246.17	65,070.30
Heating	213,801.31	217,195.07	219,041.42
Water Systems	131,917.21	131,917.21	131,926.01
Total (Electric)	4,200,817.27	4,177,069.62	4,187,640.16

Table 31: Comparison of consumption in base case and both configurations, in (kWh)

The results are compared in table 31, a better result is achieved when the long side of the modules is the one parallel to the facade since the total electric consumption is the lowest. The exterior lights and the equipment do not present any change, the interior lights and the heating are higher than the base case with better results using the long side and the cooling, fans, pumps, and heat rejection are lower than the base case, mostly with better results using the short side. Considering the overall effect, it is preferable to install with the long side facing the wall, in this case the higher consumption in the lights is outweighed by the reductions in the other loads.

A similar result was obtained in a study that used reference buildings of medium office and apartment building [60], the loads associated to the lights and the heating increased with the installation of a solar system, but the reduction in the use of the HVAC system made the total effect to be a decrease in energy requirements. It is also pointed out that the equipment consumption, that remains invariant, has a greater weight on the overall consumption and makes the percentage changes less notorious.

Before deciding to use one configuration or the other, the shading between two floors is taken into account. The sun chart [49] presented in figure 26 is used, but in this case the summer solstice is considered because the sun reaches its highest point in the year, the worst scenario in this situation. The date is December 21th since it is the southern hemisphere.

According to the sun chart, at the moment in consideration the solar elevation is 80° and the azimuth is 0° . The calculation logic is represented in figure 41. The tilt angle used to install the modules is 33° , to have a situation without shading in is needed that the vertical distance between the end of one panel and the beginning of the other (y_1) is greater than the value of the vertical projection of the shadow (y).

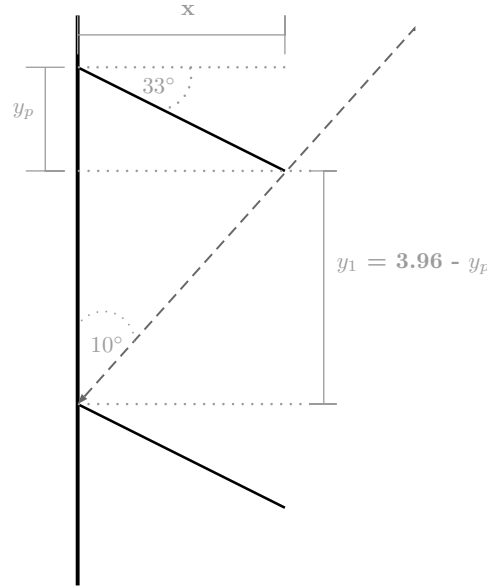


Figure 41: Geometric representation of the incident sun beams on the PV configuration

The relevant equations are the following and the results for each configuration are shown in table 32:

$$x = L \cdot \cos 33^\circ \quad (24)$$

$$y_p = L \cdot \sin 33^\circ \quad (25)$$

$$y = \frac{x}{\tan 10^\circ} \quad (26)$$

Configuration	x [m]	y_p [m]	y_1 [y]	y [m]	% shaded
Long side	0.83	0.54	3.42	4.72	14.42%
Short side	1.38	0.90	3.06	7.85	44.45%

Table 32: Results for the simulation of the shading at noon, December 21st

At noon in the summer solstice both configurations present shading, but with the long side to the facade the shadow is considerably smaller. In this case the maximum shadow over the panel has a length of 0.14 [m], while in the other it is of 0.73 m. When the elevation of the sun is reduced to 75° the selected configuration does not present any shading, while the other still has almost 20% covered. Also, as it was mentioned in section 5.1.3 the use of the bypass diodes in this module make this configuration preferable.

The consumption reduction and the better situation of shading make the configuration of the panels installed with the long side parallel to the facade the selected option. A lower number of modules will be used in the facade, but the efficiency of the whole system will be higher. In figure 42 it is displayed the final disposition of the building with the PV panels.

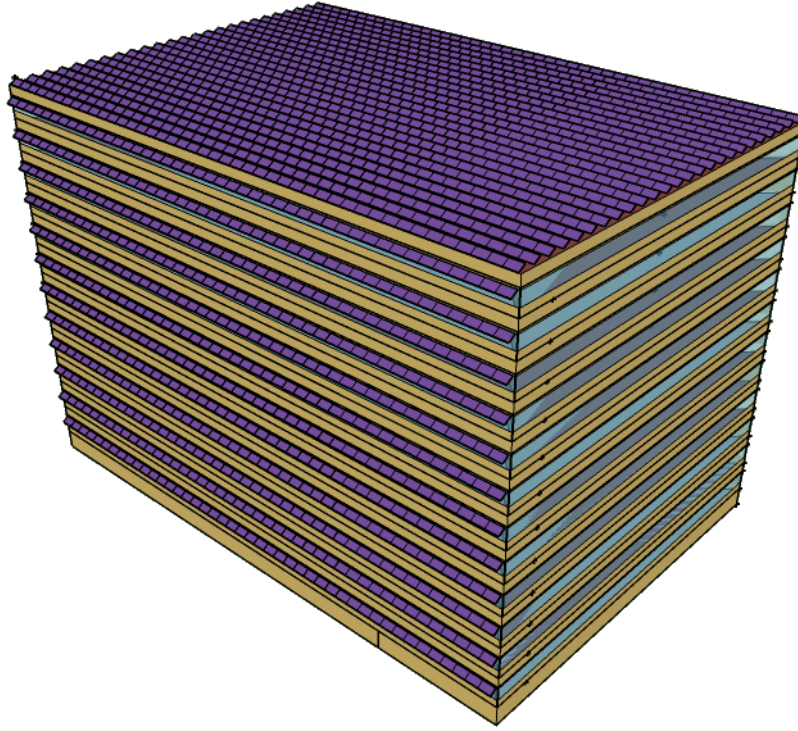


Figure 42: Representation of the building with the Sun shield and roof installations

With this model the energy simulation in EnergyPlus is performed to obtain the demand profile, it will be used later in the economic analysis. The same is done with the model of the Curtain wall configuration. The final results are presented in table 33, there is a slight reduction in the energy consumed, but the production over consumption ratio does not increase considerably.

Variable	Unit	Original	Base	Sun shield	Curtain wall
Installed power	kWp	0	0	488.4	885.87
Energy cons.	kWh	8,963,758.05	4,200,817.27	4,161,513.16	4,178,828.53
Specific energy	kWh/m^2	193.522	90.693	89.845	90.218
$E_{Sun\ shield}/E_{cons}$		11.56%	24.66%	24.90%	-
$E_{Curtain\ wall}/E_{cons}$		19.95%	42.56%	-	42.79%

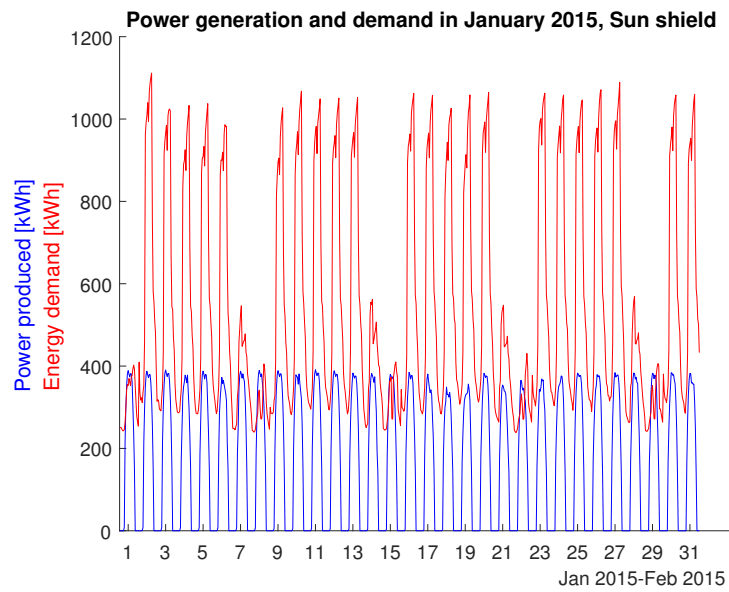
Table 33: Comparison between original, base and final cases

In annex A4 the detailed consumption by load category is presented for the Original case, Base case, Sun shield and Curtain wall. Comparing these two with the base case it is noticeable that the Sun shield allows a slightly better overall performance of the facility, especially in heat related mechanisms. Cooling and fans reduce their load around 5% while pumps and heat rejection almost 3%. With Curtain wall the interior lightning presents a bigger reduction of its load, but it is only around 1.3% and doesn't compensate the lower decrements in the other categories.

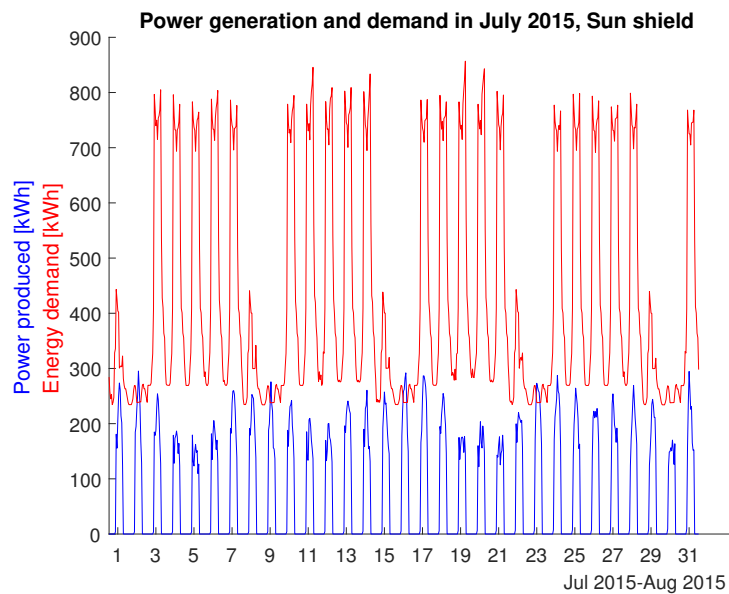
In both cases the electric equipment and exterior lights remain unchanged and since

these conform more than half the total demand of the building, they have the effect of reducing the percentage of change in the total energy consumed, which results in only 0.94% for Sun shield and 0.52% for Curtain wall.

It is possible to plot in the same graph the hourly data obtained in the simulations for the power generated and for the demand of the building, this is done to observe if there are moments during the year in which there is more energy production than the amount required in the facility. Figure 43 shows, for both configurations, the behavior in the months of January and July to represent the extreme conditions of summer and winter.

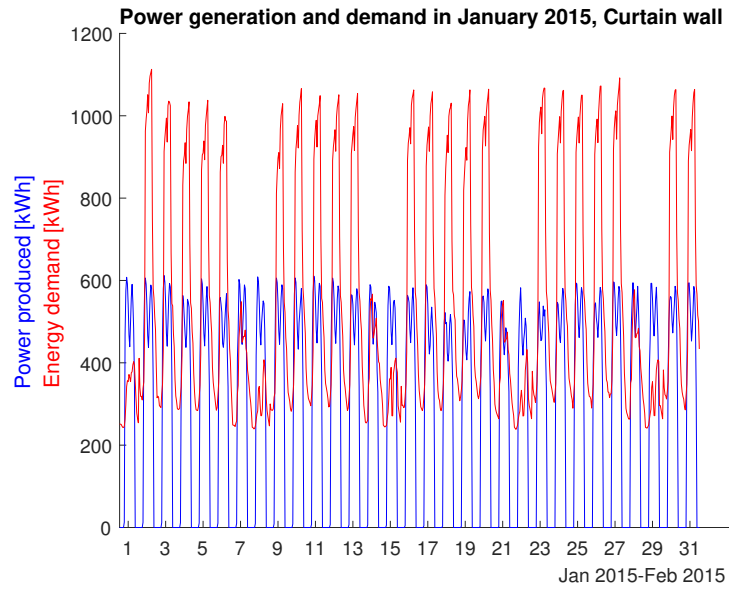


(a) Curves for January with Sun shield

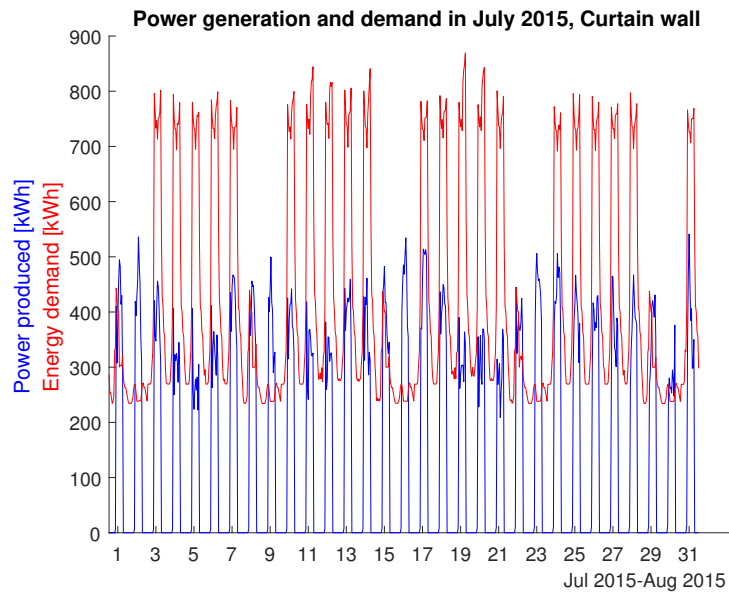


(b) Curves for July with Sun shield

Figure 43: Generation and demand during a month in summer and in winter



(c) Curves for January with Curtain wall



(d) Curves for July with Curtain wall

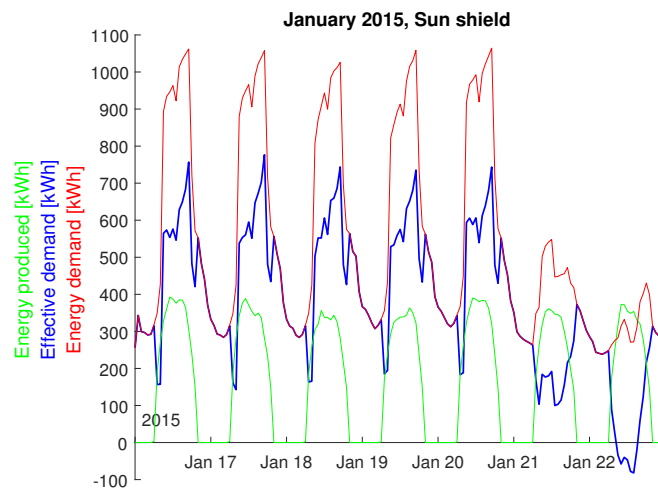
Figure 43: Generation and demand during a month in summer and in winter

The diagrams for all the months of the year are presented in annexes A6 and A7. In 43a and 43b the generation is lower than the consumption most of the time, only during weekends there is a small excess of power, specifically on Sundays. This effect occurs because of the typical shape of the demand profile for commercial buildings, as is was mentioned in section 4.1 the energy requirement is higher during the day and lower at night so both the energy production and consumption augment in the mornings and then decrease in the afternoons. Since on Sundays the demand is smaller than in the other days of the week, it is the moment when usually there is more generation and it can be injected to the electric network.

In January, when it is summer, the production is high and it can be clearly observed the effect of the synchronization between production and demand during the day. Every Sunday a little energy is delivered to the grid. In July, during winter, the irradiance is lower and there are more cloudy days. Most of the time the power generated is inferior than the minimum consumption, but even in these conditions there are some moments where energy is delivered to the grid.

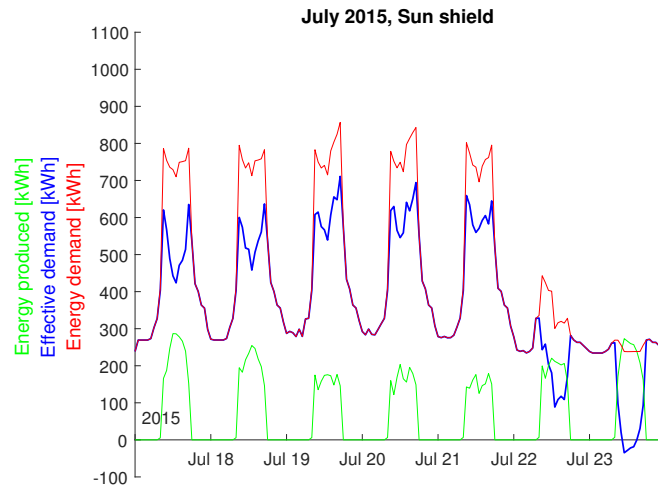
As for the case of Curtain wall, 43c and 43d show a higher amount of generated energy each day. Although the effect of the synchronization between production and demand is present, in January the production increases faster than the demand and there are moments of injection to the grid every morning in weekdays and through the day on weekends. Given that on winter sunrise occurs later, there is energy delivery to the network only on Saturdays and Sundays.

Finally, the generation, demand of the building in the base case and the effective demand to the network with the PV installation are plotted in the same graph. The effective demand refers to the actual amount of energy that is required from the network each hour, it is the difference between the total load of the building and the power generated during the day, when it is negative it means that it is being injected to the electric grid. Figure 44 shows these curves along with the generation for both configurations considered.

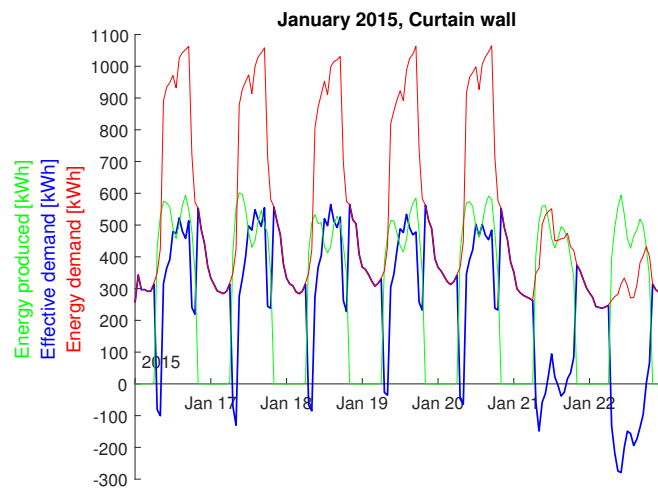


(a) Curves for January, Sun shield

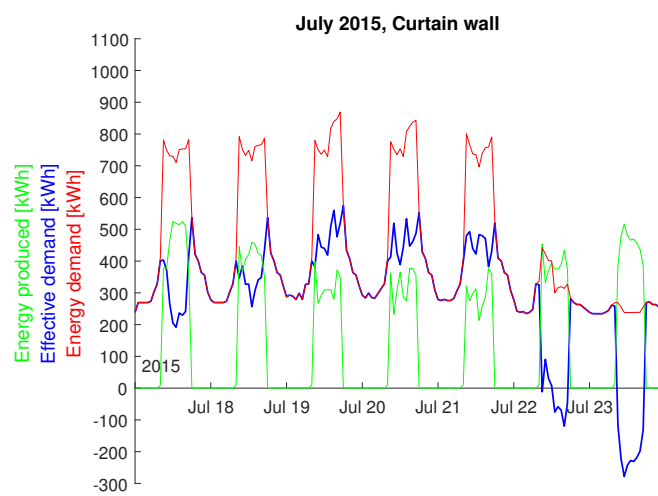
Figure 44: Generation, base and effective demands during a week in summer and in winter



(b) Curves for July, Sunshield



(c) Curves for January, Curtain wall



(d) Curves for July, Curtain Wall

Figure 44: Generation, base and effective demands during a week in summer and in winter

The diagrams illustrate the effect of peak shaving produced by the reduction of the maximum demand each day. This is more intense during summer days because the generation is higher, in winter is still possible to notice, with a reduction of approximately 150 *kW* with respect to the peak of the week for Sun shield and around 300 *kW* for Curtain wall. This outcome is useful because it helps reduce the monthly energy bill due to one component of the tariff, in section 7.1.1 it will be explained with more detail.

If the whole year is considered, the differences between the peak power for the first year is 278.1 *kW* for Sun Shield and 423.74 *kW* for Curtain wall, with the years the effect of the performance reduction makes these differences fall to 244.79 *kW* and 385.2 *kW* respectively. The peak shaving effect is stronger for the Curtain wall due to the higher power produced, but it also presents a bigger decline due to the performance reduction.

7 Economic analysis

This chapter focuses on the economic analysis performed for the photovoltaic system being simulated. The way in which the necessary parameters are estimated and the assumptions made to carry out the analysis are explained. The procedure followed to find the Net Present Value (NPV) in both configurations, the Payback Time, Internal Rate of Return (IRR) and the LCOE calculations are also described.

7.1 Tariffs

To perform an economic analysis for a project of electric generation it is important to know the tariffs of electricity that are applied because it is the way to assign a monetary value to the energy produced during the year. This section presents a small review of the tariffs used in Chile.

According to Chilean law [61], electricity tariffs are defined separately for High Voltage and Low Voltage clients, depending on whether they are connected to more than 400 V or less, respectively. In the case of low voltage rates, five main categories can be distinguished: those aimed at residential users (BT1 and TRBTx), the one determined by contracted power (BT2), the tariff per maximum demand read (BT3), the hourly tariff (BT4) and the rate for maximum demand in the distribution component (BT5). A small description of each one is provided:

- BT1: Simple tariff, the rate typically used by residential consumers, it has a limit of 10 kW of installed power. Four monthly charges are made, a fixed charge, one for the use of the network charged per kWh, one for the use of energy also charged per kWh and a charge for additional consumption during winter. There are variations called BT1a, BT1b that depend on the moment of the year when the maximum demand occurs, TRBT2 and TRBT3, that are similar to the next two rates that will be described.
- BT2: Contracted Power, the typical consumers are commercial and small industrial. A contracted power is established for a year, there are also 4 charges associated: fixed, use of network, use of energy and for contracted power. Since this is the tariff that corresponds to the building in consideration, it will be explained in more detail later.
- BT3: Maximum Demand, this rate requires a special meter to record the maximum flow rate at 15-minute intervals. There are also 4 charges associated: fixed, use of network, use of energy and in this case for the maximum read demand which is per kW.

- BT4: Hourly tariff, in this case a special meter is required to also record the maximum contracted or read power demand and maximum contracted or read power demand at peak times of the electrical system and offers three options:
 - BT4.1: Measurement of the total monthly energy consumed, contract of the maximum power demand during peak hours and the maximum power demand.
 - BT4.2: Measurement of the total monthly energy consumed, and the maximum power demand read at peak times, and contract of the maximum power demand.
 - BT4.3: Measurement of the total monthly energy consumed, the maximum power demand read at peak times and the maximum power demand supplied.
- BT5: It is aimed to for non-residential supplies and requires the metering of energy consumed, of the maximum demand power read at peak times and maximum demand supplied with 15-minute resolution or less and a mass memory for recording.

7.1.1 BT2 tariff

For the economic analysis the BT2 tariff will be used because the type of client that is usually is associated to it is of commercial type. A contracted power is established with the supplier and lasts for a 12-month period it can be used in any moment during this time, after that a new value can be accorded.

The monthly bill for this tariff is the result of the sum of four charges, for the proposes of this analysis the will be expressed in *USD* instead of Chilean pesos, the charges are:

- Monthly fixed charge (*USD/month*): It is billed every month and does not depend on the electric consumption. It is not considered in the analysis since remains invariant between the base case and the one with the photovoltaic system.
- Charge for the use of the Transmission System and Public Services (*USD/kWh*): It depends on the amount of energy consumed in the month, it considers the price associated to the structures needed to transport the electrical energy from the points of generation to the areas of consumption.
- Charge for energy (*USD/kWh*): It is the result of the multiplication of the energy consumed in the month by its unit price.
- Charge for Contracted Power (*USD/kW/month*): Obtained multiplying the contracted power by the corresponding unit price. This price can have two different values depending on whether the supply is classified as partially present at peak or present at peak.

Peak hours for the Chilean electric system are defined from 18:00 to 23:00 hours between April 1st and October 31st [62]. To determine if the supply is categorized as partially present at peak or present at peak the following ratio is used:

$$\frac{D_{peak}}{P_{contracted}} \geq 0.5 \quad (27)$$

D_{peak} is the average demand at peak hours, that is, the total consumption in that period divided by the number of peak hours. If the ratio is greater or equal to 0.5, as shown in equation (27), the supply is classified as present at peak, otherwise as partially present at peak.

In the case of the demand simulated, for a contracted power near the maximum power registered in an hour of the load profile the ratio in equation (27) is higher than 0.5 and thus the charge is for the present at peak category. Taking these definitions into consideration the values for the tariffs that will be used in the analysis are:

	Unit	Charge
Elec. Transport	<i>USD/kWh</i>	0.0157
Energy use	<i>USD/kWh</i>	0.1162
Contracted power	<i>USD/kW/month</i>	18.5413

Table 34: Tariffs applied for the monthly electric bill of the building

7.1.2 Net billing and PMGD

Since 2014 Chilean legislation allows regulated clients to generate electric energy locally, consume it and sell the surplus to the network. This initiative is focused on projects that use non-conventional renewable energy sources and the electricity sold is reduced from the monthly bill. It requires the use of a smart meter that records separately the consumption and the injection of electricity to the grid.

It is necessary that the meter records the two values because the energy injected is priced at a lower cost than the consumption in the total bill. When selling to the grid only the charge for energy is considered, while in the other case the transports charge is also included. The restriction to use this incentive is that the maximum installed power to be connected to the network is 100 *kW* [64] and there is a draft legislation that has been approved [63] to raise the limit to 300 *kW*.

In the case of the simulated system only the roof installation has an installed power of 330 *kW*, this exceeds both limits, so it is not possible to use the Net billing option. Bigger installations aimed at self-consumption can sell the excess of energy in moments of lower consumption using the Small Means of Distributed Generation (PMGD for the name in Spanish), in this case the energy is sold to the generation companies.

The PMGD model is less strict, both free and regulated consumers can use it and allows all types of generation technologies. When the project has a power under 1.5 MW there are benefits like a shorter process to connect to the grid [65]. The relevant aspect of this scheme for the economic analysis is that the energy is sold at the node price (when a stabilized price is chosen instead of the marginal price). This value is obtained from the technical report of the National Energy Commission (CNE) [66]. Table 35 shows the prices for the energy sold in the Net billing and the PMGD schemes.

	Net billing	PMGD
Price [USD/kWh]	0.1162	0.0751

Table 35: Prices estimation in Net billing and PMGD models

7.2 Net Present Value

One of the most common parameters used in the economic evaluation of projects is the Net Present Value, as the name says it takes into account the present value of all the cash flows involved in the development of the project during the period considered in the analysis. A simple definition would be as the difference between the benefits and the costs associated, but since these occur at different times, it is necessary to use the present value of all the cash flows. The criteria is that a project is profitable if the NPV is positive.

This analysis is performed in an annual basis, to bring the cash flows to the present an annual interest rate is used. Due to the characteristics of the project, there is a large initial investment related to the purchase and installation of the panels and inverters, while in the following years there are gains from the energy generated and small maintenance costs are incurred, for example in cleaning.

The calculation is performed as follows:

$$NPV = -C_0 + \sum_{t=1}^T \frac{C_t}{(1+r)^t} \quad (28)$$

C_0 represents the total initial cash flow that includes the investment required and the savings that can be considered, C_t the cash flows of each year considered as the difference between the earnings and the expenses of that year, r is the discount rate and T the years considered in the evaluation. To make a correct estimation of the factors to be considered, other parameters are required, the inflation rate to represent the evolution of prices over time and the euro-dollar exchange rate to express all amounts in the same currency. These parameters are shown in table 36.

Parameter	Value
Discount rate r	0.12
Inflation i	0.03
Euro-Dollar	1.18 (<i>USD</i>)

Table 36: Discount rate, inflation and conversion from euro to dollar

The value for the discount rate for the project is defined according to a economic study performed in Chile for a PV installation for a commercial application [67], since it is a similar project and in the same line of business, it can be assumed that the level of risk is similar and the associated discount rate would be the same. The inflation is provided by the Central bank of Chile [72] and the currency exchange rate is from the European Central Bank [73] on June 8, 2018.

7.2.1 Initial costs

The initial costs for this project include the purchase of the solar modules for the roof and the facade, the acquisition of inverters, the expenses associated with the installation, the wiring, for the fixing and stabilizing system and also the paperwork. The total cost of the modules is calculated separately for the roof, the Sun shield and the Curtain wall configurations, in the first two cases is determined considering the price per kWp and the installed power, while for the latter it is the price by square meter.

In section 5.1 the prices found are used to decide which model is selected, in this case the values are obtained from studies related to BAPV and BIPV systems. The Sun shield and the roof installations are classified as BAPV and the corresponding costs must be considered. A study on market potential and competitiveness for BIPV [68] also provides the investment expenses for an usual BAPV commercial installation.

The total cost is $0.95 \text{ } e/Wp$ and it is divided in $0.45 \text{ } e/Wp$ for the modules, which accounts for almost half of it, and the other half includes the DC and AC wiring, the mounting, the inverters, the installation, the studies required and finally a margin is considered of $0.14 \text{ } e/Wp$. The diagram that appears in the study is shown in figure 45 and in table 37 these values are expressed in *USD/Wp*.

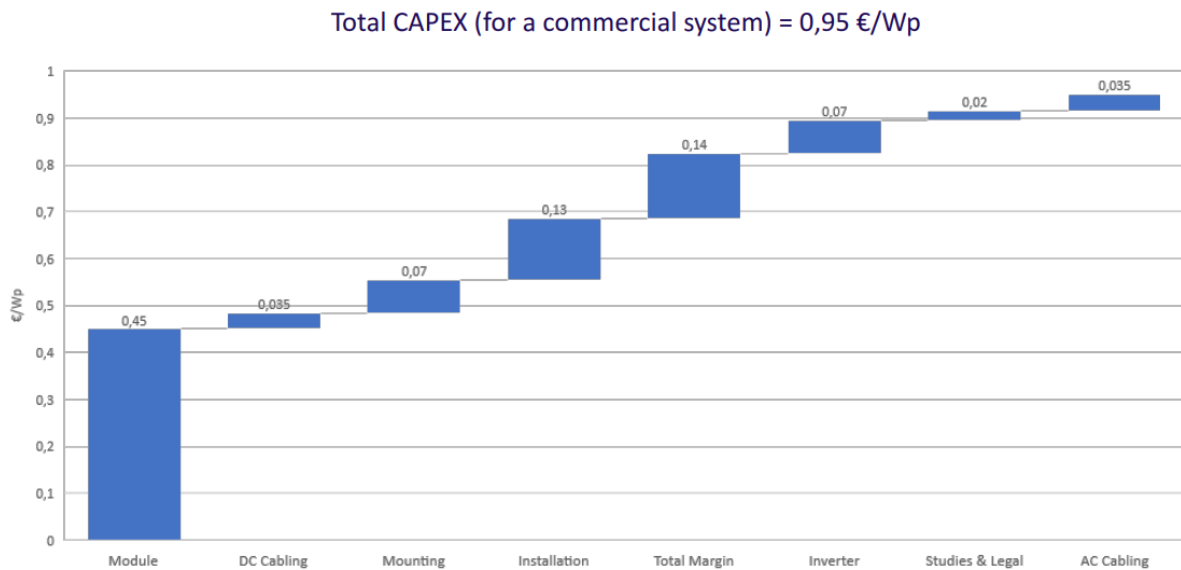


Figure 45: Capital Expenditures for a commercial BAPV system [68]

On the other hand, the Curtain wall configuration is categorized as BIPV, the associated costs are obtained from a report on solar building skins by SUPSI [69]. In this case the estimation of the initial costs is carried out considering each category as a percentage of the total initial investment, the cost of the solar modules provided by EnergyGlass is used to obtain the total value and then the other costs are determined. Figure 46 shows the percentages used.

An extra 10% is added to the original cost of the modules to take into account the shipping expenses since they were not included. Also, the cost of acquiring the inverters is used as calculated in section 5.1.4, since the number of purchased products is much lower in this category and it can be estimated directly.

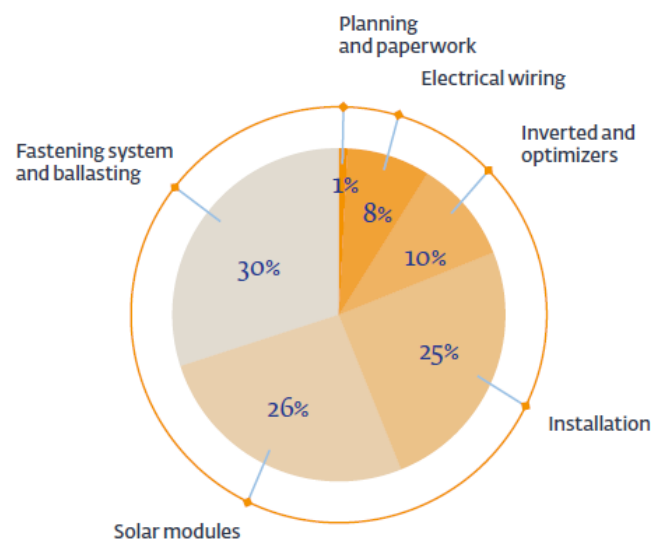


Figure 46: Percentages for each initial cost for building facades [69]

For the facades the cost of the modules is only a quarter of the total investment, the installation represents an equal expense and the fastening and ballasting is even higher. Considering these parameters and the cost for the PV panels in each case it is possible to obtain an estimation, the results are summarized in table 37. Since the roof installation is constant and added to the other two cases, the total initial costs are 545,362.09 *USD* for the Sun shield and 4,297,745.67 *USD* for the Curtain wall.

Category	[USD/W _p]	Sun shield	Roof	[USD/W _p]	Curtain wall
Solar modules	0.53	83,782.51	174,546.90	2.13	1,185,865.72
Inverters	0.08	13,032.84	27,151.74	0.1	89,706.53
Installation	0.15	24,203.84	50,424.66	1.86	1,036,595.91
Wiring	0.08	13,032.84	27,151.74	0.6	331,710.69
Mounting	0.08	13,032.84	27,151.74	2.24	1,243,915.09
Studies	0.02	3,723.67	7,757.64	0.07	41,463.84
Margin	0.16	26,065.67	54,303.48	-	-
Total	1.12	176,874.19	368,487.90	7.07	3,929,257.77

Table 37: Initial costs, in *USD*

It is easily noticeable that the inversion needed for the Curtain wall configuration is much higher than for the Sun shield, with a total initial cost almost seven times greater, if the roof is not considered it is more than twenty times higher. This is because there is more installed power and also the specific costs of each category are more expensive.

This effect is mainly due to the fact that the estimation of the costs in the BIPV system is made on the basis of percentages of the panels purchase prices, which are 4 times higher. In the case of the inverters there is not much variation because they are calculated differently than the other categories. As a result, the prices per kW_p associated with the studies are twice greater, the wiring is almost eight and the others even higher. The mounting costs stand out, for the Curtain wall configuration they get around 30 times more expensive than in a BAPV application. As a total the initial cost is around 690% greater but excluding the roof installation the difference increases to a 2,100%.

7.2.2 Fixed costs

Throughout the years of operation there are associated costs that remain relatively constant regardless of the level of production. For this project the cost of cleaning the modules is considered because, as explained in section 3.4, Santiago is characterized by a high level of pollution. During the winter months it is assumed that the water from rainfalls will be enough to maintain the modules clean. During the summer it will be necessary to clean them manually, every two months. It is assumed that the company that cleans the windows for the building also provides the service for the PV modules and it is required every two months in the warmer months.

This service can be contracted for a price of approximately 20 USD/m^2 [70]. For the case of the Curtain wall configuration only the area that corresponds to walls in the facade is considered, because in the case of windows, cleaning is not an incremental cost. If the photovoltaic installation had not been carried out, these windows would have had to be cleaned in any case, so the cost associated with them would have been paid anyway.

For the Sun shield and roof installations the cost will be considered as half, 10 USD/m^2 , because the modules in the facade will capture most of the dirt and the windows will require less frequent cleaning. In the case of the roof the modules are on a horizontal surface, which means a lower cost because the people that clean have easier access and there is no requirement for external equipment. In table 38 the costs for the first year are shown for each installation, for the following years they are adjusted to inflation.

	Sun Shield	Curtain wall	Roof
Cleaning cost [USD]	25,926.91	54,014.40	125,070.74

Table 38: Yearly additional cleaning costs for each category

7.2.3 Initial savings

One of the characteristics of BIPV is that the elements used to generate power are replacing construction components of the building, in the specific case of the Curtain wall configuration considered, semi-transparent photovoltaic modules substitute the windows of the north facade and opaque ones cover the walls. The cost of acquisition and installation of the elements that are replaced can be subtracted from the initial cost [71].

The cost associated to the purchase of the conventional windows is avoided, as well as the installation. This second factor is applied reducing the installation costs by a 40% which is the percentage of the facade covered by windows, for the opaque modules the amount remains unchanged. According to the report of SUPSI [69] the savings associated with conventional materials represent one third of the prices for the PV elements used.

It is assumed that the building in the base case does not have any kind of sun blocking system in the facade, which allows to compare the effects of Sun shield and Curtain wall. This is why in the case of Shun shield and the roof there are no initial savings, as no material is being replaced. Table 39 summarizes the values for both configurations:

Savings	Sun Shield	Curtain wall
Construction components	0	395,288.57
Installation	0	414,638.36
Mounting	0	497,566.04
Total	0	1,307,492.97

Table 39: Initial savings for each configuration, in USD

The greatest savings are achieved from the mounting of the windows, which also represented the highest value of the initial costs. The total initial savings reduce the initial cash flow of the project with Curtain wall in a 30%.

7.2.4 Gains

The profits obtained during each year will allow the initial investment to be progressively recovered and, if they are high enough, will make it possible for the project to begin generating economic gains. The yearly benefits of the installation are mainly due to the power that is self-consumed and therefore not purchased from the electricity grid. In that case the electric tariff for consumption is applied. As noted in section 6.6.2, there are some cases during the week specially on the weekends when the production is higher than the demand, in those situations the exceeding power has to be valued with the tariff for injection.

It must also be considered the change in the consumption of the building due to the installation of the photovoltaic system, not related to the power that is provided but to the energy implications of the installation, mainly modifying the cooling load. As it is pointed out in section 6.6.2 there is a reduction of the total electric load between the base case and the situation with the modules, for the Sun shield there is a decrease of 0.94% and with Curtain wall of 0.52%. This is also energy that does not have to be used from the grid, consequently it is valued with the tariff for consumption.

A third factor that is included in the economic benefits of the PV installation is the peak shaving effect. The tariff applied for the commercial building considers a charge to the contracted power that is added to the monthly electric bill, this variation of the power required from the grid allows to negotiate a lower power and thus reducing the resulting cost. Due to the performance reduction of the PV modules, as years go by the generation level will become lower and the peak shaving will have less impact.

Since the contracted power is agreed for periods of 12 months, a new maximum power can be considered for analysis each year. The difference of the maximum powers has to be calculated between the normal consumption in the base case and the resulting demand to the grid after having taken into account the contributions of the PV generation, in the case of each configuration. The value of that difference is used to estimate the savings in this component of the electric bill.

The diagrams from figures 47 and 48 illustrate the logic followed in the calculation of each factor that is part of the yearly gains. It is also important to apply an adjustment to include the effect of inflation when the economical values for the following years are being determined. The final gains for each year are the sum of these three elements.

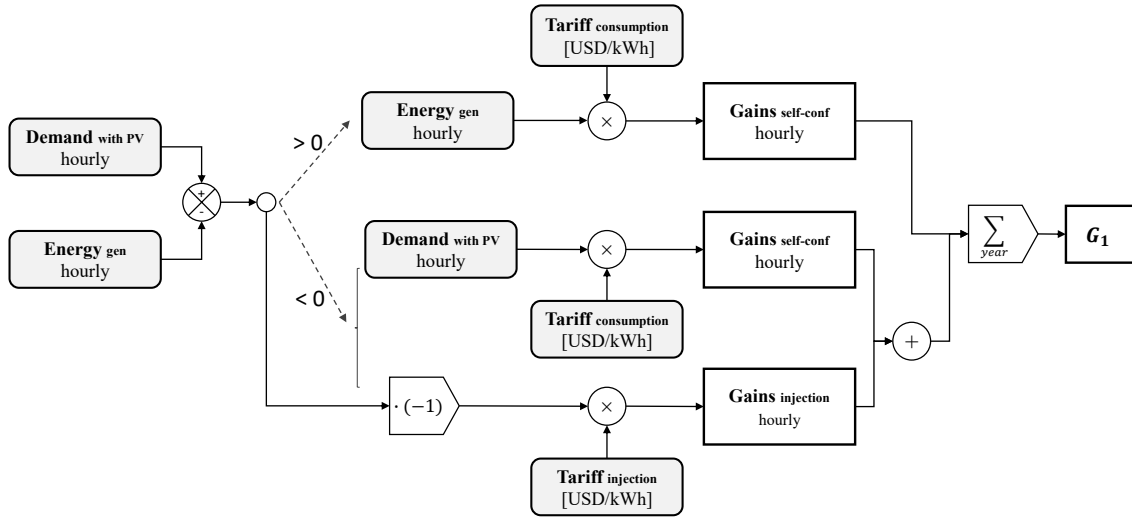


Figure 47: Calculation logic of the yearly gains related to power self-consumed or injected

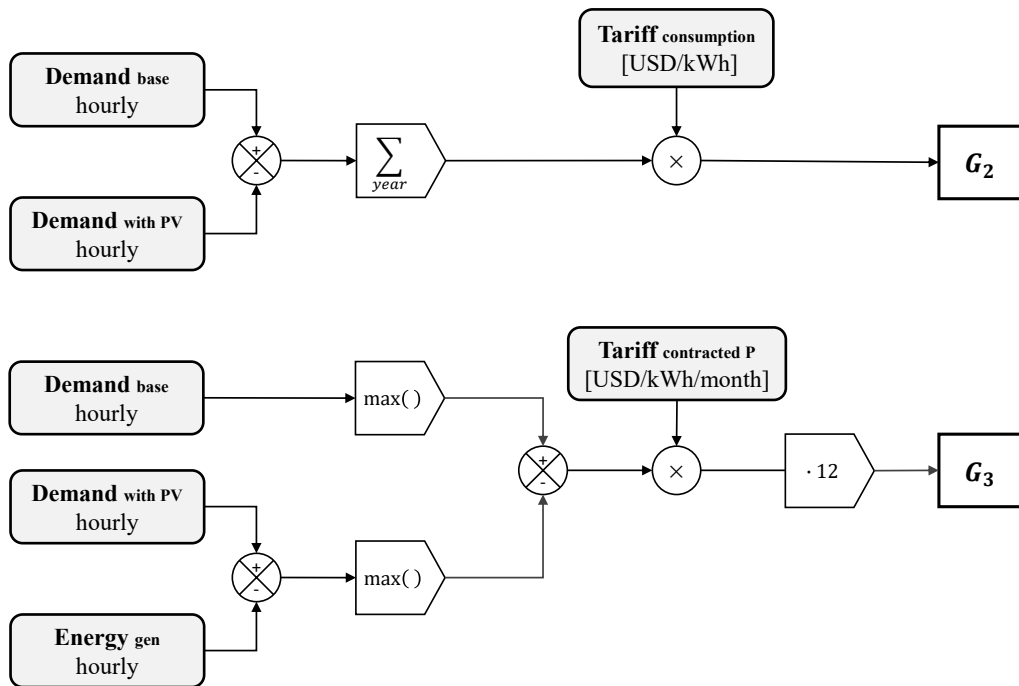


Figure 48: Calculation logic of the yearly gains related to load reduction and peak shaving

The gains are calculated for the Sun shield configuration and for the Curtain wall. The results for the first year, for each part and the global income, are summarized in table 40:

Gains	Sun shield	Curtain wall
G_1	135,783.04	228,067.25
G_2	5,184.31	2,900.41
G_3	63,684.14	95,817.36
Total	204,651.50	326,785.02

Table 40: Gains for the first year of operation, in *USD*

The Curtain wall configuration allows to have more total incomes each year, almost 60% higher than with Sun shield. This occurs mainly due to the energy self-consumed or delivered to the grid, since there is more installed power given the bigger surface available. On the other hand, the Sun shield installation presents higher gains from the reduction of the loads like cooling, but these only represent a 2.5% of the total and do not have an important effect on the overall benefits.

7.2.5 NPV, Payback Time and IRR

With the initial investment, initial savings, the fixed costs and the gains calculated for each period, the NPV is determined for both configurations. Using the notation from equation (28), the “0” index indicates that the cash flow is taken into account at the start of the project, the “t” index indicates the cash flow at the end of the corresponding year of operation. The values are used as follows:

- $C_0 = C_{module} + C_{inverter} + C_{install} + C_{wiring} + C_{mounting} + C_{studies} + C_{margin} - S_{tot}$
- $C_t = G_1 + G_2 + G_3 - C_{cleaning}$
- $T = 25$ years
- $r = 0.12$

Other parameters that are useful as economic indicators are the payback time and the internal rate of return. The payback time represents the number of years required to recover the investment in the project, it is obtained as the year in which the sum of the initial costs and the following cash flows starts being positive. A variation exists called the Discounted Payback Time and considers the present value of the variables to get the corresponding year. The IRR is the discount rate at which the NPV becomes 0, as shown in equation (29) if it is higher than the rate used, the project should be profitable.

$$-C_0 + \sum_{t=1}^T \frac{C_t}{(1 + IRR)^t} = 0 \quad (29)$$

In table 41 the resulting values for the four parameters previously described are presented. Installing the Sun shield configuration is profitable, the NPV is positive, over

565,000 *USD* in the 25 years in consideration. The investment is recovered in the 5th year, if the discounted cash flows are used, it is done in 7 years. The internal rate of return is 24.55%, higher than the 12% used, which also suggests that this photovoltaic installation is a good option.

Parameters	Unit	Sun shield	Curtain wall
NPV	<i>USD</i>	568,528.49	-1,733,576.42
Payback time	years	5	19
Disc. Payback t	years	7	25 +
IRR	-	0.2455	0.0277

Table 41: Main economical parameter for the projects

On the other hand, the Curtain wall is not profitable. Despite having greater gains each year of operation, these do not make up for the much higher initial investment required. The NPV is under $-1,700,000\text{USD}$ in the 25 years, which means the discounted payback time is higher than 25 years. If the present value is not considered, then the payback time becomes 19 years. The IRR is 2.77%, much lower than the 12% used, it also indicates that the project with this installation is not cost-effective.

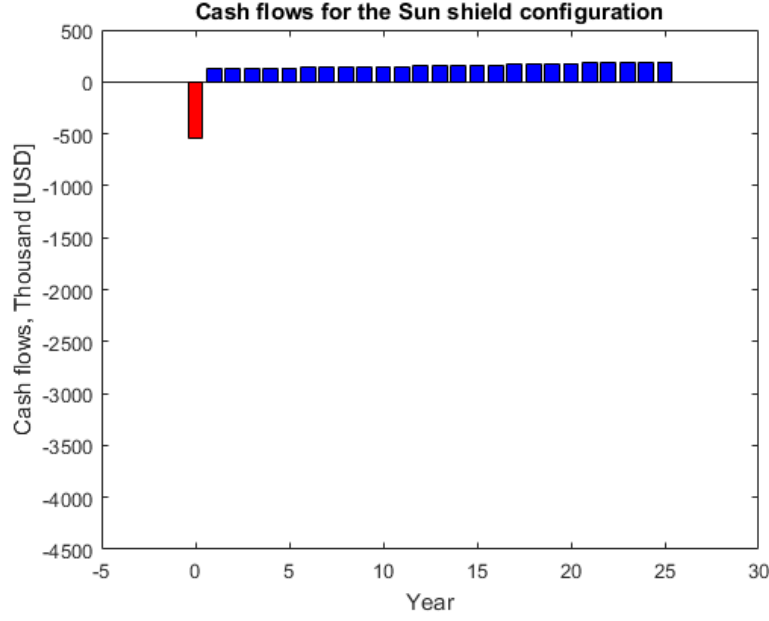
The evolution of the NPV over the 25 years and also the sum of the non-discounted cash flows is showed in table 42 to better illustrate the evolution of these variables and how is determined the discounted payback time and payback time. It is indicated with bold font the year and the corresponding value when it passes from negative to positive.

The total cash flows in each year are illustrated in figure 49, in the initial period it is possible to observe the big investment required to install the PV system, in the following 25 years the smaller incomes are portrayed. For Sun shield the initial investment is more than 4 times bigger than net profits of the first year, this is why it takes 5 years to recover it without discounting to represent present values, it would make the blue bars smaller over time. Instead, it is possible to see that the inflows increase over the years, this is caused because the inflation is taken into consideration for both the gains and the fixed costs.

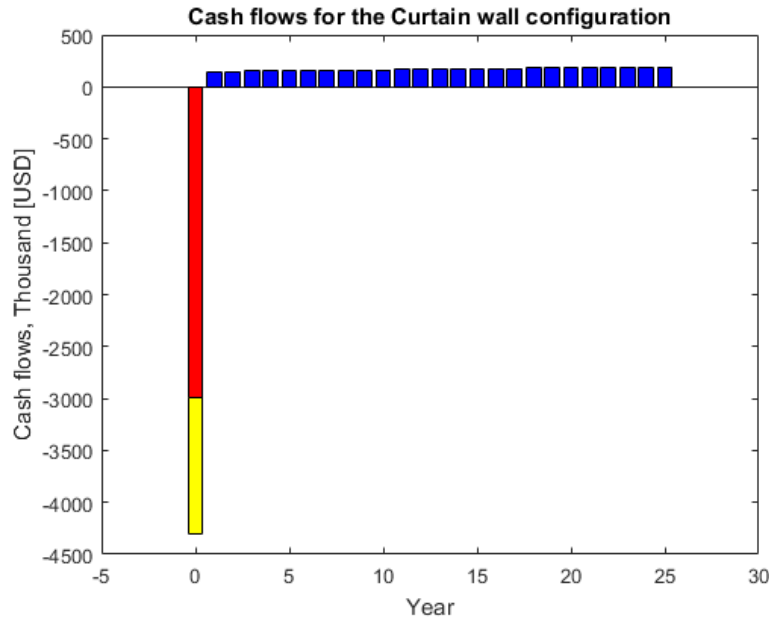
Year	Sun shield			Curtain wall		
	Cash flow	NPV	Sum CF	Cash flow	NPV	Sum CF
0	-545,362.09	-545,362.09	-545,362.09	-2,990,252.70	-2,990,252.70	-2,990,252.70
1	124,710.18	-434,013.71	-420,651.91	147,699.88	-2,858,377.80	-2,842,552.82
2	126,683.69	-333,022.25	-293,968.22	149,011.03	-2,739,587.13	-2,693,541.79
3	129,096.92	-241,133.62	-164,871.30	150,968.33	-2,632,130.85	-2,542,573.46
4	131,551.16	-157,530.48	-33,320.14	152,928.89	-2,534,941.78	-2,389,644.57
5	134,046.66	-81,468.80	100,726.51	154,891.28	-2,447,052.31	-2,234,753.29
6	136,584.26	-12,270.97	237,310.77	156,855.26	-2,367,584.55	-2,077,898.03
7	139,163.77	50,679.65	376,474.54	158,819.76	-2,295,742.56	-1,919,078.28
8	141,785.80	107,944.56	518,260.34	160,781.46	-2,230,805.62	-1,758,296.82
9	144,450.85	160,034.99	662,711.20	162,739.66	-2,172,120.07	-1,595,557.16
10	147,159.83	207,416.51	809,871.02	164,694.04	-2,119,093.00	-1,430,863.11
11	149,912.39	250,512.74	959,783.41	166,641.06	-2,071,187.67	-1,264,222.05
12	152,709.15	289,709.38	1,112,492.56	168,579.54	-2,027,917.50	-1,095,642.51
13	155,551.01	325,357.65	1,268,043.57	170,507.87	-1,988,841.50	-925,134.65
14	158,437.84	357,777.17	1,426,481.41	172,422.52	-1,953,560.44	-752,712.13
15	161,370.56	387,258.97	1,587,851.97	174,320.17	-1,921,712.80	-578,391.96
16	164,349.68	414,067.97	1,752,201.65	176,200.97	-1,892,970.60	-402,190.99
17	167,375.46	438,445.25	1,919,577.12	178,064.30	-1,867,036.54	-224,126.70
18	170,448.44	460,610.30	2,090,025.56	179,907.30	-1,843,641.47	-44,219.40
19	173,568.68	480,762.80	2,263,594.23	181,727.09	-1,822,541.73	137,507.69
20	176,736.52	499,084.50	2,440,330.75	183,522.52	-1,803,516.54	321,030.21
21	179,952.99	515,740.88	2,620,283.74	185,254.47	-1,786,369.46	506,284.69
22	183,218.43	530,882.51	2,803,502.17	186,388.32	-1,770,965.86	692,673.00
23	186,533.16	544,646.41	2,990,035.33	187,459.11	-1,757,133.63	880,132.11
24	189,897.32	557,157.25	3,179,932.65	188,462.79	-1,744,717.31	1,068,594.90
25	193,311.81	568,528.49	3,373,244.46	189,395.82	-1,733,576.42	1,257,990.72

Table 42: Cash flows, NPV and sum of the non-discounted cash flows, in *USD*

On figure 49b the initial investment is shown as the complete bar under 0, in yellow the savings are represented and in red the resulting incremental cash flow. Even with the reduction, it is more than five times the initial cost required for the Sun shield. The yearly profits instead, are only an 18% higher than the other case, although the gains are 60% bigger, the yearly cleaning costs are also larger and by 480%. With this situation the discounted profits are unable to match the initial outflow and results in a negative net present value.



(a) Cash flows for Sun shield



(b) Cash Flows for Curtain wall

Figure 49: Positive and negative cash flows in the period evaluated

7.2.6 Levelized Cost Of Energy, LCOE

The Levelized Cost Of Energy (LCOE) can be understood as the cost that has to be assigned to sell the produced energy, in order to have all the discounted inflows that occur due to electric production of the installation in its lifetime to be equal to the total life-cycle cost. This is shown in equation (30), then in equation (31) the usual definition is portrayed, C_{fix} in this case is $C_{cleaning}$.

$$\sum_{t=0}^T \frac{LCOE \cdot E_t}{(1+r)^t} = \sum_{t=0}^T \frac{-C_{0t} - C_{fix_t} + G_t}{(1+r)^t} \quad (30)$$

$$LCOE = \frac{\sum_{t=0}^T \frac{-C_{0t} - C_{fix_t} + G_t}{(1+r)^t}}{\sum_{t=0}^T \frac{E_t}{(1+r)^t}} \quad (31)$$

This parameter allows to compare the cost associated to the installation to others, that can use this type of technology or they can be related to others like wind or fossil fuels. The values for each case are as follows:

	Sun shield	Curtain wall
LCOE [<i>USD/kWh</i>]	0.1712	0.3597

Table 43: LCOE values for each configuration

For the Sun shield the cost to produce one kWh is of 0.1712 *USD*, while for the Curtain wall is approximately the double. It must be considered that in both cases the crystalline silicon technology is used, which is characterized by a high price. It is possible to compare with the other levelized costs presented in figure 50 from an analysis performed by Lazard [74].

The Curtain wall application does not seem to be competitive with any of the alternatives presented, the LCOE is higher than the upper end of the PV residential rooftop, nevertheless it must be considered that this study does not include BIPV examples and according to the report by SUPSI [69] these present a higher associated cost than the other PV solar technologies.

The Sun shield configuration on the other hand, is within the range of solar rooftop for commercial and industrial applications. Although most technologies have lower LOCE, it is competitive with some conventional like nuclear, integrated gasification combined cycle (IGCC) or gas peaking and also with some alternative like solar thermal.

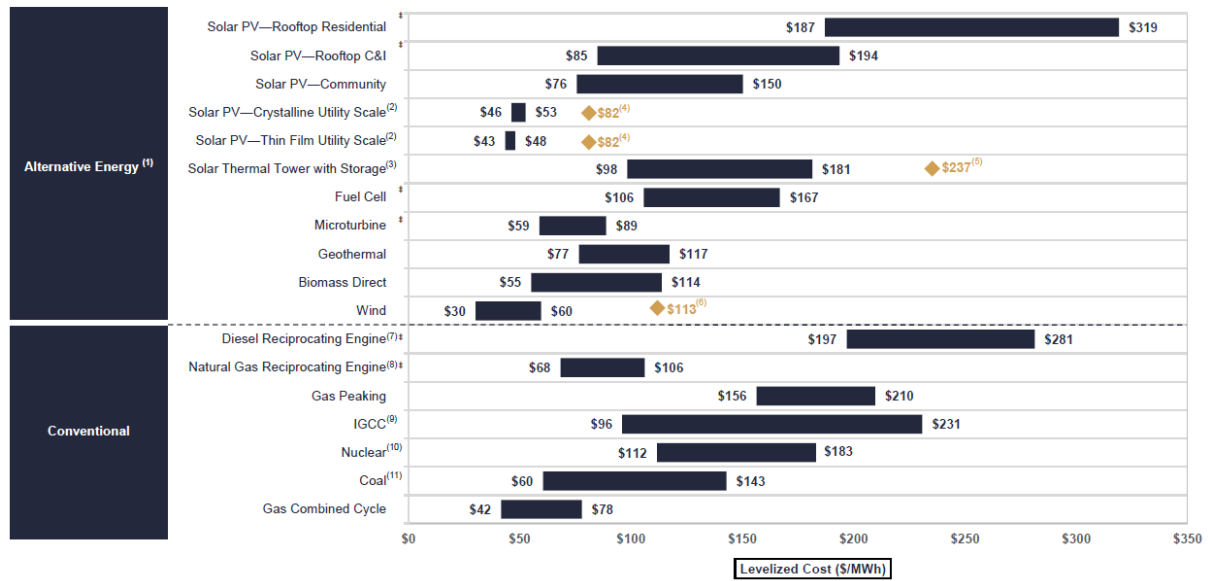


Figure 50: Levelized Cost of Energy for various technologies [74]

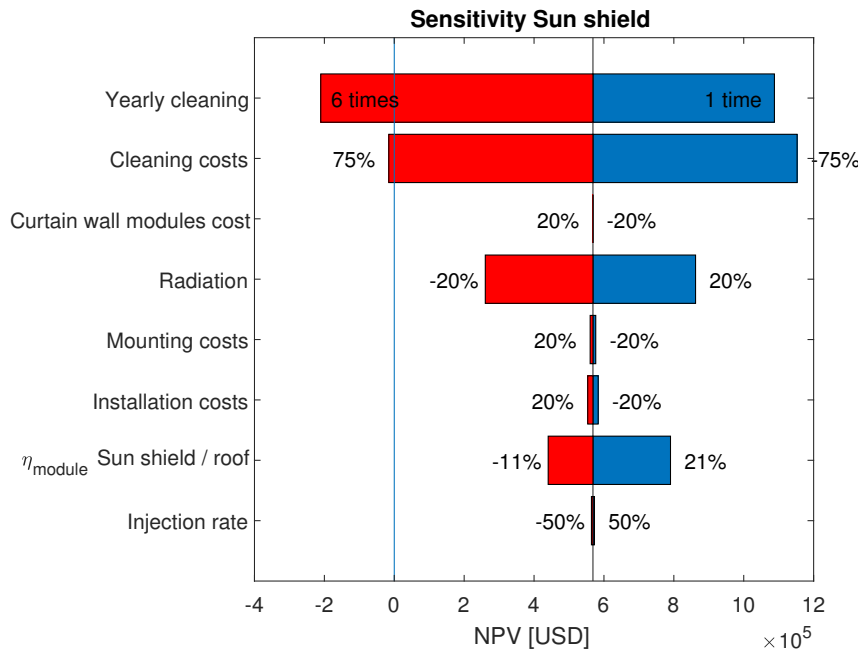
7.3 Sensitivity analysis

A simple sensitivity analysis will be performed to assess the effect of variations on some of the variables that were estimated in this economic evaluation. In each case a “*Ceteris Paribus*” situation is assumed, meaning that all other inputs remain constant. Eight criteria will be considered, the extreme values are defined as follows:

- Different cleaning costs modifying the number of times that is performed in the year. As a lower end 1 time a year is considered and as an upper end 6 times, this can be cleaning all year round every two months or during the summer every month.
- Changes in the actual cleaning charges by square meter. It is decreased a 75% to verify if the Curtain wall becomes profitable, the same percentage is increased to the original value, which can reflect the use of more sophisticated technologies to clean the glasses.
- Variations on the injection rate, for example if the Net Billing program could be applied for the installation, this would mean a rate 50% higher. A decrease by the same amount is used as the other end, it could represent a drop in the node prices of that area of the electric network.
- The use of high efficiency PV modules on the Sun shield and roof is modeled increasing the Wp/m^2 , the SunPower X22 360W [75] module has an efficiency of 22.2% and it is represented raising the Wp/m^2 approximately 21%. To represent an inferior efficiency the JKM265P-60 265W from Jinko Solar [11] is used, it has an efficiency of 16.2% which means a reduction of 11%.

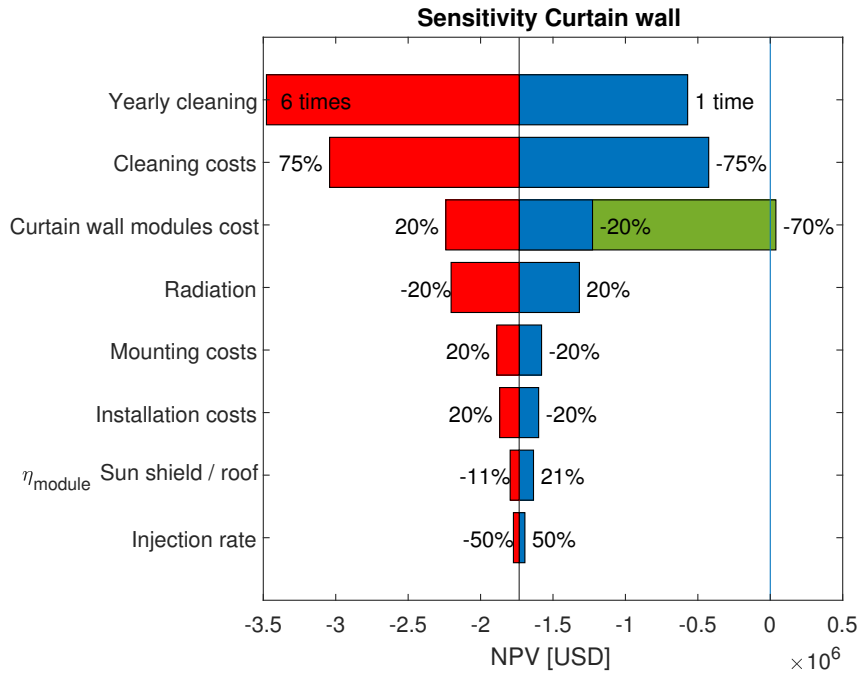
- The effect of a change in the prices for the Curtain wall modules is considered in a range of $\pm 20\%$, a higher cost can be the effect of higher transport rates than the estimated. The lower costs can be due to advancements in the technology, for example because of economies of scale or the development of new methods in the production processes.
- Changes in the installation costs, a range of $\pm 20\%$ is contemplated to take into account the possibility of a more expensive workforce and the learning effect for the manipulation of this new technology.
- Changes in the mounting costs, also between $\pm 20\%$ for the same reasons that were explained for the installation costs.
- Different levels of radiation, since the irradiance that arrives to the surface of a certain location is not the same every year, it is interesting to observe the effect on the profitability of the systems if it is a 20% higher or lower.

In figure 51 the tornado plots that are produced from the results of the sensitivity analysis are shown, the variables are sorted from the most influential to the ones that shows less changes.



(a) Tornado plot for Sun shield

Figure 51: Tornado plots for the eight variables sensitized



(b) Tornado plot for Curtain wall

Figure 51: Tornado plots for the eight variables sensitized

The most influential variable is the cleaning cost, mainly because a wider range is considered. If more regular cleaning is required as a result of increased dirt deposits due to environmental contamination, the Sun shield system also becomes unprofitable for 6 or more times a year. With respect to the Curtain wall, even if the modules are washed only one time a year the project remains unprofitable.

If no cleaning to the windows is performed during the year then the NPV for the Curtain wall system becomes approximately 11,000 *USD*, it is profitable. However, this is not a realistic result, the sensitivity analysis gives that outcome considering that all other variables remain constant, but if there is no cleaning of the PV modules, the dirt from the pollution in the air, dust and other factors will start to accumulate over the surface that receives sun irradiance. The overall efficiency will drop resulting in a lower production and thus less income.

Reducing the cleaning cost per square meter does not make Curtain wall profitable either. It has a greater effect than the change in the number of times it is cleaned in the year, but the NPV is $-425,000\text{USD}$. It would have to drop by a 99% to have positive results. Meanwhile the Sun shield presents negative results if the price for washing the modules increases by 75%. It is unlikely that the costs are reduced in the percentage considered but it is possible to have an increase of that magnitude due to the use other techniques for the cleaning of facades the can require more equipment.

The change in the cost of the Curtain wall modules has no effect on the Sun shield

results. Meanwhile the first is still in negative numbers, if the modules get a 70% cheaper the project starts producing profits in the 25-year period. This reduction in price is not feasible since mono crystalline technology is characterized by higher costs and other technologies offer lower prices but implies changes in characteristics such as efficiency and thermal coefficients, which leads to different results in production, that is why an upper limit of 20% was considered.

In both cases the increase and decrease of the irradiance level alters the output since the production varies accordingly, the reduction of the incident irradiation has a slightly bigger effect than the increase. The Sun shield is more sensitive to the changes but remains profitable in the range, with the NPV rising 52% and dropping 54% respectively. The Curtain wall does not change as much, with a 24% more and 27% less, in either case unprofitable.

The mounting and installation costs don't have a big influence on the outcome of the systems. In the Sun shield is even lower, around 1% for the mounting, in this case it is more important the installation since with the same variations the NPV changes by 3%. For Curtain wall the expenses for mounting are more significant with nearly a 9% deviation, while for installation is almost 8%.

The efficiency of the Sun shield modules does have a bigger influence on this configuration. With high efficiency there is almost a 40% improvement, a lower performance makes the NPV drop by around 130,000USD which is a little more than 20%, but it is still positive. On the Curtain wall it does have an effect since they are used in the roof, but the variations are near 6% and -3.5%.

The injection rate has a barely noticeable influence with variations under 1% on Sun shield and of 2.3% on Curtain wall. This means that the fact that these installations have to be under the PMGD normative instead of the Net billing does not affect largely the final results and also that changes on the node prices on the electrical network do not have a large effect.

8 Results and discussion

This thesis presented the sizing and 25-year simulation of two different configurations for a photovoltaic system installed in the north facade of a 12-floor office building in Santiago, Chile. In both cases mono-crystalline technology was used, one was a BAPV type and considered the installation of Sun shields, or saw-tooth curtain, on every window facing north with a rated power of 488.4 kWp . The other was BIPV and consisted of a Curtain wall in which the windows were made of semi-transparent PV modules and opaque versions covered the rest of the exterior walls, rated power of 885.87 kWp . The space in the roof was also used for solar generation with 330 kWp installed and it is already included in the total power indicated.

To obtain a demand profile an energy simulation of the building is performed and results in an annual consumption of 4,200.8 MWh without the solar installation. When the modules are added, the energy simulation shows that there is not a considerable change in the loads, decreasing 0.94% for the Sun shield and 0.52% for the Curtain wall. The simulation for the electric generation according to the solar irradiance that reaches the modules is carried out, for Sun shield the annual production is 1,036.1 MWh and for Curtain wall 1,788.0 MWh , it represents a 24.9% and 42.8% of the building consumption respectively.

Comparing the generation and demand daily profiles it is possible to corroborate the coincidence of the load behavior with the hours of solar electric production. This effect makes it possible to self-consume most of the energy and inject to the grid only part of it, mostly on weekends when the demand is lower and also in the moments when the solar radiation is higher, especially with the Curtain wall configuration. The self-consumption reduces the amount of energy that the building requires from the electric network during the day resulting in a peak-shaving effect, with differences of 278.1 kW for Sun shield and 423.74 kW for Curtain wall.

The annual and reference yields are higher for the Sun shield, 2,121.4 kWh/kWp and 2,583.2 $kWh \cdot m^{-2}/kW \cdot m^{-2}$ compared to the 2,018.4 kWh/kWp and 2,312.0 $kWh \cdot m^{-2}/kW \cdot m^{-2}$ with Curtain wall, it is mainly due to the better inclination of the modules to receive the solar radiation since the latter is vertical. The performance ratio instead is lower, 82.1% compared to 87.3% with the Curtain wall, because the PR represents the losses and gains in each system and the use of bifacial cells is modelled as a gain when the resulting power generated by Curtain wall is calculated.

The economic analysis considers 25 years of operation and indicates that, even though with Sun shield there is less power produced each year, it is profitable with an NPV of 568,000 USD and a payback time of 5 years. The Curtain wall instead is not economically viable, the NPV is -1,733,500 USD . Also, the LCOE is 0.171 USD/kWh and

0.360 *USD/kWh* respectively. These results are due to different factors, the initial costs associated with BIPV are higher than for BAPV, specially for the mounting and stability, also there is more peak power installed, these two result in a bigger initial investment that has to be overcome by the profits from the following years. Even though with BIPV there are initial savings from the materials that are replaced by PV modules and reduce by 30% the incremental cash flow, it is still more than five times greater than with Sun shield.

Another factor that has an influence on the negative NPV for Curtain wall is the fact that the annual profits are only 18% bigger compared to the ones with Sun shield and thus are not able to compensate the large initial expense. The gains from the energy produced are bigger, but the periodic cost of cleaning the modules becomes more important since there is a larger installed area to wash. There is a wide range of variability for the cleaning costs depending on the technologies used and the number of times a year that has to be performed, if it becomes too high even the Sun shield configuration becomes unprofitable. Other costs and variables like the incident radiation don't have an effect as big as the cleaning costs over the economic viability of the project.

The economic gains that are obtained with the systems for the first year are approximately 205,000 *USD* and 325,000 *USD* but, in both cases, only a 70% of those amounts is from the energy that is not consumed or injected to the grid, a 30% comes from the reduction of the peak power that is required by the building during the year. This is dependent on the available radiation, if it is low during the moments of highest consumption the corresponding gains will be greatly reduced.

One possible solution to this situation would be to include energy storage in the systems. This allows to manage the electricity generated by the solar panels and have a more stable peak shaving during the hours of high consumption. The addition changes the operation of the system, adds new costs and also modifies the gains so it is a different approach from the one used in this thesis project, but it is interesting for a future feasibility analysis.

Although with current values for costs and efficiencies only the Sun shield configuration is economically viable, future advancements may change the situation for Curtain wall installations. Third generation photovoltaics show promising results for low cost modules that also have properties like transparency or even color, also the gain of experience working with this type of applications will provide advancements in technologies and processes that will also reduce other costs related to installation, mounting and stability and then make this type of photovoltaic system profitable.

9 Bibliography

References

- [1] F. Birol, “Key World Energy Statistics”, International Energy Agency, 2017 [Online]. Available: <https://webstore.iea.org/key-world-energy-statistics-2017>. [Accessed: June 28, 2018]
- [2] M. Hosenuzzaman et al., “Global prospects, progress, policies, and environmental impact of solar photovoltaic power generation”, *Renewable and Sustainable Energy Reviews*, vol. 41, pp. 284 - 297, 2015 [Online]. Available: <http://www.sciencedirect.com/science/article/pii/S1364032114007229>. [Accessed: June 28, 2018]
- [3] A. A. Bayod-Rjula, “Future development of the electricity systems with distributed generation”, *Energy*, vol. 34, no. 3, pp. 377 - 383, 2009 [Online]. Available: <http://www.sciencedirect.com/science/article/pii/S0360544208003174>. [Accessed: Dic. 18, 2017]
- [4] A. K. Shukla, K. Sudhakar and P. Baredar, “A comprehensive review on design of building integrated photovoltaic system”, *Energy and Buildings*, vol. 128, supplement C, pp. 99 - 110, 2016 [Online]. Available: <http://www.sciencedirect.com/science/article/pii/S0378778816305667>. [Accessed: Dec. 18, 2017]
- [5] E. Biyik et al., “A key review of building integrated photovoltaic (BIPV) systems”, *Engineering Science and Technology, an International Journal*, vol. 20, no. 3, pp. 833 - 858, 2017 [Online]. Available: <http://www.sciencedirect.com/science/article/pii/S2215098616309326> [Accessed: Dic. 18, 2017]
- [6] M. Günther et al., “Solar Radiation”, in *Advanced CSP Teaching Materials*, Enermena, 2011, pp. 8-67.
- [7] G.V. Fracastoro, “Technologies for Renewable Energy Sources”, Politecnico di Torino, Italy, 2017.
- [8] F. Spertino, “Photovoltaic Power Systems (short handbook)”. 2016, pp. 3-10.
- [9] F. Spertino, “Power Generation from Renewable Sources”, Politecnico di Torino, Italy, 2016.
- [10] Trina Solar, “The Honey M Plus+ framed 60-cell module”, TSM-DD05A.08(II) datasheet, 2017 [Revised March 2018].
- [11] Jinko Solar, “JKM265P-60 245-265 Watt Poly Crystalline Module”, JKM265P-60 datasheet, 2015 [Revised March 2018].
- [12] D. Chen et al., “21.40% efficient large area screen printed industrial PERC solar cell.”, *31st European Photovoltaic Solar Energy Conference and Exhibition*, Hamburg, 2015, pp. 334-340 [Online]. Available: https://www.researchgate.net/publication/283729906_2140_EFFICIENT_LARGE_AREA_SCREEN_PRINTED_INDUSTRIAL_PERC_SOLAR_CELL. [Accessed: June 25, 2018]
- [13] R. Guerrero-Lemus et al., “Bifacial solar photovoltaics A technology review”, *Renewable and Sustainable Energy Reviews*, vol. 60, pp. 1533 - 1549, 2016 [Online]. Available: <http://www.sciencedirect.com/science/article/pii/S1364032116002768>. [Accessed: June 19, 2018]
- [14] M. Pollawa et al., “Advances in Cost-Efficient Thin-Film Photovoltaics Based on Cu(In,Ga)Se₂”, *Engineering*, vol. 3, no. 4, pp. 445 - 451, 2017 [Online]. Available: <http://www.sciencedirect.com/science/article/pii/S2095809917306033>. [Accessed: Dic. 18, 2017]
- [15] J. Jean et al., “Pathways for solar photovoltaics”, *Energy & Environmental Science*, vol. 8, no. 4, pp. 1200-1219, 2015 [Online]. Available: <http://pubs.rsc.org/-/content/articlelanding/2015/ee/c4ee04073b/unauth#!divAbstract>. [Accessed: June 19, 2018]

- [16] R. Luthander et al., "Photovoltaic self-consumption in buildings: A review", *Applied Energy*, vol. 142, pp. 80 - 94, 2015 [Online]. Available: <http://www.sciencedirect.com/science/article/pii/S0306261914012859> [Accessed: June 20, 2018]
- [17] C. A. Hill et al., "Battery energy storage for enabling integration of distributed solar power generation", *IEEE Transactions on Smart Grid*, vol. 3, no. 2, pp. 850-857, 2012 [Online]. Available: <http://ieeexplore.ieee.org/stamp/stamp.jsp?tp=&arnumber=6198748&isnumber=6204228>. [Accessed: Dic. 18, 2017]
- [18] O. M. Toledo, D. Oliveira Filho and A. Alves Cardoso. "Distributed photovoltaic generation and energy storage systems: A review", *Renewable and Sustainable Energy Reviews*, vol. 14, no 1, pp. 506-511, 2010 [Online]. Available: <http://www.sciencedirect.com/science/article/pii/S136403210900207X>. [Accessed: Dic. 18, 2017]
- [19] M. Schmela, G. Masson, T.M.N. Ngo, "Global Market Outlook for Solar Power 2016-2020", European Photovoltaic Industry Association, Brussels, Belgium, 2016.
- [20] REN21, "Renewables 2018 Global Status Report", *Renewable energy policy network for the 21st century*, 2018 [Online]. Available: <http://www.ren21.net/gsr-2018/>. [Accessed: June 27, 2018]
- [21] PVPS, IEA. "Snapshot of Global Photovoltaic Markets". *Report IEA PVPS T1-33:2018*, 2018 [Online]. Available: http://www.iea-pvps.org/fileadmin/dam/public/report/statistics/IEA-PVPS_-_A_Snapshot_of_Global_PV_-_1992-2017.pdf. [Accessed: June 27, 2018]
- [22] D. Feldman, J. Hoskins and R. Margolis, "Q4 2017/Q1 2018 Solar Industry Update", NREL, 2018 [Online]. Available: <https://www.energy.gov/eere/solar/q4-2017q1-2018-presentation-solar-industry-update>. [Accessed: June 27, 2018]
- [23] B. Marion et al., "Performance parameters for grid-connected PV systems", in *Conference Record of the Thirty-first IEEE Photovoltaic Specialists Conference, 2005.*, 2005, pp. 1601-1606.
- [24] L. R. d. Nascimento and R. Rother, "Fifteen years and counting: The reliable long-term performance of the first grid-connected, building-integrated, thin-film photovoltaic installation in Brazil", in *2014 IEEE 40th Photovoltaic Specialist Conference (PVSC)*, 2014, pp. 3372-3377.
- [25] Central Intelligence Agency, "The World Factbook 2018", 2018. [Online]. Available: <https://www.cia.gov/library/publications/the-world-factbook/index.html> [Accessed: May 26, 2018]
- [26] Chile, Instituto Nacional de Estadísticas, *Compendio Estadístico*. Santiago: INE; 2017. [Online] Available: <http://www.ine.cl/docs/default-source/publicaciones/2017/compendio-estadistico-2017.pdf?sfvrsn=6>. [Accessed: May 26, 2018]
- [27] Weatherbase.com, "Santiago, Chile", 2018. [Online]. Available: <http://www.weatherbase.com/weather/weather-summary.php3?s=47558&cityname=Santiago%2C+Santiago+Metropolitan%2C+Chile&units=>. [Accessed: May 24, 2018]
- [28] Meteoblue.com, "Climate Santiago", 2018. [online]. Available: https://www.meteoblue.com/en/weather/forecast/modelclimate/santiago_chile_3871336. [Accessed: May 25, 2018]
- [29] R. Escobar et al. "Estimating the potential for solar energy utilization in Chile by satellite-derived data and ground station measurements", *Solar Energy*, vol. 121, pp. 139-151, 2015. [Online]. Available: <http://www.sciencedirect.com/science/article/pii/S0038092X15004703>. [Accessed May 26, 2018]
- [30] A. Molina, M. Falvey and R. Rondanelli, "A solar radiation database for Chile", *Scientific Reports*, vol. 7, no.1, pp. 14823, 2017. [Online]. Available: <https://doi.org/10.1038/s41598-017-13761-x>. [Accessed: May 27, 2018]
- [31] Worlddata.info, "Sunshine and sunset in Chile", 2018. [online]. Available: <https://www.worlddata.info/america/chile/sunset.php>. [Accessed: May 27, 2018]

- [32] I. Kavouras et al. "Source Apportionment of PM10 and PM25 in Five Chilean Cities Using Factor Analysis", *Journal of the Air & Waste Management Association*, vol. 51, no. 3, pp. 451-464, 2001. [Online]. Available: <https://doi.org/10.1080/10473289.2001.10464273>. [Accessed: May 27, 2018]
- [33] Comisin Nacional de Energia, *Reporte mensual sector energtico, volumen N 38*. Santiago: CNE; 2018. [Online] Available: <https://www.cne.cl/nuestros-servicios/reportes/informacion-y-estadisticas/>. [Accessed June 27 2018]
- [34] SINCA.mma.gob.cl, "Regin Metropolitana de Santiago, Estaciones de monitoreo de la calidad del aire", 2018. [Online]. Available: <https://sinca.mma.gob.cl/index.php/region/index/id/M>. [Accessed: May 27, 2018]
- [35] S. M. Frank and P. K. Sen, "Estimation of electricity consumption in commercial buildings", in *2011 North American Power Symposium*, 2011, pp. 1-7.
- [36] Pacific Northwest National Laboratory, US, "Commercial Prototype Building Models", 2018. [Online]. Available: https://www.energycodes.gov/development/commercial/prototype_models. [Accessed: April 4, 2018]
- [37] M. DERU et al. "US Department of Energy commercial reference building models of the national building stock", National Renewable Energy Laboratory, 2011. [Online]. Available: <https://www.nrel.gov/docs/fy11osti/46861.pdf>. [Accessed: March 14, 2018]
- [38] S. Goel et al. "Enhancements to ASHRAE standard 90.1 prototype building models", Pacific Northwest National Laboratory (PNNL), Richland, WA (US), 2014. [Online]. Available: https://www.energycodes.gov/sites/default/files/documents/PrototypeModelEnhancements_2014_0.pdf. [Accessed: May 20, 2018]
- [39] DOE, US, "EnergyPlus", 2018. [Online]. Available: <https://energyplus.net/>. [Accessed: April 5, 2018]
- [40] DOE, US, "EnergyPlus Version 8.9.0 Documentation, Engineering Reference", 2018. [Online]. Available: <https://energyplus.net/documentation>. [Accessed: April 6, 2018]
- [41] DOE, US, "OpenStudio", 2018. [Online]. Available: <https://openstudio.net>. [Accessed: May 22, 2018]
- [42] DOE, US, "Building Component Library", 2018 [Online]. Available: <https://bcl.nrel.gov>. [Accessed: April 4, 2018]
- [43] PV Tech.org, "Top 10 module suppliers in 2017", 2018. [Online]. Available: <https://www.pv-tech.org/editors-blog/top-10-module-suppliers-in-2017>. [Accessed: March 22, 2018]
- [44] FreeCleanSolar "295W Trina Solar Panel Mono TSM-295DD05A.05", 2018. [Online]. Available: <http://www.freecleansolar.com/295W-Trina-Solar-Panel-Mono-TSM-295DD05A-05-p/tsm-295dd05a.05.htm>. [Accessed: March 28, 2018]
- [45] H. Darhmaoui and D. Lahjouji, "Latitude Based Model for Tilt Angle Optimization for Solar Collectors in the Mediterranean Region", *Energy Procedia*, vol. 42, pp. 426 - 435, 2013 [Online]. Available: <http://www.sciencedirect.com/science/article/pii/S1876610213017451>. [Accessed: May 7, 2018]
- [46] EnergyGlass, "EnergyGlass Solar & Glass Architecture", 2018. [Online]. Available: <https://energyglass.gruppostg.com/it/> [Accessed: April 16, 2018]
- [47] R. Macconi, "Richiesta ricevuta attraverso il sito ITALIANO EnergyGlass", 2018
- [48] NSP, "NS6QL Mono-Crystalline Silicon Solar Cell", NS6QL datasheet, 2017 [Revised June 12]
- [49] SunEarthTools.com, "Sun Position", 2018 [Revised June 2018].

- [50] PowerFromSunlight.com, “Best Solar Panel Reviews: The Complete Expert Review About Trina Solar TSM-DD05A.05 (II) 290 Watt Peak”, 2017. [Online]. Available: <https://www.powerfromsunlight.com/best-solar-panel-reviews-complete-expert-review-trina-solar-tsm-dd05a-05-ii-290-watt-peak/>. [Accessed: May 28, 2018]
- [51] NaturalEnergyHub.com, “Top Solar Inverter makers in the world (2016 2017) Germanys SMA leads world solar inverter market by revenue”, 2017. [Online]. Available: <https://naturalenergyhub.com/solar-energy/top-solar-inverter-makers-world/>. [Accessed: April 5, 2018]
- [52] SMA, “Sunny Tripower 60-US”, Sunny Tripower 60-US datasheet, [Revised: May 31, 2018]
- [53] SMA, “Installation Guide, Sunny Tripower 60”. [Online], Available: <http://files.sma.de/dl/25977/STP60-10-1A-xx-11.pdf>. [Accessed: June 12, 2018]
- [54] SolaricaShop, “SMA Sunny Tripower 60”, 2017. [Online]. Available: <https://www.solaricashop.com/solar-inverters/sma/sma-sunny-tripower-60.html>. [Accessed: April 4, 2018]
- [55] A. Molina, “Modelo de radiacin solar”, Dept. Geofisica, Universidad de Chile, 2017. [Online]. Available: <http://ernc.dgf.uchile.cl:48080/downloads/radiacion.pdf>. [Accessed: Feb. 22, 2018]
- [56] A. Molina, “Modelo de generacin fotovoltaica”, Dept. Geofisica, Universidad de Chile, 2017. [Online]. Available: <http://ernc.dgf.uchile.cl:48080/downloads/fotovoltaico.pdf>. [Accessed: June 16, 2018]
- [57] L. Yang, H. Yan and J. C. Lam, “Thermal comfort and building energy consumption implications A review”, *Applied Energy*, vol. 115, pp.164 - 173, 2014 [Online]. Available: <http://www.sciencedirect.com/science/article/pii/S0306261913008921>. [Accessed: june 3, 2018]
- [58] Action Energy “Energy Consumption Guide 19, Energy Use in Offices”, Crown, London, 2003.
- [59] N. Jung et al. “Energy performance analysis of an office building in three climate zones”, *Energy and Buildings*, vol. 158, pp. 1023 - 1035, 2018. [Online]. Available: <http://www.sciencedirect.com/science/article/pii/S0378778817316456>. [Accessed: June 3, 2018]
- [60] F. Martellota, A. Cannavale and U. Ayr, “Comparing energy performance of different semi-transparent, building-integrated photovoltaic cells applied to reference buildings”, *Energy Procedia*, vol. 126, Supplement C, pp. 219 - 226, 2017. [Online]. Available: <http://www.sciencedirect.com/science/article/pii/S1876610217336299>. [Accessed: Dec. 18, 2017]
- [61] *Decreto N 11T de 2016*, 2016. [Online]. Available: <http://bcn.cl/21x2o>
- [62] Enel, “Tarifas”. [Online]. Available: <https://www.eneldistribucion.cl/tarifas>. [Accessed: May 3, 2018]
- [63] Asociacin Chilena de Energia Solar (ACESOL), “Cambios a Ley Netbilling”, 2018. [Online]. Available: <https://www.acesol.cl/noticias/item/1300-cambios-a-ley-netbilling.html>. [Accessed: May 3, 2018]
- [64] *Ley 20571*, 2014. [Online]. Available: <http://bcn.cl/1v0bx>
- [65] Ministerio de Energia, “Generacin distribuida en Chile”, 2016. [Online]. Available <https://www.cne.cl/wp-content/uploads/2016/11/PPT-Ministro-seminario-Gx-Dx-25oct2016.pdf>. [Accessed: June 10, 2018]
- [66] Comisin Nacional de Energia, “FIJACIN DE PRECIOS DE NUDO PROMEDIO DEL SISTEMA ELCTRICO NACIONAL Y DE AJUSTES Y RECARGOS POR APLICACIN DEL MECANISMO DE EQUIDAD TARIFARIA RESIDENCIAL, INFORME TCNICO DEFINITVO”, CNE, Santiago, 2018. [Online]. Available: <https://www.cne.cl/wp-content/uploads/2017/10/20171122-ITD-PNP-ENE18.pdf> [Accessed: June 10, 2018]

- [67] BID, “Energía Fotovoltaica del Autoconsumo”, BID, 2015. [Online]. Available <https://publications.iadb.org/bitstream/handle/11319/6897/Folleto-Energia%20Fotovoltaica%20de%20Autoconsumo%20en%20Sector%20Industrial%20y%20Comercial.pdf>. [Accessed: May 20, 2018]
- [68] G. Masson, “BIPV Competitiveness and Market Potential”, Becquerel Institute, 2017. [Online]. Available: http://www.energyville.be/sites/default/files/7masson_0.pdf. [Accessed: June 8, 2018]
- [69] SUPSI and SEAC, “Building Integrated Photovoltaics: Product overview for solar building skins. Status Report”, SUPSI and SEAC, 2017. [Online]. Available: http://www.bipv.ch/images/Report%202017_SUPSI_SEAC_BIPV.pdf. [Accessed: May 8, 2018]
- [70] Vertical Chile, “Vertical Chile”, 2018 [Online]. Available: <http://verticalchile.cl/index.html>. [Accessed: June 4, 2018]
- [71] Odersun AG, “Manual for BiPV Projects”, Odersun AG, 2011. [Online]. Available: <https://www.ntnu.no/wiki/download/attachments/40800075/Odersun-BiPV-Download.pdf?version=1&modificationDate=1326906420000>. [Accessed: May 6 2018]
- [72] Banco Central de Chile, “Inflación”, 2018. [Online]. Available: <http://www.bcentral.cl/web/guest/inflacion>. [Accessed: May 20, 2018]
- [73] European Central Bank, “US Dollar (USD)”, 2018. [Online]. Available: https://www.ecb.europa.eu/stats/policy_and_exchange_rates/euro_reference_exchange_rates/html/eurofxref-graph-usd.en.html. [Accessed: June 8, 2018]
- [74] Lazard, “Lazard’s Levelized Cost of Energy Analysis - Version 11.0” Lazard, 2017. [Online]. Available: <https://www.lazard.com/perspective/levelized-cost-of-energy-2017/>. [Accessed: June 20, 2018]
- [75] SunPower, “SunPower X-Series Residential Solar Panels | X22-360”, X22-360 datasheet, 2016 [Revised June 2018].

10 Annexes

A1 Datasheet for the TSM-DD05A.08 (II) PV module

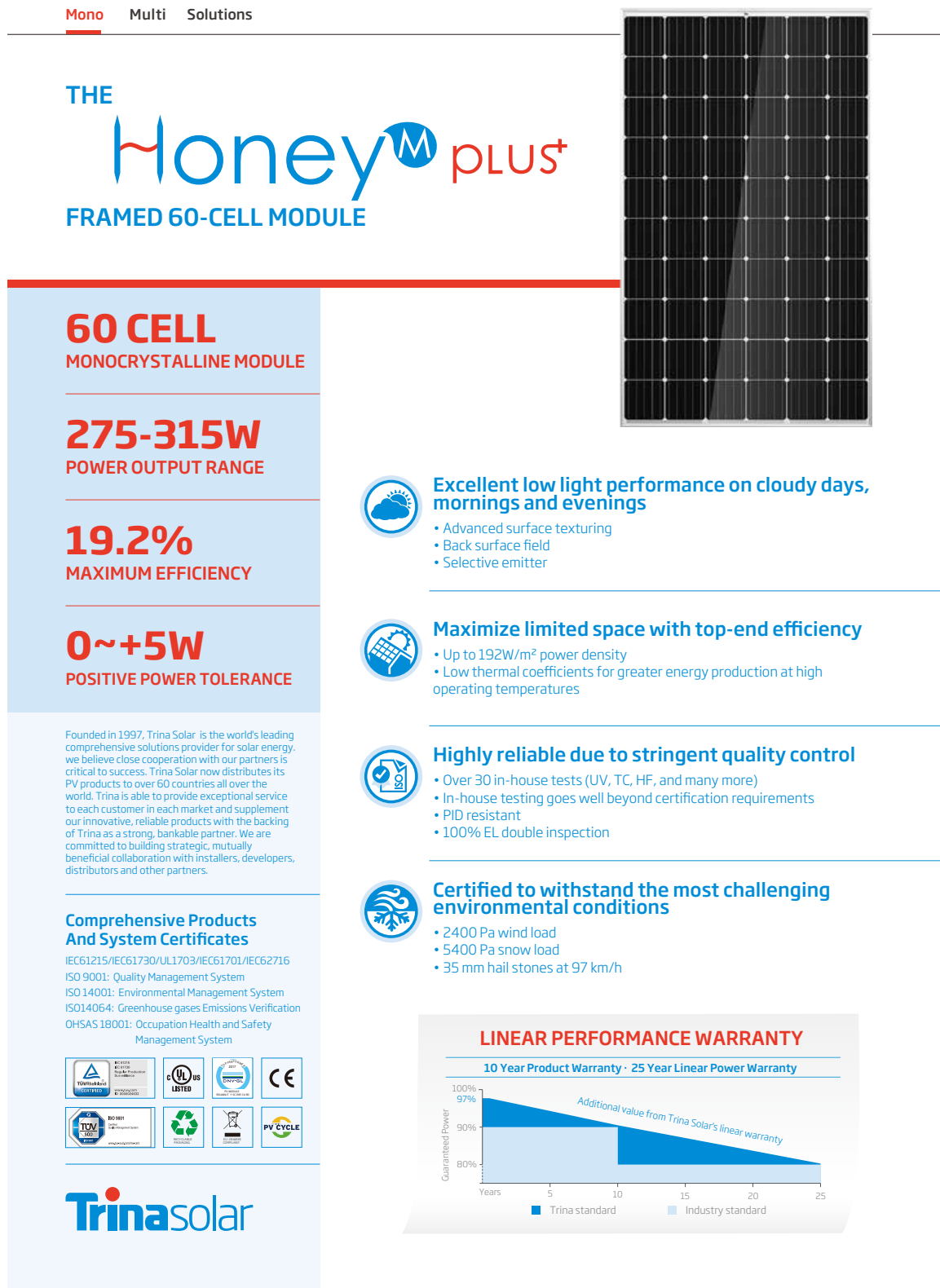


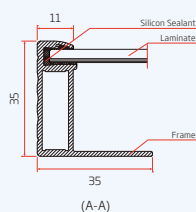
Figure 52: Complete datasheet for PV module in Sun shield configuration [10]

POWER RANGE

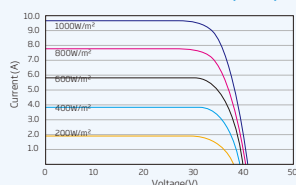
TSM-DD05A(II)	280-315W
TSM-DD05A.08(II)	280-315W
TSM-DD05A.05(II)	275-310W

Technical drawing of the front panel of the 1000 Series 12-Drain Rack. The panel is rectangular with dimensions 947mm width and 1650mm height. It features a Nameplate at the top left, a Junction Box at the top right, and a 12-Drain Hole at the bottom center. The panel is mounted on a 35mm thick base. The drawing includes labels for the 4-Ø 3/4" Installing Hole and the 6-Ø 4.3 Grounding Hole. The panel is shown with a 1000mm scale bar.

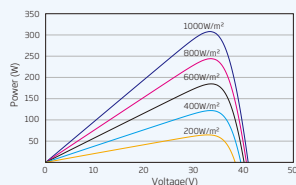
Back View



I-V CURVES OF PV MODULE(305W)



P-V CURVES OF PV MODULE(305W)



Peak Power Watts- P_{MAX} (Wp)*	275	280	285	290	295	300	305	310	315
Power Output Tolerance- P_{MAX} (W)	0 ~ +5								
Maximum Power Voltage- V_{MP} (V)	31.4	31.7	31.8	32.2	32.5	32.6	32.9	33.1	33.3
Maximum Power Current- I_{MP} (A)	8.76	8.84	8.97	9.01	9.08	9.19	9.28	9.37	9.46
Open Circuit Voltage- V_{OC} (V)	38.4	38.4	38.5	38.9	39.6	39.8	40.0	40.2	40.5
Short Circuit Current- I_{SC} (A)	9.24	9.42	9.51	9.66	9.68	9.77	9.85	9.94	10.0
Module Efficiency η_m (%)	16.8	17.1	17.4	17.7	18.0	18.3	18.6	18.9	19.2

STC: Irradiance 1000W/m², Cell Temperature 25°C, Air Mass AM1.5.
*Measuring tolerance: ±3%.

Maximum Power- P_{MAX} (Wp)	205	209	212	216	220	223	227	231	235
Maximum Power Voltage- V_{MPP} (V)	29.1	29.4	29.5	29.9	30.1	30.2	30.5	30.7	30.9
Maximum Power Current- I_{MPP} (A)	7.04	7.10	7.21	7.24	7.30	7.38	7.46	7.53	7.60
Open Circuit Voltage- V_{OC} (V)	35.7	35.7	35.8	36.2	36.8	37.0	37.2	37.4	37.6
Short Circuit Current- I_{SC} (A)	7.46	7.61	7.68	7.80	7.82	7.89	7.95	8.03	8.10

NOCT: Irradiance at 800W/m². Ambient Temperature 20°C. Wind Speed 1m/s

Solar Cells	Monocrystalline 156.75 × 156.75 mm (6 inches)
Cell Orientation	60 cells (6 × 10)
Module Dimensions	1650 × 992 × 35 mm (65.0 × 39.1 × 1.38 inches)
Weight	18.6 kg (41.0 lb)
Glass	3.2 mm (0.13 inches), High Transmission, AR Coated Tempered Glass
Backsheet	White [DD05A(II), DD05A.08(II)]; Black [DD05A.05(II)]
Frame	Silver Anodized Aluminium Alloy [DD05A(II)]; Black Anodized Aluminium Alloy [DD05A.08(II), DD05A.05(II)]
J-Box	IP 67 or IP 68 rated
Cables	Photovoltaic Technology Cable 4.0mm² (0.006 inches²), 1000 mm (39.4 inches)
Connector	MC4/UTX/TS4/QC4 *

*Please refer to regional datasheet for specified connector.

TEMPERATURE RATINGS

NOCT (Nominal Operating Cell Temperature)	44°C (±2°C)
Temperature Coefficient of P _{MAX}	- 0.39%/°C
Temperature Coefficient of V _{OC}	- 0.29%/°C
Temperature Coefficient of I _{SC}	0.05%/°C

MAXIMUM RATINGS

Operational Temperature	-40~+85°C
Maximum System Voltage	1000V DC (IEC) 1000V DC (UL)
Max Series Fuse Rating	15A (Power ≤285W) 20A (Power ≥290W)

(DO NOT connect Fuse in Combiner Box with two or more strings in parallel connection)

WARRANTY

10 year Product Workmanship Warranty

25 year Linear Power Warranty

(Please refer to product warranty for details)

PACKAGING CONFIGURATION

Modules per box: 30 pieces

Modules per 40' container: 840 pieces

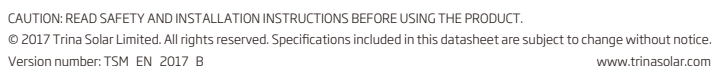


Figure 52: Complete datasheet for PV module in Sun shield configuration [10]

A2 Datasheet for Sunny Tripower 60-US inverter



SUNNY TRIPOWER 60-US



STP60-US-10

Efficient	Reliable	Cost-Effective	Innovative
<ul style="list-style-type: none">• Maximum efficiency of 98.8%• Superior power density: 60 kVA at only 165 pounds	<ul style="list-style-type: none">• Distributed architecture for maximum system availability• Central control with SMA Inverter Manager	<ul style="list-style-type: none">• DC input of up to 1,000 V• Up to 2.5 MW per inverter manager	<ul style="list-style-type: none">• Suitable for commercial and utility applications• Complete grid management feature set

SUNNY TRIPOWER 60-US

The efficient solution for medium to large-scale PV Plants

The new Sunny Tripower 60-US is part of an innovative, global system solution for commercial and utility PV plants. This solution combines the advantages of a decentralized system layout with the benefits of centralized inverter designs which results in the best of both worlds. High efficiency, easy installation, simple commissioning and low maintenance requirements contribute decisively to reducing the operating costs for the entire plant.

Figure 53: Complete datasheet for Inverter [52]

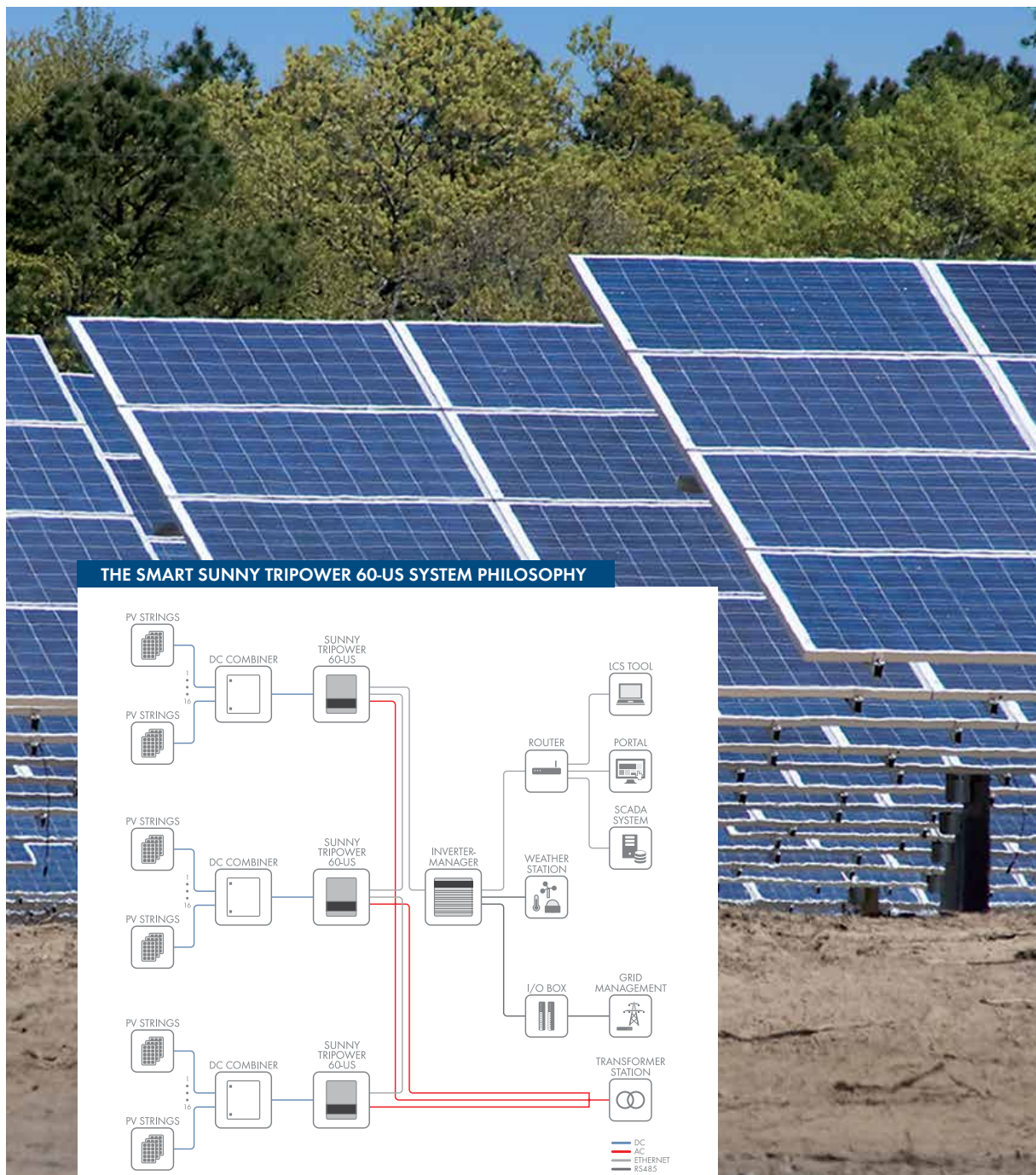


Figure 53: Complete datasheet for Inverter [52]



UNMATCHED POWER DENSITY

With Maximum Efficiency

The new SMA system solution consists of three components: highly efficient Sunny Tripower 60-US inverters, the SMA Inverter Manager and the LCS commissioning tool. It is precisely this systemized approach that makes the Sunny Tripower 60-US so unique and ensures a high level of performance.

System Cost Reduction

With a compact design of 60 kVA weighing only 165 pounds, the Sunny Tripower 60-US requires little space, reduces on-site preparation work, simplifies installation and lowers maintenance costs.

Innovative system management

The SMA Inverter Manager is the central communications component and sole interface for the entire system control. It handles all the important inverter and system management functions for up to 2.5 MW with a single inverter manager.

The Sunny Tripower 60-US benefits from a self-configuring inverter network with automatic IP configuration and device discovery, which eliminates manual setup. The SMA Inverter Manager also creates a seamless inverter control loop which enables complete grid management capabilities.

Simple commissioning

The specially developed LCS tool (Local Commissioning and Service Tool) makes commissioning easy, saves time and reduces costs. The inverter is configured by simply selecting the system-specific configuration files and then transmitting them to all inverters. In addition, individual inverter data is aggregated into a single plant profile for comprehensive plant performance analysis.

Figure 53: Complete datasheet for Inverter [52]

Technical data	Sunny Tripower 60-US
Input (DC)	
Max. input voltage	1,000 V
MPP voltage range	570 V to 800 V @400 VAC, 685 V to 800 V @480 VAC
Min. input voltage	565 V @400 VAC, 680 V @480 VAC
Max. input current / short-circuit current	110 A / 150 A
Number of independent MPP inputs / strings per MPP input	1/1 (split up by external PV array junction box)
Output (AC)	
Rated power at nominal voltage	60,000 W
Max. apparent AC power	60,000 VA
Output Phases / line connections	3 / PE
Nominal AC voltage	400 V, 480 V
Nominal AC voltage range	352 V to 440 V @400 VAC, 423 V to 528 V @480 VAC
AC power frequency	50 Hz, 60 Hz
Rated power frequency / rated grid voltage	50 Hz, 60 Hz / 400 V, 480 V
Max. output current	3 x 87 A @ 400 V, 3 x 72 A @ 480 V
Power factor at rated power/displacement power factor adjustable	1/0.8 lagging ... 0.8 leading
Feed-in phases / connection phases	3 / 3
Efficiency	
Max. efficiency / CEC @ 400 VAC / CEC @ 480 VAC	98.8% / 98.0% / 98.5%
Protective devices	
DC-side disconnection point / DC surge arrester (type II) can be integrated	● / ●
Ground fault monitoring / grid monitoring	● / ●
DC reverse polarity protection / AC short-circuit current capability / galvanically isolated	● / ● / -
All-pole sensitive residual-current monitoring unit	●
Protection class (acc. to IEC 62103)/overvoltage category (acc. to IEC 60664-1)	I / AC: III, DC: II
General data	
Dimensions (W / H / D) / weight	570 / 740 / 300 mm (22.4 / 29.1 / 11.8 inch) / 75 kg (165.3 lbs)
Operating temperature range	-25 °C ... +60 °C (-13 °F to +140 °F)
Noise emission, typical / Self-consumption (at night)	55 dB(A) / 3W
Topology / cooling concept, degree of protect. (IEC 60529/UL50E), climatic cat. (IEC 60721-3-4)	Transformerless / active, IP65 / NEMA 3R, 4K4H
Maximum permissible value for relative humidity (non-condensing)	95%
Features	
DC connection / AC connection	Screw terminal / screw terminal
Display / Interface	Graphic / Using external inverter manager: Modbus TCP
● Standard features ○ Optional features – Not available	
Type Designation Sunny Tripower 60-US: STP 60-US-10 with DC Switch SMA Inverter Manager: IM-10: SMA Inverter Manager for max. 42 inverters I/O Module: IM-DIO-10: SMA Digital I/O Box with 6 digital inputs Certificates and Approvals Sunny Tripower 60-US: IEC 62109-1/IEC 62109-2 (Class I, grounded—communication Class II, PELV), UL1741—w. Non-Isolated EPS Interactive PV Inverters, IEEE 1547, FCC Part 15, Subpart B Class A SMA Inverter Manager: UL 508, UL 60950-1, CSA C22.2 No. 60950-1-07, EN 60950-1, EN 55022 Class A, EN 61000-3-2 Class D, EN 61000-3-3, EN55024, FCC Part 15, Subpart B Class A	
Technical data	SMA Inverter Manager
Voltage supply	
Input voltage	9 - 36 Vdc
Power consumption	< 20 W
General data	
Dimensions (W / H / D) / weight	160 / 125 / 49 mm (6.3 / 4.9 / 1.9 inch) / 940 g (2 lbs)
Degree of protection / assembly	IP21 / DIN top-hat rails or wall mounting
Operating temperature range / relative humidity	-40 to +85 °C / 5 - 95 % (non-condensing)
Cooling concept	Convection
Interfaces	
User interface / Sensor interface	LCS tool for PC / RS-485 for Sunspec Alliance compatible weather stations
Active and reactive power setpoints	Constant values, curves, remotely controlled
Interface to inverter network / Interface to external network	1 Ethernet port (RJ45) / 1 Ethernet port (RJ45) Modbus TCP, SunSpec Alliance
Interface to remote control	6 x DI, Modbus TCP via external I/O module
Data at nominal conditions	

+1 888 476 2872
www.SMA-America.com

SMA America, LLC

Figure 53: Complete datasheet for Inverter [52]

A3 Generic office types from the Energy consumption guide

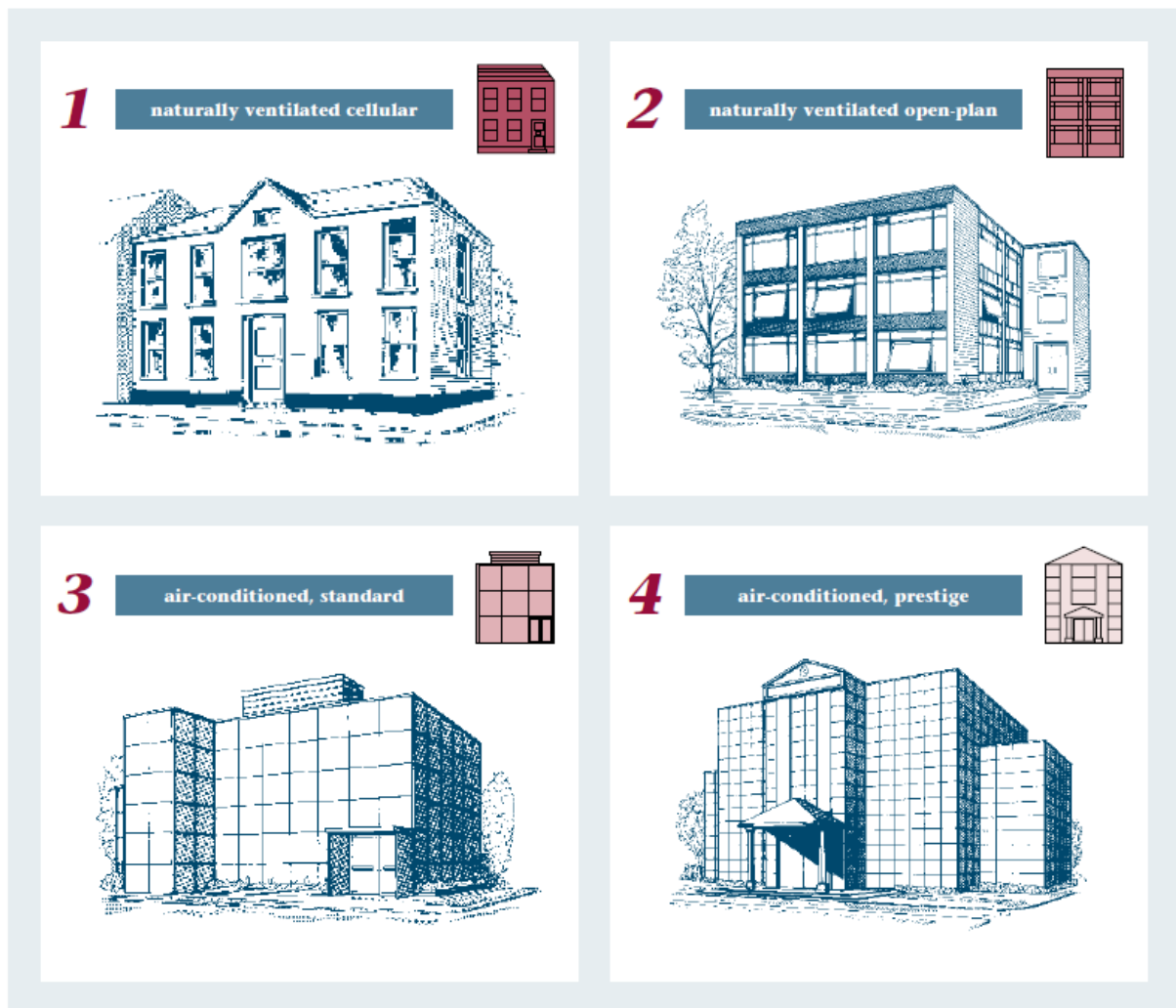


Figure 54: Four categories in which office buildings are classified in the study [58]

A4 Consumption of each load over a year, for all the cases modelled

Load	Original	Base	Sun shield	Curtain Wall
Cooling	686,295.53	274,050.75	260,523.82	270,415.53
Interior Lighting	976,973.33	968,652.50	961,284.44	956,319.44
Exterior Lighting	719,476.94	176,009.78	176,009.78	176,009.78
Interior Equipment	5,777,700.00	2,387,972.22	2,387,972.22	2,387,972.22
Exterior Equipment	-	-	-	-
Fans	600,233.61	242,561.69	228,540.56	238,058.86
Pumps	131,351.78	84,583.11	82,055.00	83,505.25
Heat Rejection	71,726.86	66,987.22	65,127.34	66,547.44
Total	8,963,758.05	4,200,817.27	4,161,513.16	4,178,828.53

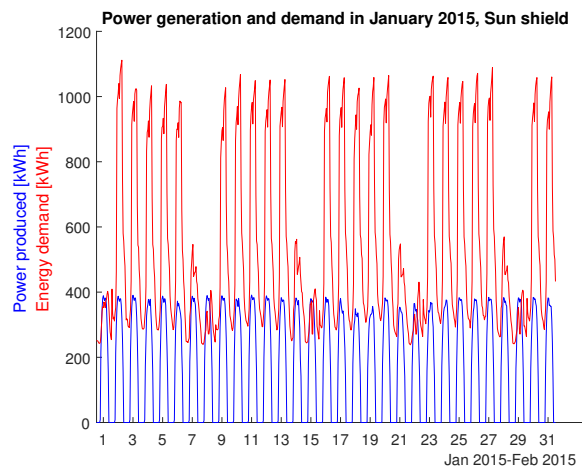
Table 44: Total consumption by load in kWh

A5 Annual yield and Performance Ratio for the 25 years

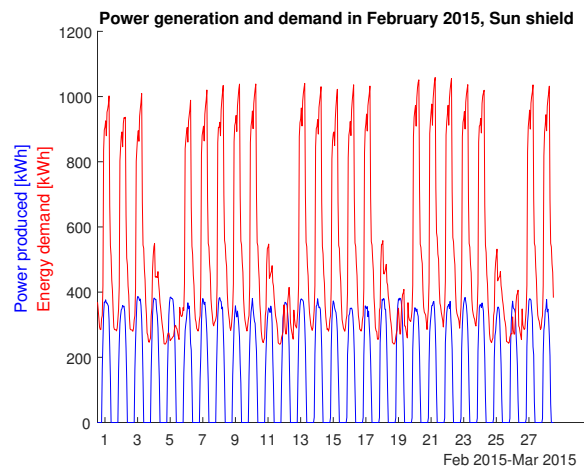
Year	Sun shield			Curtain wall		
	E_{gen} [kWh]	Y_f [kWh/kWp]	PR	E_{gen} [kWh]	Y_f [kWh/kWp]	PR
1	1,036,097.17	2,121.41	82.12%	1,788,027.65	2,018.39	87.30%
2	1,028,403.66	2,105.66	81.51%	1,770,963.48	1,999.12	86.47%
3	1,020,767.27	2,090.02	80.91%	1,754,062.16	1,980.04	85.64%
4	1,013,187.59	2,074.50	80.31%	1,737,322.15	1,961.15	84.82%
5	1,005,664.18	2,059.10	79.71%	1,720,741.89	1,942.43	84.02%
6	998,196.65	2,043.81	79.12%	1,704,319.87	1,923.89	83.21%
7	990,784.56	2,028.63	78.53%	1,688,054.57	1,905.53	82.42%
8	983,427.51	2,013.57	77.95%	1,671,944.50	1,887.35	81.63%
9	976,125.10	1,998.62	77.37%	1,655,988.18	1,869.34	80.85%
10	968,876.90	1,983.78	76.80%	1,640,184.14	1,851.50	80.08%
11	961,682.53	1,969.05	76.23%	1,624,530.93	1,833.83	79.32%
12	954,541.58	1,954.43	75.66%	1,609,027.10	1,816.32	78.56%
13	947,453.65	1,939.91	75.10%	1,593,671.24	1,798.99	77.81%
14	940,418.35	1,925.51	74.54%	1,578,461.92	1,781.82	77.07%
15	933,435.30	1,911.21	73.99%	1,563,397.76	1,764.82	76.33%
16	926,504.10	1,897.02	73.44%	1,548,477.36	1,747.97	75.60%
17	919,624.36	1,882.93	72.89%	1,533,699.36	1,731.29	74.88%
18	912,795.71	1,868.95	72.35%	1,519,062.39	1,714.77	74.17%
19	906,017.77	1,855.07	71.81%	1,504,565.11	1,698.40	73.46%
20	899,290.15	1,841.30	71.28%	1,490,206.19	1,682.20	72.76%
21	892,612.50	1,827.63	70.75%	1,475,984.30	1,666.14	72.07%
22	885,984.42	1,814.05	70.23%	1,461,898.14	1,650.24	71.38%
23	879,405.57	1,800.58	69.70%	1,447,946.41	1,634.49	70.70%
24	872,875.56	1,787.21	69.19%	1,434,127.83	1,618.89	70.02%
25	866,394.04	1,773.94	68.67%	1,420,441.13	1,603.44	69.35%

Table 45: Energy generated, Annual yield and Performance Ration for the 25 years simulated

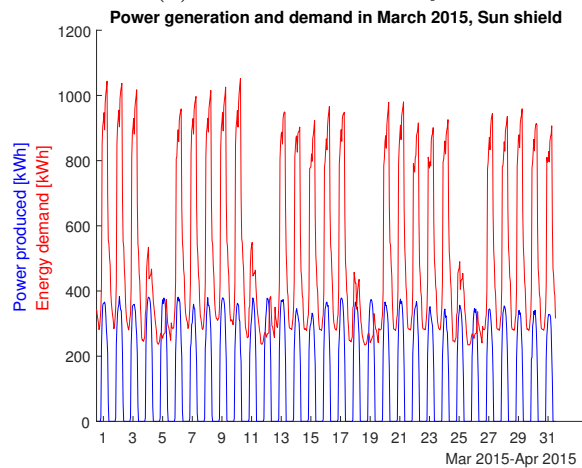
A6 Comparison of the power generated and consumed each month, for Sun shield



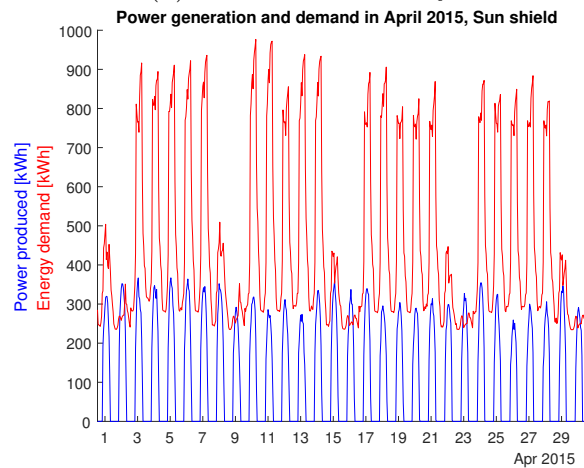
(a) Curves for January



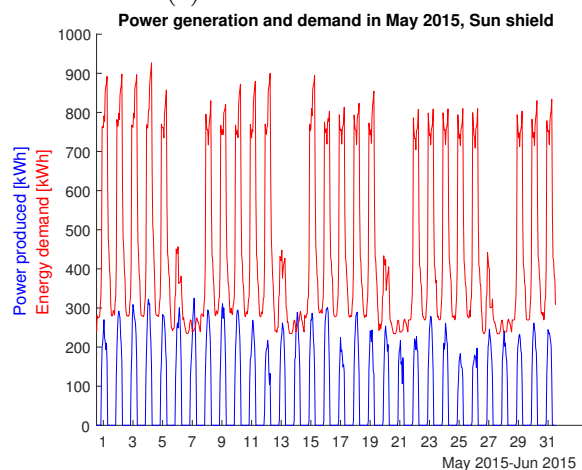
(b) Curves for February



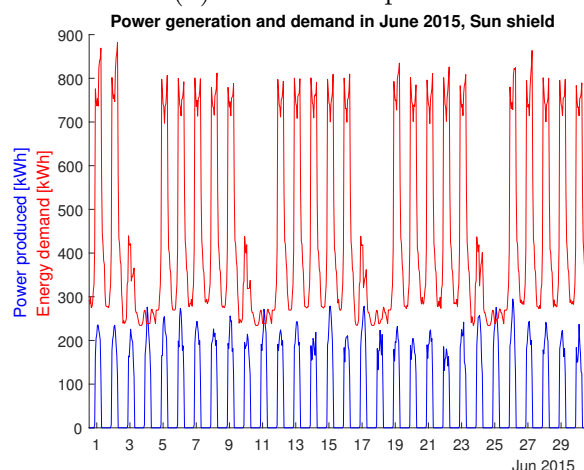
(c) Curves for March



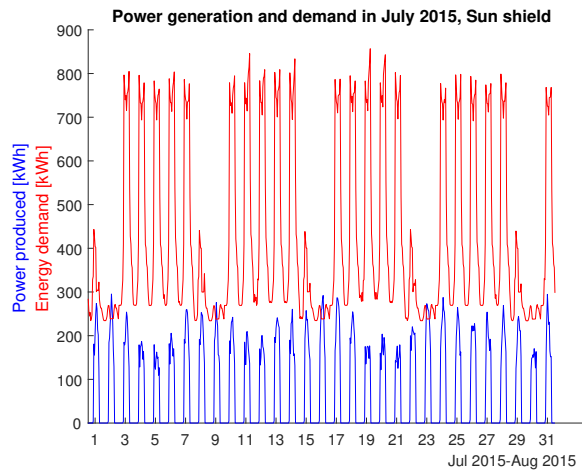
(d) Curves for April



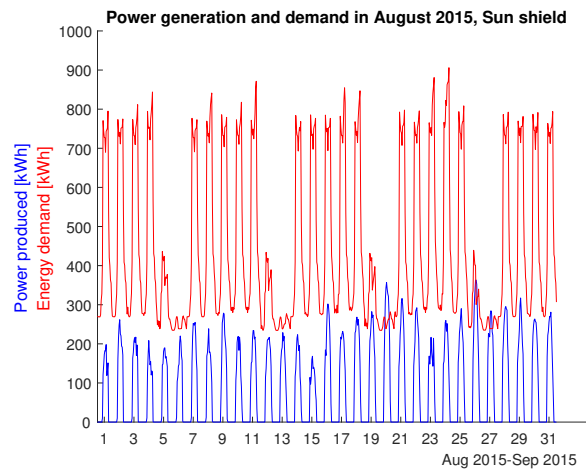
(e) Curves for May



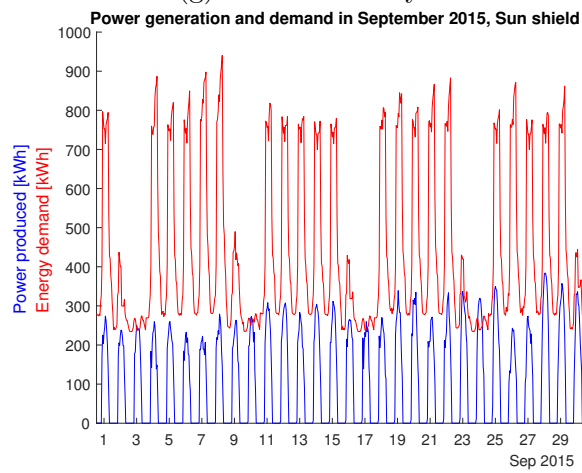
(f) Curves for June



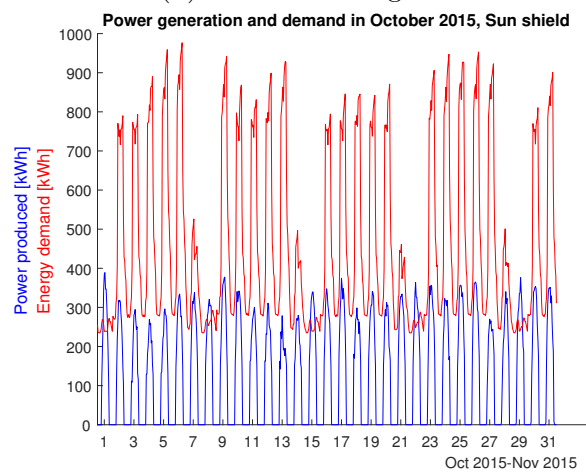
(g) Curves for July



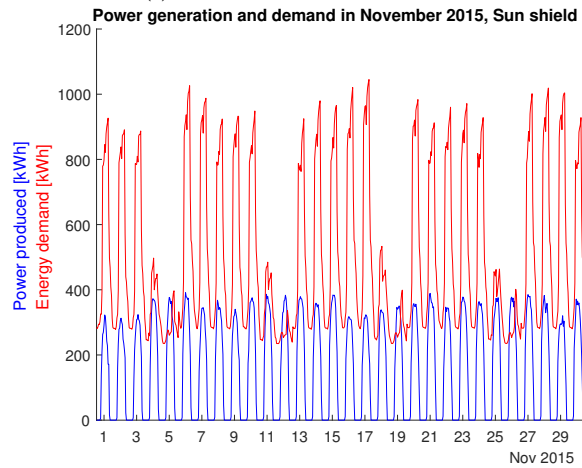
(h) Curves for August



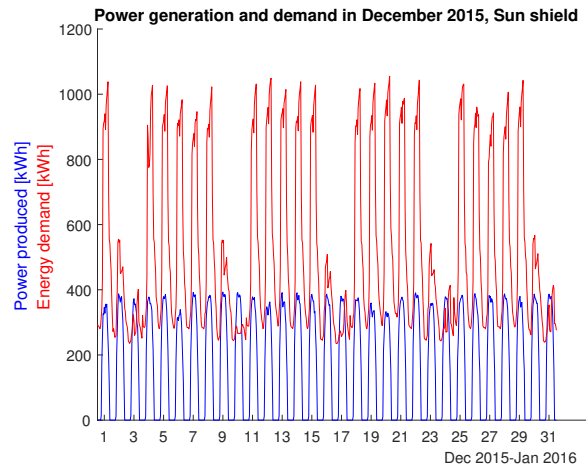
(i) Curves for September



(j) Curves for October



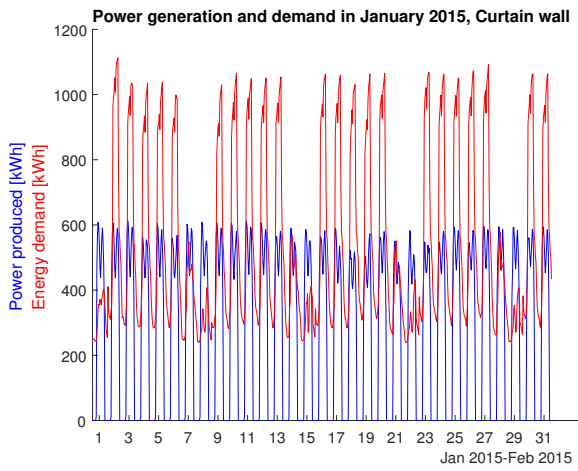
(k) Curves for November



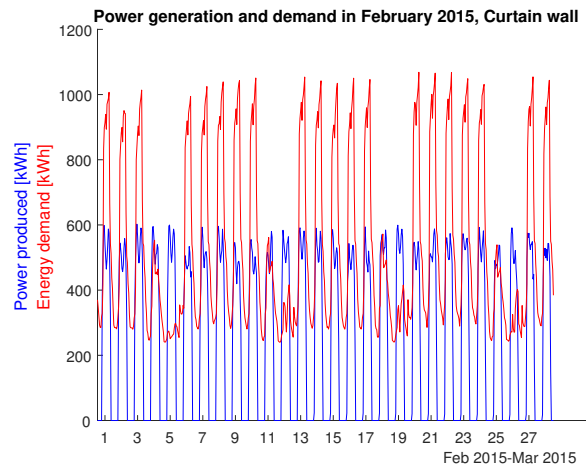
(l) Curves for December

Figure 55: Generation and demand during each month with Sun shield configuration

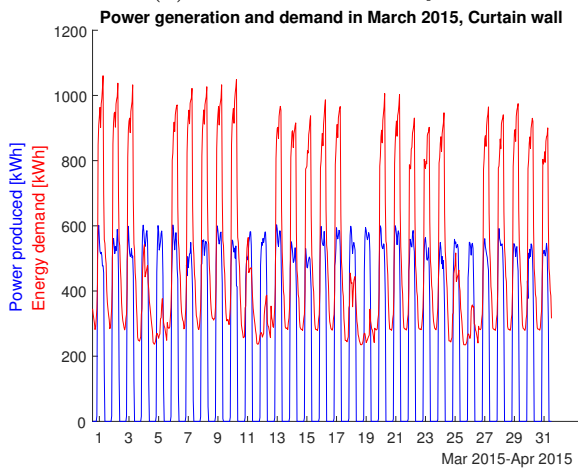
A7 Comparison of the power generated and consumed each month, for Curtain wall configuration



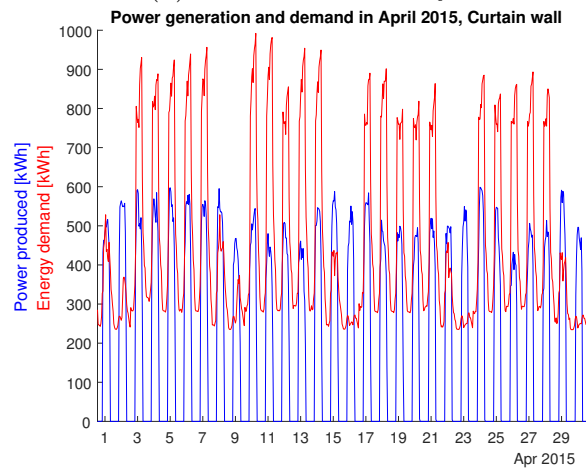
(a) Curves for January



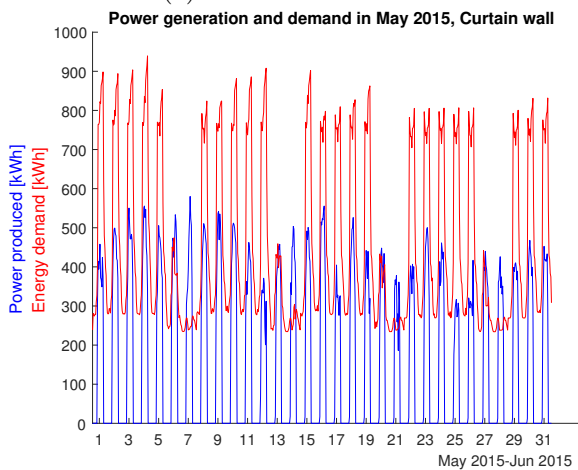
(b) Curves for February



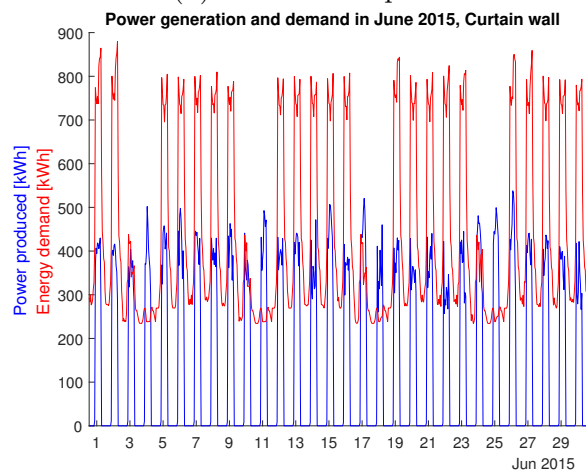
(c) Curves for March



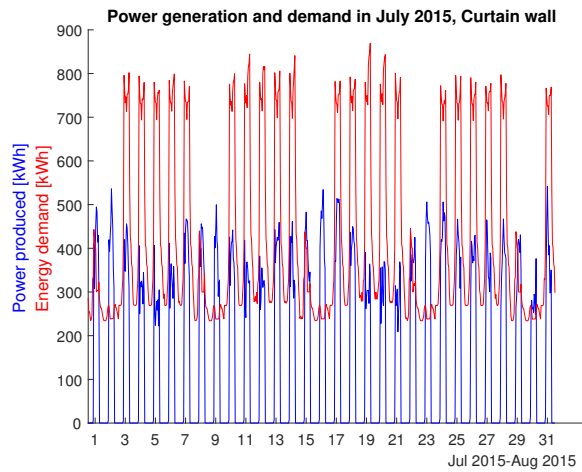
(d) Curves for April



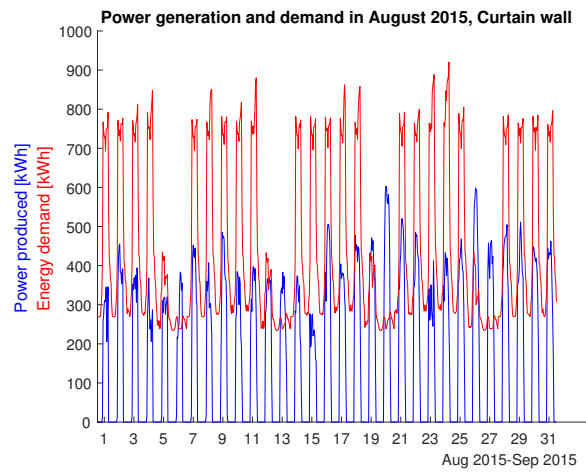
(e) Curves for May



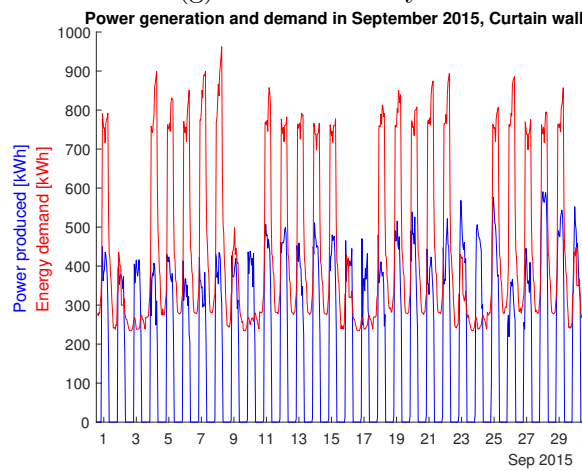
(f) Curves for June



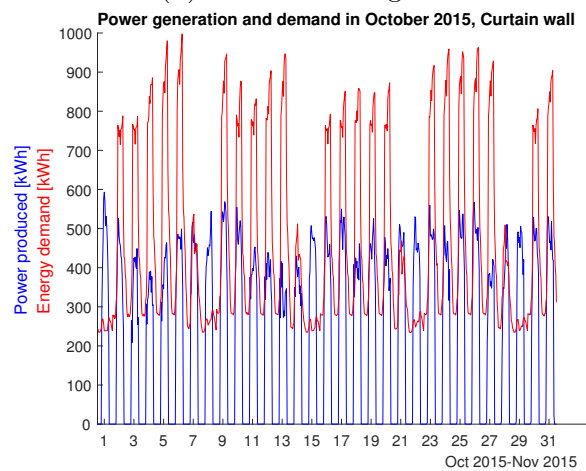
(g) Curves for July



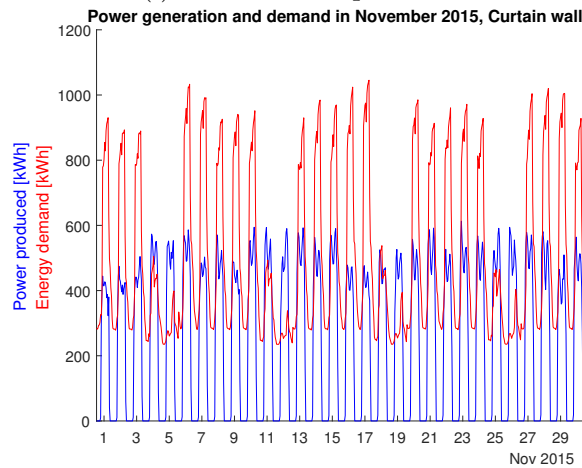
(h) Curves for August



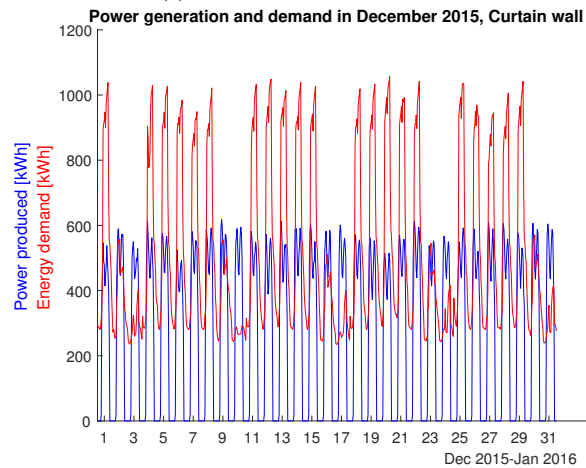
(i) Curves for September



(j) Curves for October



(k) Curves for November



(l) Curves for December

Figure 56: Generation and demand during each month with Curtain wall configuration

A8 Matlab code

```

clear

% Variables
euro2dollar = 1.1754;      %USD (08-06-2018) European Central Bank
peso2dollar = 1/630;       %USD (08-06-2018) Banco Central de Chile
Cons_tariff = 0.1319;      %USD/kWh Energy consumed
Inj_tariff = 0.0751;       %USD/kWh Energy injected PMGD
Pcont_tariff = 18.5413;    %USD/kWh/month Contracted power
inflation = 0.03;         %Banco Central (mean)
disc_rate = 0.12;         %From study on commercial project, 166 kW
Perc_Wiring = 0.08;       %Perc of wiring costs over total
Perc_Inverters = 0.1;      %Perc of inverter and optimizers costs over total
Perc_Installation = 0.25; %Perc of installation costs over total
Perc_Modules = 0.26;       %Perc of solar modules costs over total
Perc_Fastening = 0.3;     %Perc of Fastening system and ballasting costs
                        over total
Perc_Studies = 0.01;      %Perc of Planning and paperwork costs over total

%%% Panels data
%Sun Shield —> Trina Solar TSM-300DD05A.08 (II)
P_max_Ssh = 300;           %Wp
gamma_p_Ssh = -0.0039;     %thermal coeff of max power (manufacturer)
NOCT_Ssh = 44;             % C (Provided by manufacturer)
Panel_length_Ssh = 0.992;  %m
Panel_width_Ssh = 1.65;    %m
Yearly_perf_reduc_Ssh = 1-(1-0.17)^(1/25); %From 97% to 80% en 25 years
Panelprice_Ssh_eur = 157;   %euro (from web)
Panelprice_Ssh_usd = 186.68; %USD (from web)
Discount_wholesale = 0.1;
USDperW_Ssh_data = (1-Discoun_t_wholesale)*Panelprice_Ssh_usd/P_max_Ssh; %
                        USD/Wp
USDperW_Ssh = 0.45*euro2dollar; %USD/W (Becquerel Institute)

%Curtain Wall —> EnergyGlass Transparent and Opaque
P_max_Cwall_t = 130;       %Wp/m2, transparent
P_max_Cwall_o = 180;       %Wp/m2, opaque
gamma_p_Cwall = -0.004;    %thermal coeff
NOCT_Cwall = 44;           % C (Approx, not provided)
Yearly_perf_reduc_Cwall = 1-(1-0.25)^(1/30); %0.25/30; %25% in 30 years
Panelprice_Cwall_t_usd = 300*euro2dollar; %USD/m2
Panelprice_Cwall_o_usd = 240*euro2dollar; %USD/m2
USDperW_Cwall_t = 1.1*Panelprice_Cwall_t_usd/P_max_Cwall_t; %USD/Wp
USDperW_Cwall_o = 1.1*Panelprice_Cwall_o_usd/P_max_Cwall_o; %USD/Wp

%Inverter —> Sunny Tripower (SMA)
eff_DC2AC = 0.983;         %efficiency of power conversion
eff_MPPT = 0.999;          %efficiency of the MPPT
eff_inv = eff_DC2AC*eff_MPPT; %efficiency of inverter
shad_losses = 0.98;        %Sading losses
power_inv = 60;            %kW
maintenance_inv = 0.0075;  %Source, paper Brasil
Inv_price_eur = 5088;       %eur (with delivery)

%System
effi = 0.92;               %total efficiency (wiring, dust, etc)
Ta = 25;                   % C

```

```

TaNOCT = 20;      % C
GNOCT = 800;      %W/m^2
G = 1000;         %W/m^2

%Building data
Building_depth = 48.74; %m
Building_width = 73.11; %m
N_floors = 12;
Building_height = N_floors*3.96; %m
FacadeArea = Building_width*Building_height; %m^2
WindowArea = FacadeArea*0.4; %m^2
WallArea = FacadeArea*0.6; %m^2

%%%Number of modules to use and P-rated
%Sun Shield
N_modFloor_Ssh = floor( Building_width/Panel_width_Ssh); %Hori
N_mod_Ssh = N_modFloor_Ssh*N_floors; %N of modules used
Panel_Area_Ssh = Panel_length_Ssh*Panel_width_Ssh; %m^2
P_max_area_Ssh = P_max_Ssh/Panel_Area_Ssh; %Wp/m^2
Total_area_Ssh = N_mod_Ssh*Panel_Area_Ssh; %m^2
P_nom_Ssh = N_mod_Ssh*P_max_Ssh/1e3; %kWp
%%% Sunpower (high efficiency m-Si)
% P_max_sunPower = 360; %Wp
% Area_sunPower = 1.558*1.046; %m^2
% Wper_m2_sunPower = P_max_sunPower/Area_sunPower; %Wp/m^2
% P_nom_Ssh = N_mod_Ssh*Wper_m2_sunPower*Panel_Area_Ssh/1e3; %kWp
%%% Jinko (lower efficiency)
% P_max_jinko = 265; %Wp
% P_nom_Ssh = N_mod_Ssh*P_max_jinko/1e3; %kWp

%Curtain Wall
P_nom_Cwall_t = P_max_Cwall_t*WindowArea/1e3; %kWp
P_nom_Cwall_o = P_max_Cwall_o*WallArea/1e3; %kWp
P_nom_Cwall = P_nom_Cwall_t+P_nom_Cwall_o; %kWp

%Roof (Same modules as Ssh)
N_modRow = floor( Building_width/Panel_width_Ssh);
N_mod_Roof = 25*N_modRow; %25 rows according to simulation
Total_area_Roof = N_mod_Roof*Panel_Area_Ssh; %m^2
P_nom_Roof = N_mod_Roof*P_max_Ssh/1e3; %kWp
%%% High efficiency
% P_nom_Roof = N_mod_Roof*Wper_m2_sunPower*Panel_Area_Ssh/1e3; %kWp
% %%% Low efficiency
% P_nom_Roof = N_mod_Roof*P_max_jinko/1e3; %kWp

% Number of inverters
N_inv_Ssh = ceil((P_nom_Ssh+P_nom_Roof)/power_inv);
N_inv_Cwall = ceil((P_nom_Cwall+P_nom_Roof)/power_inv);

%%% Intial costs

Cost_Ssh_panels = USDperW_Ssh*P_nom_Ssh*1e3; %USD
Cost_Cwall_t_panels = WindowArea*Panelprice_Cwall_t_usd*1.1;%USD (10%
shipping)
Cost_Cwall_o_panels = WallArea*Panelprice_Cwall_o_usd*1.1; %USD (10%
shipping)
Cost_Cwall_panels = Cost_Cwall_t_panels+Cost_Cwall_o_panels;%USD

```

```

Cost_Roof_panels = USDperW_Ssh*P_nom_Roof*1e3; %USD
USDperW_Cwall = (Cost_Cwall_panels/1.1)/(P_nom_Cwall*1e3); %USD/W

InvertPerW_Ssh = 0.07*euro2dollar;
Cost_inv_Ssh = InvertPerW_Ssh*P_nom_Ssh*1e3; %USD
Cost_inv_Cwall = N_inv_Cwall*Inv_price_eur*euro2dollar; %USD
Cost_inv_Roof = InvertPerW_Ssh*P_nom_Roof*1e3; %USD

WiringPerW_Ssh = 0.07*euro2dollar; %USD/W (Becquerel Institute)
WiringPerW_Cwall = USDperW_Cwall*(Perc_Wiring/Perc_Modules); %USD/W
InstPerW_Ssh = 0.13*euro2dollar; %USD/W (Becquerel Institute)
InstPerW_Cwall = USDperW_Cwall*(Perc_Installation/Perc_Modules); %USD/W
FastenPerW = USDperW_Cwall*(Perc_Fastening/Perc_Modules); %USD/W
MountPerW_Ssh = 0.07*euro2dollar; %USD/W (Becquerel Institute)
StudiesPerW_Ssh = 0.02*euro2dollar; %USD/W (Becquerel Institute)
StudiesPerW_Cwall = USDperW_Cwall*(Perc_Studies/Perc_Modules); %USD/W
MarginPerW_Ssh = 0.14*euro2dollar; %USD/W (Becquerel Institute)

Cost_Wiring_Ssh = P_nom_Ssh*WiringPerW_Ssh*1e3; %USD
Cost_Wiring_Cwall = P_nom_Cwall*WiringPerW_Cwall*1e3; %USD
Cost_Wiring_Roof = P_nom_Roof*WiringPerW_Ssh*1e3; %USD
Cost_Inst_Ssh = P_nom_Ssh*InstPerW_Ssh*1e3; %USD
Cost_Inst_Cwall = P_nom_Cwall*InstPerW_Cwall*1e3; %USD
Cost_Inst_Roof = P_nom_Roof*InstPerW_Ssh*1e3; %USD
Cost_Mount_Ssh = P_nom_Ssh*MountPerW_Ssh*1e3; %USD
Cost_Fasten_Cwall = P_nom_Cwall*FastenPerW*1e3; %USD
Cost_Mount_Roof = P_nom_Roof*MountPerW_Ssh*1e3; %USD
Cost_Studies_Ssh = P_nom_Ssh*StudiesPerW_Ssh*1e3; %USD
Cost_Studies_Cwall = P_nom_Cwall*StudiesPerW_Cwall*1e3; %USD
Cost_Studies_Roof = P_nom_Roof*StudiesPerW_Ssh*1e3; %USD
Cost_Margin_Ssh = P_nom_Ssh*MarginPerW_Ssh*1e3; %USD
Cost_Margin_Roof = P_nom_Roof*MarginPerW_Ssh*1e3; %USD

InitialCost_Ssh = Cost_Ssh_panels+Cost_inv_Ssh+Cost_Wiring_Ssh...
+Cost_Inst_Ssh+Cost_Mount_Ssh+Cost_Studies_Ssh+Cost_Margin_Ssh; %USD
InitialCost_Cwall = Cost_Cwall_panels+Cost_inv_Cwall+Cost_Wiring_Cwall...
+Cost_Inst_Cwall+Cost_Fasten_Cwall+Cost_Studies_Cwall; %USD
InitialCost_Roof = Cost_Roof_panels+Cost_inv_Roof+Cost_Wiring_Roof...
+Cost_Inst_Roof+Cost_Mount_Roof+Cost_Studies_Roof+Cost_Margin_Roof; %USD

%%% Initial Savings

SavIni_win_Cwall = Cost_Cwall_panels/3;
SavIni_inst_Cwall = Cost_Inst_Cwall*0.4;
SavIni_fastening_Cwall = Cost_Fasten_Cwall*0.4;
InitialSavings_Cwall = SavIni_win_Cwall+SavIni_inst_Cwall+
SavIni_fastening_Cwall;

%%% Fixed costs
%Cleaning cost/m2
cleanM2 = 20; %USD/m2
% % % Cleaning windows/facade
Cost_Cleaning_Ssh_ini = cleanM2*Total_area_Ssh*0.5; %USD
Cost_Cleaning_Roof_ini = cleanM2*Total_area_Roof*0.5; %USD
% % % Only consider the area that is not windows for the additional
% % % cleaning cost

```

```

Cost_Cleaning_Cwall_ini = WallArea*cleanM2; %USD
%Assuming cleanning every 2 months in summer semester and in winter with
%the rain
n = 3;
Cost_Cleaning_Ssh = Cost_Cleaning_Ssh_ini*n; %USD annual
Cost_Cleaning_Roof = Cost_Cleaning_Roof_ini*n; %USD annual
Cost_Cleaning_Cwall = Cost_Cleaning_Cwall_ini*n; %USD annual
%Costs for the next 25 years in both cases add the Roof costs
YearCleaning_Ssh = zeros(1,25);
YearCleaning_Roof = zeros(1,25);
YearCleaning_Cwall = zeros(1,25);
for i = 1:25
    YearCleaning_Ssh(i) = (Cost_Cleaning_Ssh+Cost_Cleaning_Roof) ...
        *(1+inflation)^(i-1);
    YearCleaning_Cwall(i) = (Cost_Cleaning_Cwall+Cost_Cleaning_Roof) ...
        *(1+inflation)^(i-1);
    YearCleaning_Roof(i) = Cost_Cleaning_Roof*(1+inflation)^(i-1);
end

%Define function for Tc
T_c_Ssh = @(x,y) x+(NOCT_Ssh-Ta_NOCT)*y/G_NOCT;
T_c_Cwall = @(x,y) x+(NOCT_Cwall-Ta_NOCT)*y/G_NOCT;
%Define function for P_ac:
P_ac_Ssh = @(x,y) P_nom_Ssh*(x/G)*effi*eff_inv*shad_losses*...
    (1+gamma_p_Ssh*(y-Ta));
% For Cwall 6% and 8% (transparent and opaque)increase because of Bifacial
P_ac_Cwall_t = @(x,y) P_nom_Cwall_t*(x/G)*effi*eff_inv*shad_losses*...
    (1+gamma_p_Cwall*(y-Ta))*1.06;
P_ac_Cwall_o = @(x,y) P_nom_Cwall_o*(x/G)*effi*eff_inv*shad_losses*...
    (1+gamma_p_Cwall*(y-Ta))*1.08;
P_ac_Roof = @(x,y) P_nom_Roof*(x/G)*effi*eff_inv*shad_losses*...
    (1+gamma_p_Ssh*(y-Ta));
%Define function for Elec_dem:
Elec_dem = @(x) x/(3.6*1e6);

% Load file
D = readtable('DHC_EIIMNWP.csv');
%Create timetable
DD = table2timetable(D);

%Determine if timetable is regular (same time differences)
tf = isregular(DD);
%Remove times with missing data
DD = rmmissing(DD);

%Yearly irradiation
DD_rad = retime(DD(:, 'ghi'), 'yearly', 'sum'); %W/m2
DD_rad.ghi = DD_rad.ghi/1e3; %kW/m2

%% %Use 10 years and the mean of the values of: temp, ghi, dni, difh
Tamb_year = DD(ismember(year(DD.Fecha_Hora),2015), 'temp');
Tamb_year.Properties.VariableNames{ 'temp' } = 'T_2015';
GHI_year = DD(ismember(year(DD.Fecha_Hora),2015), 'ghi');
GHI_year.Properties.VariableNames{ 'ghi' } = 'GHI_2015';
DNI_year = DD(ismember(year(DD.Fecha_Hora),2015), 'dni');
DNI_year.Properties.VariableNames{ 'dni' } = 'DNI_2015';
DIFh_year = DD(ismember(year(DD.Fecha_Hora),2015), 'difh');
DIFh_year.Properties.VariableNames{ 'difh' } = 'DIFh_2015';

```

```

for i = 2006:2014
    temp1 = DD(ismember(year(DD.Fecha_Hora),i),'temp');
    todelete1 = (month(temp1.Fecha_Hora) == 2) &...
        (day(temp1.Fecha_Hora) == 29);
    temp1(todelete1,:) = [];
    Tamb_year.New = temp1.Variables;
    Tamb_year.Properties.VariableNames{'New'} = strcat('T_',num2str(i));
    temp2 = DD(ismember(year(DD.Fecha_Hora),i),'ghi');
    todelete2 = (month(temp2.Fecha_Hora) == 2) &...
        (day(temp2.Fecha_Hora) == 29);
    temp2(todelete2,:) = [];
    GHI_year.New = temp2.Variables;
    GHI_year.Properties.VariableNames{'New'} = strcat('GHI_',num2str(i));
    temp3 = DD(ismember(year(DD.Fecha_Hora),i),'dni');
    todelete3 = (month(temp3.Fecha_Hora) == 2) &...
        (day(temp3.Fecha_Hora) == 29);
    temp3(todelete3,:) = [];
    DNI_year.New = temp3.Variables;
    DNI_year.Properties.VariableNames{'New'} = strcat('DNI_',num2str(i));
    temp4 = DD(ismember(year(DD.Fecha_Hora),i),'difh');
    todelete4 = (month(temp4.Fecha_Hora) == 2) &...
        (day(temp4.Fecha_Hora) == 29);
    temp4(todelete4,:) = [];
    DIFh_year.New = temp4.Variables;
    DIFh_year.Properties.VariableNames{'New'} = strcat('DIFh_',num2str(i));
end
Mean10 = @(x1,x2,x3,x4,x5,x6,x7,x8,x9,x10) ...
    (x1+x2+x3+x4+x5+x6+x7+x8+x9+x10)/10;
Tamb_prom = rowfun(Mean10,Tamb_year,'OutputVariableNames','temp');
GHI_prom = rowfun(Mean10,GHI_year,'OutputVariableNames','ghi');
DNI_prom = rowfun(Mean10,DNI_year,'OutputVariableNames','dni');
DIFh_prom = rowfun(Mean10,DIFh_year,'OutputVariableNames','difh');
D_15 = [Tamb_prom GHI_prom DNI_prom DIFh_prom];

%% Calc in-plane irradiation
% Get the angle between beam and normal to module plane
tilt_Ssh = 33; %
tilt_Cwall = 90; %
% a = ghi, b = difh, c = dni
getTheta_Ssh = @(a,b,c) acosd((a-b)/c)-tilt_Ssh;
getTheta_Cwall = @(a,b,c) acosd((a-b)/c)-tilt_Cwall;
indNo0 = find(D_15.dni);
dniNon0 = D_15(D_15.Fecha_Hora(indNo0),:);
theta_Ssh = rowfun(getTheta_Ssh,dniNon0,'InputVariables',...
    {'ghi','difh','dni'},'OutputVariableNames','theta_Ssh'); %
theta_Cwall = rowfun(getTheta_Cwall,dniNon0,'InputVariables',...
    {'ghi','difh','dni'},'OutputVariableNames','theta_Cwall'); %
%Add thetasto D_15
D_15 = synchronize(D_15,theta_Ssh,theta_Cwall,'union','fillwithconstant');
% Calc the irradiation Gt
% a = ghi, b = difh, c = dni, d = theta
G_t_Ssh = @(a,b,c,d) c*cosd(d)+b*0.5*(1+cosd(tilt_Ssh))+a*0.5*0.24*...
    (1-cosd(tilt_Ssh));
G_t_Cwall = @(a,b,c,d) c*cosd(d)+b*0.5*(1+cosd(tilt_Cwall))+a*0.5*0.24*...
    (1-cosd(tilt_Cwall));

Gt_Ssh = rowfun(G_t_Ssh,D_15,'InputVariables',...
    {'ghi','difh','dni','theta_Ssh'},'OutputVariableNames','Gt_Ssh');

```

```

Gt_Cwall = rowfun(Gt_Cwall,D_15,'InputVariables',...
    {'ghi','difh','dni','theta_Cwall'},'OutputVariableNames','Gt_Cwall');
%Add Gt to D_15
D_15 = [D_15 Gt_Ssh Gt_Cwall];

% %Sensi: +/- 20% rad
% D_15.Gt_Ssh = D_15.Gt_Ssh*1.2;
% D_15.Gt_Cwall = D_15.Gt_Cwall*1.2;
% D_15.Gt_Ssh = D_15.Gt_Ssh*0.8;
% D_15.Gt_Cwall = D_15.Gt_Cwall*0.8;

% Calc Tc (Cell temperature)
Tc_Ssh = rowfun(Tc_Ssh,D_15,'InputVariables',{'temp','Gt_Ssh'},...
    'OutputVariableNames','Tc_Ssh'); % C
Tc_Cwall = rowfun(Tc_Cwall,D_15,'InputVariables',{'temp','Gt_Cwall'},...
    'OutputVariableNames','Tc_Cwall'); % C
% Add Tc to D_15
D_15 = [D_15 Tc_Ssh Tc_Cwall];

%Min Cell Temperature
Tamb_all = rowfun(Tc_Ssh,D_15,'InputVariables',{'temp','Gt_Ssh'},...
    'OutputVariableNames','Tc_all'); % C
Tamb_day = Tamb_all(ismember(hour(Tamb_all.Fecha_Hora),8:17),:);
[M,I] = min(Tamb_day.Tc_all);

% Calc Pac
Pac_Ssh_noR = rowfun(Pac_Ssh,D_15,'InputVariables',...
    {'Gt_Ssh','Tc_Ssh'},'OutputVariableNames','Pac_Ssh_noR'); %W
Pac_Cwall_t = rowfun(Pac_Cwall_t,D_15,'InputVariables',...
    {'Gt_Cwall','Tc_Cwall'},'OutputVariableNames','Pac_Cwall_t'); %W
Pac_Cwall_o = rowfun(Pac_Cwall_o,D_15,'InputVariables',...
    {'Gt_Cwall','Tc_Cwall'},'OutputVariableNames','Pac_Cwall_o'); %W
Pac_Roof = rowfun(Pac_Roof,D_15,'InputVariables',...
    {'Gt_Ssh','Tc_Ssh'},'OutputVariableNames','Pac_Roof'); %W
%Add the power of the roof to each case
Suma = @(x,y) x+y;
Pac_Cwall_noR = rowfun(Suma,[Pac_Cwall_t Pac_Cwall_o],...
    'OutputVariableNames','Pac_Cwall_noR'); %Transparent + Opaque
Pac_Ssh = rowfun(Suma,[Pac_Ssh_noR Pac_Roof],...
    'OutputVariableNames','Pac_Ssh'); %Ssh + Roof
Pac_Cwall = rowfun(Suma,[Pac_Cwall_noR Pac_Roof],...
    'OutputVariableNames','Pac_Cwall'); %Cwall + Roof

% Add Pac to DD
D_15 = [D_15 Pac_Ssh_noR Pac_Cwall_t Pac_Cwall_o Pac_Cwall_noR ...
    Pac_Roof Pac_Ssh Pac_Cwall];

% Demand profile
% Load file
B_base = readtable('Consumo_Ssh_Base.csv');
B_Ssh = readtable('Consumo_Ssh_HorizRoof.csv');
B_Cwall = readtable('Consumo_Cwall.csv');

%Create timetable
BB_base = table2timetable(B_base);
BB_Ssh = table2timetable(B_Ssh);
BB_Cwall = table2timetable(B_Cwall);

```

```

% Change year from 2009 to 2015 so it matches the year of the radiation
% data
BB_base.Hourly = BB_base.Hourly + calyears(6);
BB_Ssh.Hourly = BB_Ssh.Hourly + calyears(6);
BB_Cwall.Hourly = BB_Cwall.Hourly + calyears(6);

%Use same hours as in irradiance data (fix first and last)
Bb_base = retime(BB_base,D_15.Fecha_Hora,'linear');
Bs_Ssh = retime(BB_Ssh,D_15.Fecha_Hora,'linear');
Bc_Cwall = retime(BB_Cwall,D_15.Fecha_Hora,'linear');

%Calculate demand in kWh
Bb_pow = rowfun(Elec_dem,Bb_base,'OutputVariableNames','Elec_dem_base');%
    kWh
Bs_pow = rowfun(Elec_dem,Bs_Ssh,'OutputVariableNames','Elec_dem_Ssh'); %
    kWh
Bc_pow = rowfun(Elec_dem,Bc_Cwall,'OutputVariableNames','Elec_dem_Cwall');%
    kWh

%Add Bx_pow to D_15
D_15 = [D_15 Bb_pow Bs_pow Bc_pow];

%%%% Simulation for the 25 wanted years %%%%
%%% Power gen
P_ac_Ssh_period = D_15(:, 'Pac_Ssh');
P_ac_Cwall_period = D_15(:, 'Pac_Cwall');
%Functions for the performance reduction of the panels over the yeras
Pac_Ssh_years = @(x) x*(1-Yearly_perf_reducion_Ssh);
Pac_Cwall_years = @(x) x*(1-Yearly_perf_reducion_Cwall);
%Assign name and include the downtime for the maintenace of the inverters
P_ac_Ssh_period.Properties.VariableNames = {'Pac_Ssh_1'};
P_ac_Ssh_period.Pac_Ssh_1 = P_ac_Ssh_period.Pac_Ssh_1*(1-maintenance_inv);
P_ac_Cwall_period.Properties.VariableNames = {'Pac_Cwall_1'};
P_ac_Cwall_period.Pac_Cwall_1=P_ac_Cwall_period.Pac_Cwall_1*(1-
    maintenance_inv);

%%% Power: Self-consumed vs Injected
Resta = @(x,y) x-y;
DiffConsGen_Ssh = rowfun(Resta,D_15,'InputVariables',...
    {'Elec_dem_Ssh','Pac_Ssh'},'OutputVariableNames','DiffConsGen_Ssh_1');
DiffConsGen_Cwall = rowfun(Resta,D_15,'InputVariables',...
    {'Elec_dem_Cwall','Pac_Cwall'},'OutputVariableNames','
    DiffConsGen_Cwall_1');
%Calc of generated power for the next 25 years
for i = 2:25
    temp1 = rowfun(Pac_Ssh_years,P_ac_Ssh_period,'InputVariables',...
        {strcat('Pac_Ssh_',num2str(i-1))});
    P_ac_Ssh_period.New = temp1.Variables;
    P_ac_Ssh_period.Properties.VariableNames{'New'} =...
        strcat('Pac_Ssh_',num2str(i));

    temp2 = rowfun(Pac_Cwall_years,P_ac_Cwall_period,'InputVariables',...
        {strcat('Pac_Cwall_',num2str(i-1))});
    P_ac_Cwall_period.New = temp2.Variables;
    P_ac_Cwall_period.Properties.VariableNames{'New'} =...
        strcat('Pac_Cwall_',num2str(i));

    temp3 = rowfun(Resta,[D_15(:, 'Elec_dem_Ssh'),temp1],...

```



```

        'OutputVariableNames', strcat('DiffConsGen_Ssh_', num2str(i)));
DiffConsGen_Ssh.New = temp3.Variables;
DiffConsGen_Ssh.Properties.VariableNames{'New'} = ...
    strcat('DiffConsGen_Ssh_', num2str(i));

temp4 = rowfun(Resta, [D_15(:, 'Elec_dem_Cwall'), temp2], ...
    'OutputVariableNames', strcat('DiffConsGen_Cwall_', num2str(i)));
DiffConsGen_Cwall.New = temp4.Variables;
DiffConsGen_Cwall.Properties.VariableNames{'New'} = ...
    strcat('DiffConsGen_Cwall_', num2str(i));
end

%%% Demand not consumed when panels are installed
%Assuming consumption remains the same in the 25 years
EnotConsumed_Ssh = rowfun(Resta, D_15, 'InputVariables', {'Elec_dem_base', ...
    'Elec_dem_Ssh'}, 'OutputVariableNames', 'EnotConsumed_Ssh');
EnotC_Ssh_y = retime(EnotConsumed_Ssh, 'yearly', 'sum');
EnotConsumed_Cwall = rowfun(Resta, D_15, 'InputVariables', {'Elec_dem_base', ...
    'Elec_dem_Cwall'}, 'OutputVariableNames', 'EnotConsumed_Cwall');
EnotC_Cwall_y = retime(EnotConsumed_Cwall, 'yearly', 'sum');

%%% Maximum values of demand
Dmax_base = max(D_15.Elec_dem_base);
%Take data only of peak hours
Dpunta_h = Bb_pow(ismember(hour(Bb_pow.Hourly), 18:23), :);
Dpunta_m = Dpunta_h(ismember(month(Dpunta_h.Hourly), 4:9), :);
Dmedia_punta = retime(Dpunta_m, 'daily', 'sum');
Dmedia_punta.Elec_dem_base = Dmedia_punta.Elec_dem_base/5;
Tp_base = max(Dmedia_punta.Elec_dem_base)/Dmax_base;

%For Ssh
Dmax_Ssh = max(DiffConsGen_Ssh.Variables);
%Take data only of peak hours
Dpunta_h_Ssh = DiffConsGen_Ssh(ismember(hour(DiffConsGen_Ssh.Fecha_Hora),
    18:23), :);
Dpunta_m_Ssh = Dpunta_h_Ssh(ismember(month(Dpunta_h_Ssh.Fecha_Hora), 4:9), :);
;
Dmedia_punta_Ssh = retime(Dpunta_m_Ssh, 'daily', 'sum');
Dmedia_punta_Ssh.Variables = Dmedia_punta_Ssh.Variables/5;
Tp_base_Ssh = max(Dmedia_punta_Ssh.Variables)./Dmax_Ssh;
D_peak = retime(D_15(:, 'Elec_dem_base'), 'daily', @max);
Dpunta2 = Bb_pow(ismember(D_15.Elec_dem_base, D_peak.Elec_dem_base), :);
%For Cwall
Dmax_Cwall = max(DiffConsGen_Cwall.Variables);

%%% Savings - Energy self-consumed and injected - Money
Zero = @(x) x*0;
Esavings_Ssh = varfun(Zero, P_ac_Ssh_period);
Esavings_Cwall = varfun(Zero, P_ac_Cwall_period);
YearlyEnotC_Ssh = zeros(1, 25);
YearlyEnotC_Cwall = zeros(1, 25);
YearlyPmaxChange_Ssh = zeros(1, 25);
YearlyPmaxChange_Cwall = zeros(1, 25);
Tcons = zeros(1, 25);
Tinj = zeros(1, 25);
Tcontr = zeros(1, 25);
for i = 1:25

```

```

Tcons(i) = Cons_tariff*(1+inflation)^(i-1);
Tinj(i) = Inj_tariff*(1+inflation)^(i-1);
Tcontr(i) = Pcont_tariff*(1+inflation)^(i-1);
YearlyEnotC_Ssh(i) = EnotC_Ssh_y.Variables*Tcons(i);
YearlyEnotC_Cwall(i) = EnotC_Cwall_y.Variables*Tcons(i);
YearlyPmaxChange_Ssh(i) = (Dmax_base-Dmax_Ssh(i))*Tcontr(i)*12;
YearlyPmaxChange_Cwall(i) = (Dmax_base-Dmax_Cwall(i))*Tcontr(i)*12;
end
%Matrix with 1 if positive (more consumption)
DiffPos_Ssh = DiffConsGen_Ssh.Variables;
DiffPos_Ssh(DiffPos_Ssh<0) = 0;
DiffPos_Ssh(DiffPos_Ssh>0) = 1;
DiffPos_Ssh = DiffPos_Ssh.*Tcons;
DiffPos_Ssh = DiffPos_Ssh.*P_ac_Ssh_period.Variables;
%matrix with 1 if negative (more generation)
DiffNeg_Ssh = DiffConsGen_Ssh.Variables;
DiffNeg_Ssh(DiffNeg_Ssh>0) = 0;
DiffNeg_Ssh(DiffNeg_Ssh<0) = 1;
DiffNeg_Ssh_cons = DiffNeg_Ssh.*Tcons;
DiffNeg_Ssh_inj = DiffNeg_Ssh.*Tinj;
DiffNeg_Ssh_cons = DiffNeg_Ssh_cons.*D_15.Elec_dem_Ssh;
DiffNeg_Ssh_inj = -DiffNeg_Ssh_inj.*DiffConsGen_Ssh.Variables;
Esavings_Ssh.Variables = DiffPos_Ssh+DiffNeg_Ssh_cons+DiffNeg_Ssh_inj;

%Matrix with 1 if positive (more consumption)
DiffPos_Cwall = DiffConsGen_Cwall.Variables;
DiffPos_Cwall(DiffPos_Cwall<0) = 0;
DiffPos_Cwall(DiffPos_Cwall>0) = 1;
DiffPos_Cwall = DiffPos_Cwall.*Tcons;
DiffPos_Cwall = DiffPos_Cwall.*P_ac_Cwall_period.Variables;
%matrix with 1 if negative (more generation)
DiffNeg_Cwall = DiffConsGen_Cwall.Variables;
DiffNeg_Cwall(DiffNeg_Cwall>0) = 0;
DiffNeg_Cwall(DiffNeg_Cwall<0) = 1;
DiffNeg_Cwall_cons = DiffNeg_Cwall.*Tcons;
DiffNeg_Cwall_inj = DiffNeg_Cwall.*Tinj;
DiffNeg_Cwall_cons = DiffNeg_Cwall_cons.*D_15.Elec_dem_Cwall;
DiffNeg_Cwall_inj = -DiffNeg_Cwall_inj.*DiffConsGen_Cwall.Variables;
Esavings_Cwall.Variables = DiffPos_Cwall+DiffNeg_Cwall_cons+
    DiffNeg_Cwall_inj;

YearEnergy_Ssh = retime(P_ac_Ssh_period,'yearly','sum');
YearSavings_Ssh = retime(Esavings_Ssh,'yearly','sum');
YearEnergy_Cwall = retime(P_ac_Cwall_period,'yearly','sum');
YearSavings_Cwall = retime(Esavings_Cwall,'yearly','sum');
YearEnergy_Roof = retime(D_15(:, 'Pac-Roof'),'yearly','sum');
YearEnergy_Roof.Pac-Roof = YearEnergy_Roof.Pac-Roof*(1-maintenance_inv);
YearEnergy_SshNoR = retime(D_15(:, 'Pac-Ssh_noR'),'yearly','sum');
YearEnergy_SshNoR.Pac-Ssh_noR = YearEnergy_SshNoR.Pac-Ssh_noR*(1-
    maintenance_inv);
YearEnergy_CwallNor = retime(D_15(:, 'Pac-Cwall_noR'),'yearly','sum');
YearEnergy_CwallNor.Pac-Cwall_noR = YearEnergy_CwallNor.Pac-Cwall_noR*...
(1-maintenance_inv);

%%% Net present Value
%Cash flow for years 1 to 25
%Add initial costs and savings

```

```

CashFlow_Ssh = YearSavings_Ssh.Variables+YearlyEnotC_Ssh+...
YearlyPmaxChange_Ssh-YearCleaning_Ssh;
CashFlow_Ssh = [-InitialCost_Ssh-InitialCost_Roof CashFlow_Ssh];
CashFlow_Cwall = YearSavings_Cwall.Variables+YearlyEnotC_Cwall+...
YearlyPmaxChange_Cwall-YearCleaning_Cwall;
CashFlow_Cwall = [-InitialCost_Cwall-InitialCost_Roof+...
InitialSavings_Cwall CashFlow_Cwall];

NPV_Prueba_Ssh = pvvar(CashFlow_Ssh,disc_rate);
NPV_Prueba_Cwall = pvvar(CashFlow_Cwall,disc_rate);
IRR_Ssh = irr(CashFlow_Ssh);
IRR_Cwall = irr(CashFlow_Cwall);
NPV_Ssh = - InitialCost_Ssh-InitialCost_Roof;
disc_payback_Ssh = 0;
Sum_Ssh = 0;
payback_Ssh = 0;
NPV_Cwall = - InitialCost_Cwall-InitialCost_Roof+InitialSavings_Cwall;
disc_payback_Cwall = 0;
Sum_Cwall = 0;
payback_Cwall = 0;
for i = 1:25
    Sum_Ssh = Sum_Ssh+CashFlow_Ssh(i);
    if Sum_Ssh <0
        payback_Ssh = payback_Ssh+1;
    end
    if NPV_Ssh < 0
        disc_payback_Ssh = disc_payback_Ssh+1;
    end
    NPV_Ssh = NPV_Ssh + (YearSavings_Ssh(:,i).Variables+YearlyEnotC_Ssh(i)+
        YearlyPmaxChange_Ssh(i) - YearCleaning_Ssh(i))/(1+disc_rate)^(i);

    Sum_Cwall = Sum_Cwall+CashFlow_Cwall(i);
    if Sum_Cwall <0
        payback_Cwall = payback_Cwall+1;
    end
    if NPV_Cwall < 0
        disc_payback_Cwall = disc_payback_Cwall+1;
    end
    NPV_Cwall = NPV_Cwall + (YearSavings_Cwall(:,i).Variables+
        YearlyEnotC_Cwall(i)+...
        YearlyPmaxChange_Cwall(i) - (YearCleaning_Cwall(i)))/...
        (1+disc_rate)^(i);
end

%%% LCOE
discE_Ssh = pvvar([0 YearEnergy_Ssh.Variables],disc_rate); %kWh
discCosts_Ssh = pvvar([InitialCost_Ssh+InitialCost_Roof ...
YearCleaning_Ssh],disc_rate); %USD
LCOE_Ssh = discCosts_Ssh/discE_Ssh; %USD/kWh
discE_Cwall = pvvar([0 YearEnergy_Cwall.Variables],disc_rate);
discCosts_Cwall = pvvar([InitialCost_Cwall+InitialCost_Roof -...
InitialSavings_Cwall YearCleaning_Cwall],disc_rate);
LCOE_Cwall = discCosts_Cwall/discE_Cwall;

%%% Calc Anual Energy Yield
%Sun Shield
Tot_gen_Ssh = YearEnergy_Ssh.Pac_Ssh_1; %kWh/year
Tot_gen_SshNoR = YearEnergy_SshNoR.Pac_Ssh_noR; %kWh/year

```

```

%Curtain Wall
Tot_gen_Cwall = YearEnergy_Cwall.Pac_Cwall_1; %kWh/year
Tot_gen_CwallNoR = YearEnergy_CwallNor.Pac_Cwall_noR; %kWh/year
%%%Calc Specific yield
An_E_Yield_Ssh = Tot_gen_Ssh/(P_nom_Ssh+P_nom_Roof); %kWh/kWp
An_E_Yield_SshNoR = Tot_gen_SshNoR/(P_nom_Ssh); %kWh/kWp
An_E_Yield_Cwall = Tot_gen_Cwall/(P_nom_Cwall+P_nom_Roof); %kWh/kWp
An_E_Yield_CwallNoR = Tot_gen_CwallNoR/(P_nom_Cwall); %kWh/kWp
%%%Calc PR for thr year
Hi_Ssh = sum(D_15.Gt_Ssh); %W/m2
Hi_Cwall = (sum(D_15.Gt_Cwall)*FacadeArea+sum(D_15.Gt_Ssh)*...
    Total_area_Roof)/(FacadeArea+Total_area_Roof); %W/m2
Hi_CwallNoR = sum(D_15.Gt_Cwall); %W/m2
Yr_Ssh = Hi_Ssh/G;
Yr_Cwall = Hi_Cwall/G;
Yr_CwallNoR = Hi_CwallNoR/G;
%An_E_Yield_Ssh/Yr_Ssh
PR_Ssh = Tot_gen_Ssh*G/(sum(D_15.Gt_Ssh)*(P_nom_Ssh+P_nom_Roof));
%An_E_Yield_SshNoR/Yr_Ssh
PR_SshNoR = Tot_gen_SshNoR*G/(sum(D_15.Gt_Ssh)*(P_nom_Ssh));
PR_Cwall = An_E_Yield_Cwall/Yr_Cwall;
%An_E_Yield_CwallNoR/Yr_CwallNoR
PR_CwallNoR = Tot_gen_CwallNoR*G/(sum(D_15.Gt_Cwall)*(P_nom_Cwall));

%%% PR every year
Yieldf_Ssh = @(x) x/(P_nom_Ssh+P_nom_Roof);
Yieldf_Cwall = @(x) x/(P_nom_Cwall+P_nom_Roof);
PerfRatio_Ssh = @(x) x/Yr_Ssh;
PerfRatio_Cwall = @(x) x/Yr_Cwall;
Yf_Ssh = varfun(Yieldf_Ssh, YearEnergy_Ssh);
Yf_Cwall = varfun(Yieldf_Cwall, YearEnergy_Cwall);
PRy_Ssh = varfun(PerfRatio_Ssh, Yf_Ssh);
PRy_Cwall = varfun(PerfRatio_Cwall, Yf_Cwall);
plot(1:25, PRy_Ssh.Variables)
hold on
plot(1:25, PRy_Cwall.Variables)
%Power gen over power consumed
Total_Dem_Ssh = retime(Bs_pow(:, 'Elec_dem_Ssh'), 'yearly', 'sum');
Total_Dem_Ssh = Total_Dem_Ssh.Elec_dem_Ssh;
Total_Dem_Cwall = retime(Bc_pow(:, 'Elec_dem_Cwall'), 'yearly', 'sum');
Total_Dem_Cwall = Total_Dem_Cwall.Elec_dem_Cwall;
PgenOPcons_Ssh = Tot_gen_Ssh/Total_Dem_Ssh;
PgenOPcons_SshNoR = Tot_gen_SshNoR/Total_Dem_Ssh;
PgenOPcons_Cwall = Tot_gen_Cwall/Total_Dem_Cwall;
PgenOPcons_CwallNoR = Tot_gen_CwallNoR/Total_Dem_Cwall;

```